

**Development of a targeted proteomic assay for rapid detection of Shiga-like toxins 1 and 2 in Shiga toxin-producing *Escherichia coli***

by

Leanne Gene Scharikow

A Thesis submitted to the Faculty of Graduate Studies of

The University of Manitoba

in partial fulfillment of the requirements of the degree of

MASTER OF SCIENCE

Department of Medical Microbiology and Infectious Diseases

University of Manitoba

Winnipeg, Manitoba, Canada

## Abstract

Shiga toxin-producing *Escherichia coli* (STEC) are extensive contributors to foodborne illness and can cause severe renal and central nervous system damage due to the production of Shiga toxin (Stx). Stx genes are found on integrated lambdoid bacteriophages and activation of the phage lytic cycle by DNA-damaging agents, such as antibiotics, promotes *stx* gene transcription and increases toxin production. The administration of antibiotics to STEC-infected patients is contraindicated due to the increased toxin production. Rapid Stx detection is important to distinguish STEC from other enteric pathogens. Current detection techniques are time consuming, expensive, and lack sensitivity. We have developed and evaluated a novel targeted mass spectrometry-based assay for detection of signature Stx peptides using parallel reaction monitoring (PRM).

Shotgun proteomics was used to determine the appropriate bacterial sample fraction, cell pellet or culture supernatant, and duration of induction to provide a robust sample preparation method. The acquired data established that inductions would be sufficient after two hours and the cell pellet fraction was most suitable to obtain the protein.

Using trypsin-digested Stx protein, 11 target tryptic peptides were selected. After developing the PRM assay methodology, the PRM assay was validated using a cohort of STEC and non-STEC bacterial cultures that were processed using the robust sample preparation method. Together, the processing method and PRM assay were confirmed as capable of detecting Stx in 56 of 62 STEC isolates and did not detect Stx in any of the 29 non-STEC isolates. In addition to detection, the PRM assay successfully determined the Stx2 subtype in 32 of 46 Stx2-positive isolates.

By applying a targeted proteomics assay, we were able to simultaneously detect both Stx toxins 1 and 2 and to subtype Stx2 into six toxin subgroups in Stx2-positive isolates. With additional refinement of the

sample processing procedures, this PRM assay shows potential to replace laborious and expensive techniques currently in use.

## **Acknowledgements**

First, I would like to thank my supervisor Dr. Morag Graham, as well as my committee members Dr. Grant McClarty, Dr. Celine Nadon, and Dr. Claudia Narvaez, for providing invaluable guidance and encouragement throughout my time as a Master's student. I am grateful for the opportunity to work with such accomplished and driven scientists.

A very heartfelt thank you goes out to the Public Health Agency's Mass Spectrometry and Proteomics Core Facility members, Dr. Garrett Westmacott, Stuart McCorrister, Derek Davlut, Dr. Patrick Chong, and Dr. Chris Grant. This project would not have been possible without their knowledge and support. Thank you for answering my millions of questions and providing a valuable lesson in patience.

I would like to thank Dr. Clifford Clark, Joanne McCrea, and Cai Guan of the Public Health Agency's Division of Enteric Diseases for the laboratory support provided throughout the project, as well as Dr. Michael Carpenter and his laboratory for their support with sample preparation. I would also like to thank the Public Health Agency of Canada and the Genomics Research and Development Initiative for supporting this research.

I am deeply indebted to Cheryl Reimer, Angela Nelson, and Jude Zieske for the administrative support I received as a graduate student and as a member of student council. The department as a whole would be lost without you.

Finally, I would like to thank my family and friends for their endless love and encouragement. To my parents, Bev and Gene Scharikow, you have taught me how to be a strong, independent young woman and ensured that I was provided with all of the tools and lessons necessary to be successful in anything that I chose to pursue. To my fiancé, Adam Pukalo, this would have been impossible without you. I cannot put into words how much your never-ending love and support means to me.

# Table of Contents

Abstract .....	2
Acknowledgements .....	4
List of Tables .....	8
List of Figures .....	9
List of Abbreviations.....	10
1. Introduction .....	11
1.1. History .....	11
1.2. Classification.....	11
1.3. Shiga toxin-producing <i>E. coli</i> .....	13
1.4. Epidemiology .....	16
1.4.1. Modes of transmission .....	16
1.4.2. Notable outbreaks .....	17
1.5. Virulence factors.....	17
1.5.1. Virulence factors other than Shiga toxin.....	18
1.6. Shiga toxins.....	19
1.6.1. Shiga toxin nomenclature.....	21
1.6.2. Toxin activity.....	23
1.6.3. Differences in toxicity.....	24
1.6.4. Induction and SOS response .....	25
1.6.5. Toxin binding and transport .....	28
1.7. Symptoms.....	31
1.8. Treatment of STEC infections .....	31
1.8.1. Novel treatment options .....	32
1.8.2. STEC prevention strategies.....	32
1.9. Current diagnostic methods.....	33
1.9.1. Culture.....	34
1.9.2. Molecular and antibody-based assays .....	36
1.9.2.1. Vero cell assay.....	37
1.9.2.2. Enzyme immunoassays.....	37
1.9.2.3. Polymerase chain reaction .....	39

1.9.3. Limitations of current diagnostic methods .....	41
1.10. Mass spectrometry for proteomic-based diagnostics .....	42
1.10.1. Targeted proteomics .....	44
2. Objectives.....	51
2.1. Objective 1: Stx induction optimization/characterization .....	51
2.2. Objective 2: Evaluate PRM for Stx 1 & 2 detection from culture .....	52
3. Materials and Methods.....	54
3.1. Shotgun Proteomics: Characterizing Stx induction.....	54
3.1.1. Isolate selection .....	56
3.1.2. Induction procedure.....	57
3.1.3. Protein extraction and quantitation .....	58
3.1.4. Protein digestion.....	59
3.1.5. iTRAQ® labelling.....	62
3.1.6. Nano-flow liquid chromatography-tandem mass spectrometry (LC/MS/MS) .....	65
3.1.7. Data analysis .....	65
3.2. Targeted Proteomics: PRM detection of Shiga toxin .....	66
3.2.1. Selecting target peptides for Shiga toxin detection.....	68
3.2.1.1. <i>in silico</i> digestion.....	68
3.2.1.2. Shiga toxin peptide identification .....	68
3.2.2. Synthetic peptide standard .....	70
3.2.2.1. Determining lower limit of detection.....	70
3.2.3. Validation of the PRM Shiga toxin detection assay .....	72
3.2.4. Improving sample preparation .....	73
3.2.5. Nano-flow liquid chromatography-tandem mass spectrometry (LC/MS/MS) .....	74
3.2.5.1. Peptide identification .....	74
3.2.5.2. Parallel reaction monitoring .....	74
3.2.6. Parallel reaction monitoring data analysis .....	75
3.3. Common Shiga toxin detection methods.....	76
3.3.1. Vero cell assay.....	76
3.3.2. Vero cell neutralization assay .....	80
3.3.3. Paton polymerase chain reaction .....	83
4. Results.....	88

4.1. Shotgun Proteomics: Characterizing Stx Induction .....	88
4.2. Targeted Proteomics: PRM detection of Shiga toxin .....	92
4.2.1. Selecting target peptides for Shiga toxin detection.....	92
4.2.2. Determining lower limit of detection.....	92
4.2.3. Validation of the PRM Shiga toxin detection assay .....	96
4.3. Common Shiga toxin detection methods.....	101
4.3.1. Vero Cell Assay.....	101
4.3.2. Polymerase chain reaction .....	102
5. Discussion.....	104
5.1. Shotgun Proteomics: Characterizing Shiga toxin Induction .....	104
5.1.1. Methodology and analysis.....	105
5.1.2. Appropriate fraction and induction time .....	106
5.1.3. Limitations .....	109
5.1.4. Future considerations for sample preparation.....	110
5.2. Targeted Proteomics: Characterizing Stx induction.....	111
5.2.1. Shiga toxin peptide identification .....	112
5.2.2. Shiga toxin detection.....	114
5.2.3. Shiga toxin 2 subtyping .....	117
5.2.4. Comparison to common Shiga toxin detection methods.....	119
5.2.5. Limitations of the PRM detection assay .....	122
5.2.6. Future steps .....	123
5.2.6.1. Sample preparation.....	123
5.2.6.2. Absolute peptide quantitation.....	124
5.3. Broader applications .....	126
6. Conclusion.....	128
7. References .....	129
8. Supplementary Data .....	135

## List of Tables

Table 1. Primers for amplification of the Paton Multiplex genes .....	84
Table 2. PCR reaction mix conditions for Paton multiplex PCR .....	85
Table 3. Run parameters for Paton Multiplex PCR.....	86
Table 4. Evaluation of LLOD for Stx peptides .....	94
Table 5. Analysis of clinical STEC and non-STEC samples using PRM, VCA, and PCR. ....	98
Table 6. Stx1 and Stx2 subtype fingerprint map .....	99
Table 7. Subtype analysis of Stx2-carrying isolates using the PRM assay. ....	100
Supplementary Table S1. Method development runs using recombinant, non-toxic Stx peptides .....	135
Supplementary Table S2. Method development runs using Stx peptides from active, intact Stx.....	136
Supplementary Table S3. Method development runs using synthetic Stx peptides .....	137
Supplementary Table S4. Validation of the PRM Stx detection assay using bacterial cultures.....	138
Supplementary Table S5. Summary of the STEC isolates used for evaluation of Stx detection. ....	139
Supplementary Table S6. Summary of the Stx-negative isolates used to evaluate the PRM Stx detection assay .....	141

## List of Figures

Figure 1. Incidence rates of O157 and non-O157 STEC in Canada.....	14
Figure 2. Structure of the AB <sub>5</sub> Stx holotoxin .....	20
Figure 3. Phylogenetic distribution of Stx subtypes .....	22
Figure 4. Regulation of Stx expression by the phage cycle.....	27
Figure 5. Comparing SRM and PRM targeted proteomics.....	46
Figure 6. QExactive™ Plus (QE+) Hybrid Quadrupole-Orbitrap™ mass spectrometer .....	47
Figure 7. Workflow for characterization of Stx induction .....	55
Figure 8. Representative 2D-LC chromatogram for fractionation of iTRAQ® samples .....	64
Figure 9. Workflow for developing and validating the PRM Stx detection assay. ....	67
Figure 10. Vero cell assay procedure.....	79
Figure 11. Vero cell neutralization assay methods .....	82
Figure 12. Stx1 induction timeline results .....	90
Figure 13. Stx2 induction timeline results .....	91
Figure 14. Dilution series plot for peptide ISNVLPEYR .....	95
Figure 15. Submarine agarose gel electrophoresis analysis of Paton PCR products.....	103

## List of Abbreviations

°C – degrees Celsius	LLOD – lower limit of detection
A/E – attaching and effacing	LLOQ – lower limit of quantitation
AB buffer – ammonium bicarbonate	LPS – lipopolysaccharide
ACN – acetonitrile	M – molar
bp – base pair	m/z – mass-to-charge ratio
BSA – bovine serum albumin	MALDI-TOF – Matrix-Assisted Laser-Desorption/Ionisation – Time-of-Flight
CDC – Centers for Disease Control	mg - milligram
CFU – colony forming units	ml – milliliter
cm – centimetre	mm – millimeter
CNS – central nervous system	mM - millimolar
CT-SMAC – cefixime tellurite sorbitol MacConkey	MMC – mitomycin C
CV – coefficient of variation	mol – mole
DAEC – diffusely adherent <i>E. coli</i>	MRM – multiple reaction monitoring
DNA – deoxyribonucleic acid	MS – mass spectrometry
dotp – dot product	NaCl – Sodium chloride
DTT – dithiothreitol	ng – nanogram
<i>E. coli</i> – Escherichia coli	NH <sub>4</sub> FA – ammonium formate
EAEC – enteroaggregative <i>E. coli</i>	nl – nanoliter
EIA – enzyme immunoassay	nm – nanometer
EIEC – enteroinvasive <i>E. coli</i>	NML – National Microbiology Laboratory
EPEC – enteropathogenic <i>E. coli</i>	nmol - nanomole
ER – endoplasmic reticulum	NRS – normal rabbit serum
ETEC – enterotoxigenic <i>E. coli</i>	nt – nucleotide
FA – formic acid	ON - overnight
FC – fold change	PBS – phosphate buffered saline
FDA – Food and Drug Administration	PCR – polymerase chain reaction
fmol – femtomole	PHAC – Public Health Agency of Canada
Fur – Ferric Uptake Regulator	Qq-OT – quadrupole-orbitrap mass spectrometer
FWS – Food and Water Safety	QqQ – triple quadrupole mass spectrometer
g/L – grams per litre	rcf – relative centrifugal force
Gb3 – globotriaosylceramide	rpm – revolutions per minute
Gb4 – globotetraosylceramide	RT – room temperature
GRDI – Genomics Research and Development Initiative	SDS – sodium dodecyl sulfate
HCD – higher-energy collision dissociation	SMAC – sorbitol MacConkey agar
HEPES - 4-(2-hydroxyethyl)-1-piperazineethanesulfonic acid	SRM – selected reaction monitoring
HUS – haemolytic uremic syndrome	STEC – Shiga toxin-producing <i>E. coli</i>
IAA - iodoacetamide	Stx – Shiga toxin
iTRAQ® – isobaric tag for relative and absolute quantitation	TCA – trichloroacetic acid
LC – liquid chromatography	TSB – trypticase soy broth
LEE – locus to enterocyte effacement	UEB – urea exchange buffer
LFI – lateral flow immunoassay	WGS – whole genome sequencing
	µg – microgram
	µl – microliter

# 1. Introduction

## 1.1. History

*Escherichia coli* is a Gram-negative, rod-shaped bacteria discovered by Theodore Escherich in 1885<sup>1</sup>. *E. coli* can be a harmless commensal normally found in the gut microbiota of healthy humans, but also has the potential to cause severe diarrheal and extraintestinal diseases. Through the gain and loss of genes found on mobile genetic elements, such as bacteriophages, these harmless commensal isolates can become diverse and adapted pathogens. Pathogenic *E. coli* carry an enormous potential to cause illness not only in developing nations, where *E. coli* infections are an immense burden, but also in developed nations, such as Canada and the United States, with mature public health infrastructure. Infections due to *E. coli* are one of the most common causes of diarrhea around the globe with high incidence in children under five in sub-Saharan Africa and South Asia<sup>2</sup>. Upon infection with *E. coli*, severity of disease and the associated morbidity and mortality are determined by the combination of virulence factors carried by and expressed by that specific strain<sup>1</sup>.

## 1.2. Classification

The earliest typing scheme for classification of *E. coli* is based on serotype. Serotyping of *E. coli* isolates requires identifying three antigens; somatic lipopolysaccharide (O), capsule (K), and flagellum (H). Originally, serotyping required the use of anti-*E. coli* polyclonal antiserum, which is time consuming, expensive, and requires in-depth understanding of the serum agglutination for interpretation<sup>3</sup>. This technique is sometimes still performed, but today, many reference laboratories have employed newer and emerging molecular technologies to classify isolates based on their phylogenetic relationships. These techniques include examples such as multi-locus enzyme electrophoresis (MLEE), multi-locus sequence typing (MLST), and whole-genome sequencing (WGS). Information obtained using MLEE and MLST is based on the characterization of only a few genes, which does not provide enough

discriminating power to differentiate between closely related isolates<sup>4</sup>. The use of WGS and the bioinformatics required to analyze the WGS outputs allow researchers to extract information based on an isolate's entire genomic sequence. This information is used for multiple molecular analyses, including serotyping and other subtyping schemes<sup>4</sup>. Whole genome sequencing is especially useful in the characterization of *E. coli* isolates as they contain large accessory genomes due to their ability to acquire genes through horizontal gene transfer. Large databases of fully sequenced *E. coli* genomes now exist as foundational information sources for reference in many modern applications.

Pathogenic *E. coli* isolates can be divided into six pathotypes characterized by the type of disease they cause<sup>1</sup>. Enteropathogenic *E. coli* (EPEC) was the first pathotype to be defined and is classified based on its ability to cause distinctive lesions on the surfaces of intestinal epithelial cells. For this reason they are referred to as attaching and effacing (A/E) pathogens. Enteroinvasive *E. coli* (EIEC) are grouped together with *Shigella* spp. due to their ability to cause bacillary dysentery and shigellosis. These pathogens are highly invasive and can adapt to harsh environmental challenges. Enteroaggregative *E. coli* (EAEC) are the most common bacterial pathogen cultured from diarrheal stool samples. They cause traveler's diarrhea and persistent diarrhea in children and HIV-infected patients. Enterotoxigenic *E. coli* (ETEC) use heat-labile or heat-stable enterotoxins to cause traveler's diarrhea and significant mortality in children. Diffusely adherent *E. coli* (DAEC) is a poorly defined pathotype describing diarrheal *E. coli* isolates that do not exhibit the classical patterns of adherence. They require further epidemiological studies for characterization. Lastly, Shiga toxin-producing *E. coli* (STEC) are a diverse group of isolates carrying the Shiga-like toxin 1 (*stx1*) and/or the Shiga-like toxin 2 (*stx2*) genes on a mobile lambdoid bacteriophage. Although hundreds of serotypes of STEC can be found across the globe, only a subset is able to cause illness in humans<sup>2</sup>.

### **1.3. Shiga toxin-producing *E. coli***

Shiga toxin-producing *E. coli* are extensive contributors to foodborne illness and are considered a global public health issue<sup>5</sup>. According to the Public Health Agency of Canada (PHAC), STEC was first recognized in 1982 during an outbreak of bleeding colitis in the United States. These infections have now become widespread public health concerns in North America, Japan, Europe, South Africa, southern South America, and Australia<sup>6</sup>, with the majority of cases occurring in the developed world<sup>7</sup>. An estimated 2.8 million cases of STEC infection occur annually across the globe leading to approximately 230 deaths. Although the number of deaths is considered low compared to other enteric bacterial pathogens, such as typhoid fever (21.7 million cases, 216,000 deaths) or salmonellosis (93.8 million cases, 155,000 deaths), the long term sequelae from STEC infection can be severe (e.g., kidney dysfunction, hypertension and neurological abnormalities) and costly<sup>5</sup>.

Incidence rates are generally subdivided and reported as two different categories; infections caused by O157 STEC serotypes and infections caused by non-O157 STEC serotypes. Global incidence rates and the proportion of O157 STEC and non-O157 STEC infections vary depending on geographical location. Argentina has reported their annual O157 STEC incidence as 13.9 cases per 100,000 people, which can be considered high compared to reported numbers from Australia (0.12 cases/100,000 people), Sweden (0.81 cases/100,000 people)<sup>4</sup> or Canada's most recent posted rate (2013) (1.34 cases/100,000 people)<sup>6</sup>. Although O157 STEC infections are routinely diagnosed in developed nations, the higher incidence in a country such as Argentina may not be due to the bacterium itself, but possibly to socioeconomic factors<sup>8</sup>, differences in the diet of the host, and variations in the host microbiome<sup>4</sup>.

The rates of O157 and non-O157 STEC infections in Canada have changed between 2002 and 2012. A drastic decrease in the number of O157 STEC infections can be seen, while an increase in non-O157 STEC infections can be observed over the sample timeline (Figure 1)<sup>6</sup>. As well, the incidence rates in Canada

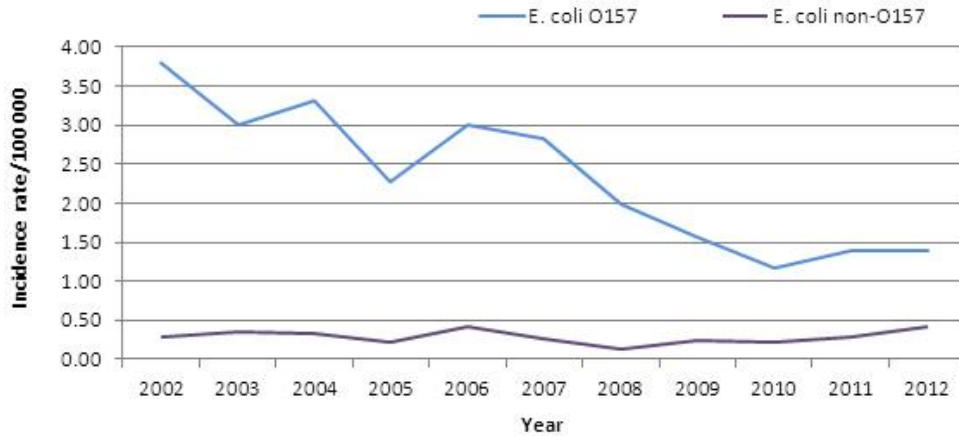


**Figure 1.** Incidence rates of O157 and non-O157 STEC in Canada. The data, acquired through the National Enteric Surveillance Program, shows a decrease in the prevalence of laboratory-confirmed O157 STEC between 2002 and 2012, while an increase in laboratory-confirmed non-O157 STEC can be seen over the same period of time. Some possible explanations for the decrease in O157 STEC infections include more awareness of proper food handling processes and pathogen reduction interventions at slaughter. As for the increase in non-O157 STEC, it has been hypothesized that better recovery and/or detection methods have led to a higher number of reported isolates. (source: <http://www.phac-aspc.gc.ca/fs-sa/fs-fi/ecoli-eng.php>)

have remained relatively unchanged since 2010 despite three multi-jurisdictional outbreaks in 2013<sup>115</sup>. Of the estimated four million episodes of domestically acquired foodborne illness in 2006, Thomas *et al.* estimate that 33,350 cases can be attributed to O157 and non-O157 STEC. Of the 30 pathogens known to cause domestically acquired foodborne illness, STEC were ranked as the fifth most common<sup>117</sup>. The incidence rates and trends in the United States mirror those of Canada; a significant reduction (32% decrease) in the incidence of O157 STEC infections was observed in 2014 compared to 2006-2008, whereas a significant increase of non-O157 STEC infections was observed over the same timeline. The reduction in O157 STEC can be attributed to increased education in food handling, as well as improved diagnostic technologies and diligence in outbreak tracking<sup>9</sup>. Consequently, the annual economic burden of STEC infections in the United States remains high, estimated at \$405 million USD<sup>10</sup>.

Although all age groups can be infected with STEC, the very young, the elderly, and the immunocompromised are more likely to become infected. One study demonstrated that, when compared with adults 18 years of age or older, children 0-4 years of age have a 4.81-fold higher incidence of STEC infection and those 5-17 years of age have a 3.96-fold higher incidence<sup>11</sup>. Young children are more likely to develop hemolytic uremic syndrome (HUS), a severe complication of STEC infection affecting the kidneys and central nervous system (CNS)<sup>12</sup>. In the United States, it is estimated that 14% of STEC-infected children under the age of 10 will progress to HUS; compared to only 4% occurrence in individuals 10 years and older<sup>2</sup>. Data from multiple outbreaks suggest females may be more susceptible to STEC infection than males. Although, this could also be due to the fact that in many cultures women are responsible for food preparation and are, therefore, more likely to be exposed to the infectious agent than men<sup>13</sup>.

## **1.4. Epidemiology**

Surveillance networks all over the globe have been established to track outbreaks and sporadic cases in order to reduce the public health impact of STEC infections. PulseNet, a network of national and regional laboratories, applies foodborne infection surveillance to track isolates and investigate foodborne disease outbreaks. Each laboratory applies standardized genotyping methods, sharing collected information in real-time to determine if isolates can be considered related and tied to a common outbreak source/contamination event, in order to intervene to limit additional foodborne illness and potential impact on public health<sup>6</sup>.

### **1.4.1. Modes of transmission**

Cases of STEC infection can occur sporadically or due to an outbreak. The bacteria are spread through the fecal-oral route and can be acquired through person-to-person contact, contact with animals or feces, ingestion of contaminated foods, or consuming feces-contaminated water<sup>13</sup>. Outbreaks are often associated with the consumption of undercooked beef, however a wide variety of food products have been implicated including leafy greens, dairy products, and unpasteurized juices<sup>1, 59</sup>. Cattle have been pinpointed as the main reservoir for STEC<sup>14, 15</sup>, with 22-67% of cattle being infected depending on the herd<sup>15</sup>. Domestic and wildlife animal species, specifically ruminants, asymptotically carry STEC and are able to shed the bacteria in high numbers in their feces. It is through contact with the feces or products contaminated with feces that humans most often acquire the infection. One study determined that viable O157:H7 bacterial cells could be recovered from feces for up to twenty months. This extended period of time allows for spread throughout the environment and eventually into food sources<sup>14</sup>. For example O157 STEC has been isolated with increasing frequency from fresh produce, including leaf lettuce, owing to contaminated water sources used in field irrigation<sup>16</sup>.

### **1.4.2. Notable outbreaks**

Outbreaks occur regularly across the globe, varying in number of patients infected and severity of infection. Outbreaks are more prevalent in areas with extreme weather such as increased temperature and heavy rainfall<sup>14</sup>. In Canada, one notable STEC outbreak occurred in Walkerton, Ontario in 2000. It saw 2,300 cases and seven deaths due to inadequately chlorinated drinking water<sup>4</sup>. Another Canadian outbreak occurred in 2012 at an Alberta beef processing plant where 18 consumers fell ill from infection with O157:H7 STEC. No deaths or cases of HUS were reported. Approximately 4,000 tonnes of beef products were recalled in Canada and the United States, representing at least 12,000 head of cattle<sup>17</sup>. A 2011 outbreak originating in Germany was linked to fenugreek seed sprouts and is a prime example of the emergence of non-O157 STEC isolates causing severe infection. The etiological agent was determined to belong to the serotype O104:H4, which has historically caused few human illnesses. This outbreak caused 4,075 infections in 16 countries. Of those infected, 22% developed HUS and the outbreak resulted in 50 deaths<sup>4</sup>. These STEC outbreaks are not only harmful to the health of the public, but also cause extensive economical losses especially in the agriculture and food processing sectors. Fast and effective diagnostics and molecular subtyping can aid in the identification and containment of an outbreak, possibly reducing the number of infections and preventing deaths.

### **1.5. Virulence factors**

Shiga toxin-producing *E. coli* have multiple virulence factors encoded within their genomes, with the presence or absence of a virulence factor being heterogeneous between isolates. The variability of virulence factors between isolates may be explained by the fact that these pathogens contain an extensive 'accessory genome', which is encoded within plasmids and other mobile genetic elements, in addition to the 'core genome'<sup>18</sup>. Many STEC virulence factors are found on large virulence plasmids or genomic islands and can be transferred between bacterial cells via horizontal gene transfer. The term 'O island' was used to designate genomic islands unique to the O157:H7 STEC strain EDL933, but this

nomenclature has since been applied in designating mobile genomic O islands carrying virulence factors in other strains<sup>2</sup>.

### **1.5.1. Virulence factors other than Shiga toxin**

Aside from Stx, other factors are also important contributors to the virulence of a STEC isolate. The *E. coli* genome contains an extensive number of virulence factors, mainly owing to horizontal gene transfer. The text below emphasizes some of the more common factors that allow STEC isolates to exert virulence on their hosts.

Some STEC are able to produce other phage-encoded toxins, such as the cytolethal distending toxin (Cdt) and the EHEC hemolysin, both of which are known to increase the likelihood of developing HUS<sup>2, 19, 20</sup>. Cdt is a DNA-damaging toxin structurally similar to Stx. It introduces double-stranded breaks in the host DNA, eventually leading to host cell apoptosis<sup>20</sup>. EHEC hemolysin, a pore-forming toxin, is produced by multiple serotypes of STEC and causes damage to epithelial and microvascular endothelial cells eventually leading to apoptosis<sup>19</sup>. Multiple other toxins may also be encoded within the accessory genome of STEC isolates.

The locus of enterocyte effacement (LEE) is another important virulence factor and is commonly found in STEC serotypes affecting humans. It is known to contribute to differential virulence phenotypes between serotypes<sup>18</sup>. The LEE genes are phage-encoded and contribute to the formation of A/E lesions, building of pili for attachment to host cells leading to increased adherence and colonization, and biofilm formation for persistence<sup>2, 18</sup>. The LEE also encodes for a Type III secretion system used to inject bacterial proteins, referred to as Type III effectors, into host cells. The effectors are then able to modulate host cellular processes to benefit the pathogen<sup>21</sup>. LEE-negative STEC have been isolated from patients with HUS, but they use a pathogenic mechanism similar to EAEC where they apply a different

repertoire of virulence genes. LEE-negative STEC are still successful in causing severe disease by attachment, invasion, and toxicity<sup>2</sup>.

As explained in a review by Vogelee *et al.*, STEC are able to persist within the environment for long periods of time, partially due to the formation of biofilms. This persistence allows for seeding and shedding of bacteria, which can ultimately lead to a contamination event and/or potential host ingestion. Pathogenic and non-pathogenic *E. coli* cells are able to attach to both biotic and abiotic surfaces by enclosing themselves in an extracellular polymeric matrix<sup>22</sup>. STEC cells are then able to create new biofilms by attaching themselves to surfaces using flagella-driven motility<sup>23</sup>. They can also integrate themselves into pre-existing biofilms, providing an excellent environment for the exchange of genetic information and acquisition of phage-encoded virulence factors between pathogenic and non-pathogenic bacteria. Biofilms are especially important for persistence in abattoirs and food processing plants<sup>22</sup>. Equipment becomes contaminated during the processing of STEC-infected animal carcasses<sup>24</sup>. Once the biofilm has been formed it is able to disperse for cross-contamination of other equipment, other foods processed within the plant, and of workers. STEC biofilms have also been found in freshwater streams that drain from or are connected to farmland such as irrigation systems and drains<sup>22</sup>.

## **1.6. Shiga toxins**

Although STEC have only been identified as a pathogen since 1982, Stx was discovered in 1898 from *Shigella dysenteriae*<sup>25</sup>. Stx is the critical virulence factor associated with human STEC infection. It belongs to the AB<sub>5</sub> group of bacterial holotoxins (Figure 2), which, in combination with the cholera and pertussis toxins, cause approximately one million deaths per year globally<sup>26</sup>. The homopentameric Stx B subunit (7 kDa) is responsible for binding to the host cell receptor. The Stx A subunit (30 kDa) is cleaved into two parts, A<sub>1</sub> and A<sub>2</sub>, at a protease-sensitive site near the C-terminus. The A<sub>1</sub> subunit is the catalytically active portion, while the A<sub>2</sub> subunit is responsible for binding A<sub>1</sub> to the B subunit pentamer<sup>27</sup>.

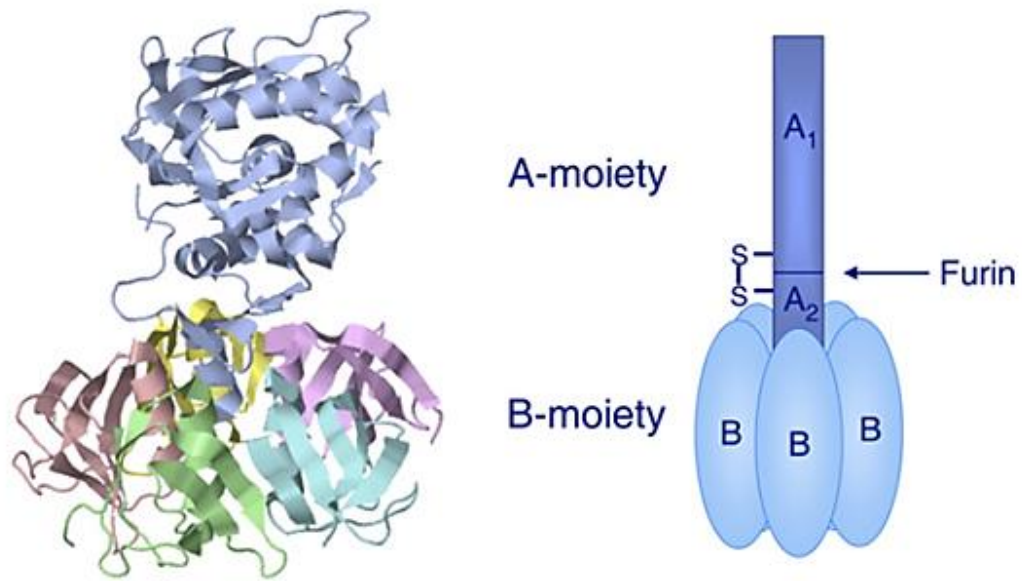


**Figure 2.** Structure of the AB<sub>5</sub> Stx holotoxin. The above figure, from Sandvig *et al.*, shows the 3D structure of Stx using a ribbon diagram and a cartoon representation. The toxin contains five B subunits arranged in a donut-like shape with the A subunit situated within the centre hole of the donut. The subunits are non-covalently attached to each other<sup>31</sup>.

### 1.6.1. Shiga toxin nomenclature

The Shiga toxins found in STEC isolates are generally referred to as Shiga-like toxins and can be divided into two immunologically distinct isoforms; Stx1 and Stx2. The two isoforms share approximately 60% amino acid homology<sup>28</sup>, with Stx1 being almost identical to the true Shiga toxin found in *S. dysenteriae*. Toxin nomenclature can be further broken down into subtypes. Stx1 is divided into three subtypes; Stx1a, Stx1c, and Stx1d<sup>29</sup>. STX1B is used to describe the gene encoding Syntaxin 1B and is not used to denote a Stx subtype. One study determined the sequence differences between Stx1 subtypes were minor with Stx1a and Stx1c being slightly more similar to each other than Stx1a and Stx1d (Figure 3)<sup>30</sup>.

Stx2 is divided into seven subtypes; Stx2a-g<sup>29</sup>. Stx2 subtypes contain more genetic variation in their nucleotide sequence than is seen among Stx1 subtypes, with Stx2f showing the most variation. In all Stx subtypes, the amino acid sequence is conserved through the active site and the disulfide bridge between A<sub>1</sub> and A<sub>2</sub><sup>25</sup>. Stx production is not limited to *E. coli* species, as Stx has been detected in several non-*E. coli* bacteria<sup>32</sup>. Recently, a new subtype of Stx1, Stx1e, was identified in an isolate of *Enterobacter cloacae*. Interestingly, the amino acid sequence of the Stx1e toxin shared only 87% identity with the closest Stx1 reference sequence and was not neutralized by anti-Stx1 monoclonal antibodies<sup>33</sup>. If a diagnostic assay is created based on the detection of the toxin protein and not of the bacteria, then, hypothetically, the species harbouring the Stx genes is irrelevant. That being said, if the culture/expression methods developed for Stx expression and detection in STEC are not transferrable to other bacterial species, then toxin may not be produced at sufficient levels for detection.

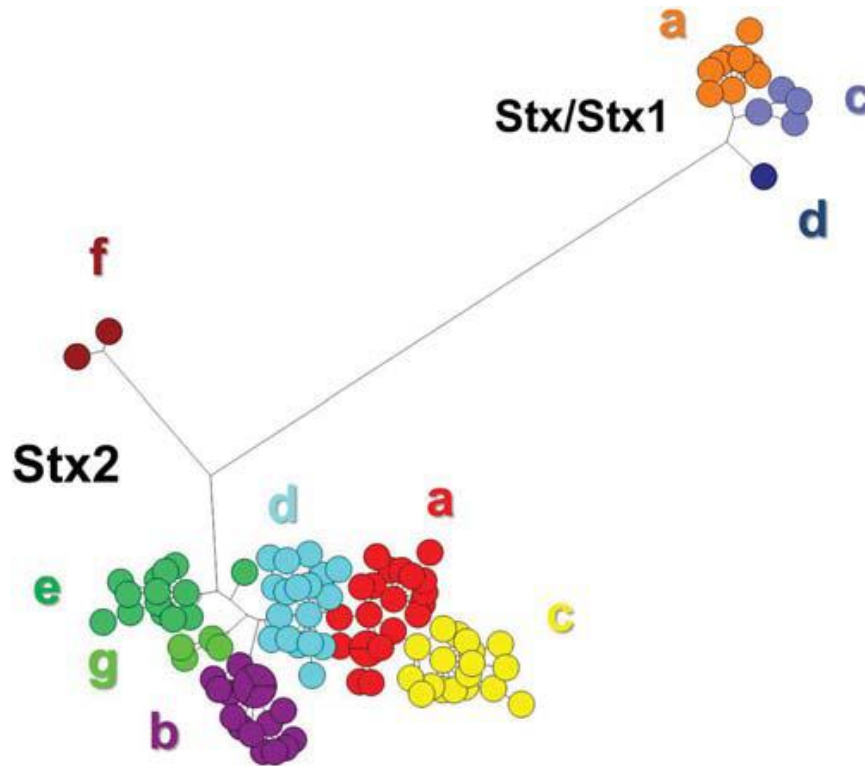


**Figure 3.** Phylogenetic distribution of Stx subtypes. Scheutz *et al.* analyzed the Stx nucleotide sequences from a total of 107 Stx variants to determine the relatedness between the different Stx subtypes. The nucleotide sequences for *S. dysenteriae* 1 strain 3818T and O157:H7 strain EDL933 were used as references for Stx1 and Stx2, respectively<sup>30</sup>. The figure shows that the Stx1 and Stx2 isolates cluster separately and that Stx2f is not as closely related to the reference strain as the rest of the Stx2 subtypes. When analyzing the amino acid sequence of the Stx subtypes, the subtypes tend to cluster in the same pattern as when analyzing the nucleotide sequences<sup>30</sup>.

### 1.6.2. Toxin activity

Shiga toxin causes damage to blood vessels within the intestinal lumen, leading to bloody diarrhea. The additional blood found released in the area allows for increased bacterial survival as it provides the cells with nutrients, such as iron<sup>45</sup>. Shiga toxin that has accumulated within the cytosol of host cells acts as a ribotoxin with a similar mechanism as ricin. The A<sub>1</sub> portion of Stx is able to remove a single adenine residue from the 28S rRNA molecule through *N*-glycosidase activity. The ribosome is inactivated and host protein synthesis is inhibited resulting in apoptosis of host cells<sup>46</sup>. As well, the inactivation of ribosomes triggers the host stress-activated protein kinase signalling pathway, the p38 mitogen-activated protein kinase pathway, and the extracellular-signalling regulated kinase pathway. All of these activated host pathways are termed the ribotoxic stress response, which appears to be essential for expression of pro-inflammatory cytokines and chemokines. Tissue damage in the colon and development of HUS and CNS complications can be exacerbated by the production of the cytokines and chemokines<sup>10,46</sup>.

Renal microvascular endothelial cells are the primary target of Stx in patients who develop HUS, as these cells have a high concentration of Gb3 receptors on their surface. Additional cell types within the renal glomerulus are also targeted by Stx and adversely affected<sup>47</sup>. Endothelial cells that have undergone apoptosis detach from the basement membrane and form a thrombus, which is a repeated deposit of fibrin that narrows the capillary lumen. This leads to a reduced blood supply to the kidneys and eventually loss of kidney function<sup>13</sup>. Endothelial damage caused by Stx recruits leukocytes to the area and activates altered complement pathways, both causing additional kidney damage<sup>35</sup>. Kidney damage in STEC-infected patients can be severe and cause long-term sequelae including chronic kidney disease and Guillain-Barré syndrome<sup>48</sup>.

Shiga toxin can also target cells of the CNS and cause severe, debilitating damage. The Gb3 receptor has been detected on the neurons in the spinal cord, glial cells, and other regions of the CNS. Although few studies have investigated CNS damage in humans, mice have been used to model the infection. After infection with STEC, the mice show vascular and glial changes that block spinal motor neuron synapses and exhibit endothelial damage in multiple areas<sup>49</sup>. Lipopolysaccharide (LPS) has been implicated as a strong inducer of inflammation and exacerbates STEC-associated CNS symptoms. The action of Stx/LPS in the CNS was explored using LPS non-responder mice (C3H/HeJ) and LPS responder mice (C3H/HeN). CNS symptoms were observed when C3H/HeJ mice were inoculated with STEC, but absent when infected with non-STEC *E. coli*. Both C3H/HeJ and C3H/HeN mice displayed CNS symptoms when inoculated with STEC, but C3H/HeJ mice showed a more aggressive time course of symptoms compared to C3H/HeN mice<sup>47</sup>. Long term CNS sequelae include coma, seizures, and psychomotor retardation<sup>48</sup>.

### **1.6.3. Differences in toxicity**

Although Stx1 and Stx2 are biologically similar, more severe disease is observed in infections caused by Stx2-encoding isolates compared to infections caused by Stx1-encoding isolates or Stx1-/Stx2-encoding isolates<sup>18</sup>. This can be confirmed *in vitro* as purified Stx2 is 1,000 times more toxic when applied to human endothelial cells than Stx1<sup>34</sup>. Severity of infection can also be attributed to the Stx subtype with which a patient has been infected. Literature states that Stx1c and Stx1d are rarely implicated in human disease and, when diagnosed, are associated with mild symptoms. In contrast, Stx2d is most often observed in severe human disease, especially with patients who progress to HUS. Stx2b is mostly implicated in mild STEC infections, while Stx2e, Stx2f, and Stx2g have historically been associated with animal and bird sources<sup>35</sup>.

Shiga toxin 2 production is tightly coupled with phage induction and replication; consequently, research suggests that variations among Stx2 phages could be indirectly responsible for the observed toxicity

differences between subtypes. Phages have short generation times and can easily recombine their genetic material with other phages. This could explain why variations in toxicity are observed within the same Stx subtype and even within the same STEC serotype<sup>34</sup>. For example, isolates from one O157:H7 outbreak were shown to be lysogenized with different Stx-encoding phages. Patients infected during this outbreak exhibited symptoms with a large spectrum of severity, which was correlated to the amount of toxin produced by their specific isolate (as determined by the phage expression characteristics)<sup>36</sup>. Differences in toxicity can also be linked to the presence of defective phages that have been lysogenized into the isolate's genome. Sequence data from one study showed an O157:H7 strain EDL933 to contain only one functional Stx-2 encoding phage, but also multiple, unrelated and defective phage insertions. Increased diversity, even in highly related strains, can be created due to recombination between the phage genomes<sup>37</sup>.

#### **1.6.4. Induction and SOS response**

Unlike *S. dysenteriae*, which houses its Shiga toxin genes within its chromosome, STEC carry the Stx genes on lambdoid bacteriophages. The phages are able to travel between bacterial cells through horizontal gene transfer and once taken up by the cell, they become lysogenized into the host chromosome<sup>38</sup>. Thus the expression of *stxAB* in *E. coli* is under the control of the phage cycle, which can be induced by any of a number of stress-inducing factors such as antibiotics, environmental conditions, or other DNA-damaging agents<sup>28</sup>. It is not until the bacterial cell is placed under stress that the phage enters the lytic cycle and an increase in toxin is observed<sup>38</sup>. Production of Stx2 is entirely under the control of the phage cycle, whereas Stx1 is regulated by both the phage cycle and intracellular iron concentrations<sup>28</sup>. Low-iron conditions lead to increased amounts of Stx1 production as the *stx1* gene is under the control of the Ferric Uptake Regulator (Fur), a low iron-derepressed transcriptional regulator influencing a large number of bacterial genes that regulate metal iron uptake<sup>39</sup>. The antibiotic

mitomycin C (MMC) is a potent phage inducer and is often used *in vitro* to induce Stx-carrying prophages through the SOS response<sup>40</sup>.

The SOS response is a global stress response that allows for the repair of DNA following damage. Lysogenized phages take advantage of the bacterial SOS response to allow the expression of their genes. If certain antibiotics are administered to an STEC-infected patient, the bacterial SOS response is induced and toxin production increases, which is detrimental to the patient<sup>28</sup>. The higher concentration of circulating toxin increases the severity of infection and the likelihood of developing HUS. Studies have shown that within two to four hours of prophage induction, the toxin concentrations have increased by two to three orders of magnitude<sup>40</sup>.

The SOS response is exploited for induction of the Stx prophage and expression of Stx genes (Figure 4). In the absence of DNA-damaging agents, binding of the *cl* repressor to the right (OR) or left (OL) operator sites inhibits activity from the phage early promoters, PR or PL, respectively. This maintains the lysogenic state of the phage cycle. Upon triggering of the SOS response, RecA is produced and activated. It cleaves the *cl* repressor allowing for PR and PL to become active. Anti-terminator protein N is transcribed from PL and allows for RNA polymerase to transcribe through the PR termination signals. Anti-terminator protein Q is then transcribed from PR. The Q protein binds to PR' to activate transcription of the late phage genes, including *stxAB*. The bacterial cell is lysed and the Stx toxin is released into the gastrointestinal (GI) tract of the host<sup>28, 38</sup>. As transcription of *stx1* can be driven without phage induction under low-iron concentrations through the release of Fur-mediated repression, the Stx1 toxin can be transcribed, but remains within the bacterial cell since the late phage lysis genes are not transcribed and translated to cause bacterial cell lysis<sup>41</sup>.

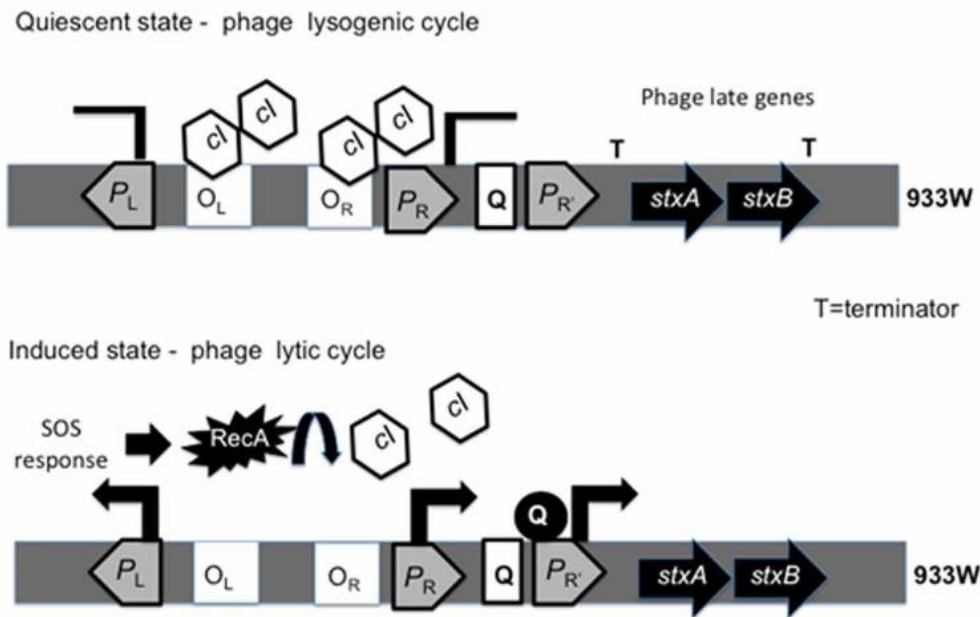


**Figure 4.** Regulation of Stx expression by the phage cycle. The above figure, from Pacheco *et al.*, shows the effect of the *cl* repressor on maintaining the lysogenic state of the phage or allowing the induction of the lytic cycle. The Stx-carrying bacteriophage is lysogenized into the bacterial chromosome and remains inactive until induction of the SOS response through DNA damage. Activation of the lytic cycle initiates transcription of the Stx genes and production of toxin. The toxin is then released into the gastrointestinal tract upon bacterial cell lysis<sup>28</sup>.

### **1.6.5. Toxin binding and transport**

Once Stx is released from the lysed bacterial cells into the host GI tract, it passes through the intestinal mucosal barrier allowing the toxin to circulate within the bloodstream before reaching its main target organ, the kidneys<sup>42</sup>. Numerous studies have attempted to determine if Stx circulates freely within the bloodstream or is cell-bound. Serum samples from HUS patients contain low amounts of Stx, indicating that the toxin may bind to yet undefined blood cells to be carried to their target<sup>43</sup>.

The preferred host binding site of Shiga toxin is globotriaosylceramide (Gb3), expressed in the kidneys, as well as some other tissues including colonic tissue. Studies have shown that glomerular microvascular endothelial cells are sensitive to sub-nanomolar concentrations of Stx in vitro due to the 50-fold higher expression of Gb3. This is in comparison to large vesicle umbilical vein endothelial cells, which are relatively resistant to Stx action owing to their low Gb3 expression<sup>43</sup>. Currently, the host function of this receptor is unknown. It is a glycosphingolipid composed of a lipid or ceramide plus a trisaccharide, called Pk trisaccharide<sup>35</sup>. These areas are also cholesterol rich, which may aid in the binding of Stx by stabilizing the Gb3 in a favourable conformation. Cholesterol-deficient cells are less efficient in the uptake of the B-pentamer<sup>44</sup>. Certain Stx subtypes are able to bind with lower affinity to globotetraosylceramide (Gb4). This receptor is derived from Gb3, but instead contains a tetrasaccharide<sup>35</sup>.

Individual host binding sites bind Stx with low affinity, therefore, recruitment of several host receptors and attachment to multiple binding sites is required. The crystal structure of Stx1 binding to Pk trisaccharide exhibits three binding sites per B-monomer for a total of 15 Pk-binding sites per B-pentamer. Although, this may differ between subtypes as Stx2a showed only two Pk-binding sites per B-pentamer. Studies comparing binding strengths and preferences among the Stx subtypes show that each subtype has a unique binding profile. Differences in toxicity can be attributed, at least in part, to the strength with which the toxin binds to the receptor. Results from a study by Karve et al. show that

subtypes exhibiting increased toxicity in humans have stronger binding affinities between the B-pentamer and Gb3, as compared to less toxic subtypes<sup>44</sup>. When considering toxin uptake, binding of the entire holotoxin results in increased toxin uptake compared to when the B-pentamer alone is bound<sup>35</sup>. It is believed that this is due to the interaction of the A subunit with other proteins at the host plasma membrane. Increasing the B subunit concentration does not affect the rate of endocytosis to the same degree as increasing the amount of intact Stx holotoxin<sup>31</sup>. In addition to binding strength, differences in Stx uptake can be attributed to preferential binding to host receptors. For example, human disease-associated Stx2a prefers to bind to Gb3, whereas swine disease-associated Stx2e prefers to bind to Gb4<sup>35, 44</sup>.

Shiga toxin is internalised from the exterior of host cells to the cytosol by an elaborate retrograde transport pathway<sup>26</sup>. Once the B-pentamer is bound to Gb3 the entire complex is endocytosed into the host cell. The protein clathrin is used to build small vesicles for transportation of molecules within cells. The toxin/receptor complex is endocytosed into the host cell within clathrin-coated pits. Evidence of clathrin-independent mechanisms is observed in some host cell types; however, the clathrin-dependent process appears to be used most commonly<sup>35</sup>. Depletion of clathrin using small interfering RNA reduced endocytosis by approximately 40% and mutations in espins (proteins required for clathrin mediated endocytosis) reduced endocytosis by 40-50%<sup>26</sup>. As well, inhibition of the enzyme Syk, which phosphorylates clathrin, results in the inhibition of Stx uptake in multiple cell lines<sup>31</sup>. Clathrin-independent pathways must be responsible for a portion of Stx uptake, as interfering with clathrin does not completely inhibit uptake. The overall understanding of clathrin-independent mechanisms is limited. Currently two pathways have been proposed; one requires dynamin while the other does not. As well, it is believed that actin-based endocytic processes such as micropinocytosis and phagocytosis may play a role in Stx toxin uptake<sup>26</sup>.

Once the Stx toxin/receptor complex has been endocytosed, the toxin is transported to the sorting endosomes and then onto the Golgi apparatus. Direct transport from the sorting endosome to the Golgi is important as continuing transport to late endosomes and lysosomes leads to proteolytic damage of the toxin<sup>26</sup>. This toxin transport process is quite complex and not completely understood at this time. Researchers have determined that the type of glycolipid surrounding the Stx toxin is crucial, as lipid rafts are used for transportation. Studies have concluded that transportation of Stx from the endosome to the Golgi is lost when glycosphingolipid synthesis is prevented<sup>31</sup>. As well, a large array of host factors are involved in fusion with the trans Golgi network once the toxin has reached the Golgi<sup>26</sup>.

Multiple mechanisms are employed to transport Stx from the Golgi apparatus to the endoplasmic reticulum (ER). The process is complicated and not well understood. Research within this area is difficult as genetic knockout or knockdown of elements involved with the transport can also affect movement of Stx from the endosome to the Golgi. One theory indicates that movement to the ER is dependent on the expression of a GDP-restricted dominant-negative variant of Rab6 GTPase known as Rab6a'<sup>26</sup>. As well, studies have not been able to determine if the Stx toxin is transported through the entire cisternae of the Golgi or if it is able to bypass certain areas on its way to the ER<sup>31</sup>.

It is believed that cleavage of the Stx A subunit occurs in either the endosome or the Golgi but separation of the two A portions does not occur until the toxin reaches the ER. Host furin is required for cleavage of the A subunit and the two resulting portions are held together by a disulfide bond until it reaches the ER. The A subunit contains a furin cleavage-site (RXXR) between the A<sub>1</sub> and A<sub>2</sub> portions. The RXXR motif, in addition to the structure at the site, is important for recognition and processing at the cleavage site<sup>31</sup>. The mechanism for reducing the disulfide bond in Stx is unknown. The AB<sub>5</sub> cholera toxin uses a disulfide isomerase, which binds and unfolds A<sub>1</sub> to release the A<sub>2</sub> portion. The sec61 translocon is used to move the A<sub>1</sub> portion across the membrane and into the host cell cytosol<sup>26</sup>.

## **1.7. Symptoms**

The most severe STEC infections generally are diagnosed in children under five years of age and in elderly or immunocompromised patients<sup>1</sup>. Symptoms include watery diarrhea with abdominal cramping at three to four days post infection. In approximately 90% of cases, the watery diarrhea will become bloody at five to six days post infection. Five to 13 days after the onset of bloody diarrhea, approximately 5-15% of patients will develop HUS, presenting as thrombocytopenia and microangiopathic hemolytic anemia with possible renal failure<sup>13</sup>. Studies have been unable to determine the exact mechanism behind the development of HUS, but evidence points to a genetic predisposition in the patient, including complement gene mutations that can lead to a poorer patient outcome<sup>12</sup>. The majority of HUS cases requiring extended hospitalization are due to O157:H7 infection, but less severe HUS can also develop from infection due to non-O157 serotypes<sup>13</sup>. Patients infected with Stx2-producing isolates are more likely to progress to HUS as the production of pro-inflammatory molecules is more efficient when induced by Stx2<sup>50</sup>.

## **1.8. Treatment of STEC infections**

Antibiotics are contraindicated for treatment of STEC infections as they are able to induce the Shiga toxin-carrying prophage into the lytic cycle and increase the production of Stx toxin<sup>1, 12, 51</sup>. This increase in toxin has been linked to worsened clinical outcome and an increase in the progression of HUS in children. Consequently, the most effective treatment option is early and targeted diagnosis, coupled with supportive care with fluid resuscitation, peritoneal dialysis, and plasma exchange. The prognosis for patients treated with supportive care is excellent and the use of intravenous fluids can reduce the risk of renal failure and other long term sequelae<sup>1</sup>.

Mortality rates for STEC-infected patients is low (approximately 250 deaths per year in North America), but long-term complications can be observed especially in those with HUS. Eight years after the

Walkerton, Ontario outbreak, 15.4% of infected individuals experienced irritable bowel syndrome and dyspepsia<sup>1</sup>. It is hypothesized that long-term complications are attributed to a sustained alteration in the gut flora. Other complications include hypertension and cardiovascular disease, diabetes, and reactive arthritis. In patients with CNS damage, coma, seizures, cortical blindness, and psychomotor retardation can occur. The complications experienced post-infection tend to be more debilitating than those of the acute infection<sup>48</sup>.

### **1.8.1. Novel treatment options**

Supportive care is not so much a treatment of STEC infection, but a management of the associated symptoms. It does not counteract the effects of the Stx toxin nor prevent subsequent disease progression. Pacheco *et al.* describe two novel therapies for the direct treatment of the toxin. One approach inhibits bacterial cells from interacting with their environment through a reduction in quorum sensing. The goal is to diminish the bacterial cells ability to colonize the host. LED209, a small therapeutic molecule that targets the adrenergic sensor QseC in STEC isolates, is able to inhibit the induction of the bacterial SOS response and decrease *stx2* expression<sup>28</sup>. Another approach requires the use of Stx-mimicking ligands, which act as competitive inhibitors. The ligands bind to Gb3 on host endothelial cell surfaces preventing the receptors from binding Stx. An alternative to this approach would be to create a compound that mimics the Gb3 receptor trisaccharide; such a compound would bind Stx in the blood, preventing it from binding to endothelial Gb3<sup>28</sup>.

### **1.8.2. STEC prevention strategies**

Vaccine candidates have long been studied but none are commercially available. Current vaccine studies are looking to increase antibody levels, especially in children who are most at risk for development of HUS<sup>28</sup>. An article by Page *et al.* describes multiple methods to avoid STEC infection. As STEC are spread through the fecal-oral route, all meats should be properly cooked and cross-contamination between

uncooked meat and raw food is to be avoided. Unpasteurized food such as fresh pressed apple juice and raw milk should also be avoided, especially in small children. The most effective practice to avoid STEC contact from the environment is to engage in proper hand washing after using the washroom, before consuming foods, and after being in contact with animals as they can be asymptomatic carriers. Within hospitals, infected patients should be isolated in single-bed rooms and anyone in contact with the patient should wear appropriate person protection equipment. Patients no longer experiencing acute symptoms should avoid settings with a high risk of transmission as long-term asymptomatic shedding has been reported for up to seven months post-infection<sup>52</sup>.

### **1.9. Current diagnostic methods**

Hospital-based, clinical detection of pathogens focuses on methods that are efficient and economical, while maintaining sensitivity and specificity. The goal is to report the required information to clinicians in the shortest amount of time. This is in contrast to diagnostics and reference services performed at provincial and federal public health laboratories where in-depth characterization using complex testing is completed more as a reference for the purpose of achieving accurate molecular subtyping for public health surveillance. The use of complex and time-consuming assays provide additional phylogenetic information on the isolate. If samples require such testing, delays in diagnosis can be detrimental to the patient. STEC-infected patients present to healthcare facilities with a broad range of common, but non-specific, GI symptoms. Differentiation between STEC and other enteric pathogens is crucial to ensure that antibiotics are not administered, as this can lead to the progression of HUS and long-term complications, owing to induced Stx toxin production. Fast and efficient diagnostics are essential to prevent patient morbidity and mortality<sup>51</sup>.

To distinguish STEC from other pathogenic *E. coli* pathotypes and enteric bacteria, the Stx protein or *stx* genes must be detected. Below are highlights of the most common diagnostic assays used in clinical,

provincial, and federal government laboratories to confirm STEC infections and isolates. Ideal assays detect the presence of the Stx toxin genes or proteins. Detecting serotypes that have historically been linked to Stx production is ineffective as horizontal gene transfer allows for the ready gain or loss of Stx genes within an STEC population. Unfortunately, due to resource shortages, some clinical laboratories are only able to perform a limited number of assays<sup>53</sup>.

### **1.9.1. Culture**

Identification of O157 STEC by culturing is relatively simple, inexpensive, and widely performed in clinical laboratories. It has been estimated that the cost for culturing, including consumable materials and labour, is approximately \$1 per sample. In comparison, the cost to perform an enzyme immunoassay is approximately \$15 per sample<sup>54</sup>. Culturing requires multiple differential media formulations to distinguish O157 STEC from non-O157 STEC isolates, other pathogenic *E. coli* strains, and commensal intestinal flora. Selective and chromogenic media, described below, exploit externally visible phenotypic differences between STEC isolates<sup>55</sup>.

Sorbitol MacConkey (SMAC) agar contains sorbitol as the carbon source, in comparison to standard MacConkey agar, which contains lactose. O157 STEC is unable to ferment sorbitol, producing colourless colonies on SMAC agar; whereas sorbitol fermenting bacteria produce pink colonies. Other non-sorbitol fermenting bacteria exist, yielding colourless colonies and allow for false-positive identification. Cefixime tellurite sorbitol MacConkey (CT-SMAC) agar is often used to improve sensitivity and reduce false-positive results. The addition of cefixime inhibits growth of *Proteus mirabilis* and tellurite inhibits growth of non-O157 STEC and other bacterial species. Bile salts and crystal violet are also added to inhibit the growth of Gram-positive organisms<sup>56</sup>. One disadvantage to using CT-SMAC is its inability to detect sorbitol-fermenting O157:H- isolates. When culture-exclusive methods are performed, these isolates are

often overlooked. This leads to inaccurate diagnostics and an underestimation of the prevalence of this serotype<sup>57</sup>.

Chromogenic agars for detection of O157 STEC are commercially available. CHROMagar O157 is widely used in clinical laboratories to distinguish between O157 and non-O157 isolates. The chromogenic substrate, which, when hydrolyzed by a specific enzyme, will produce insoluble colour. O157 colonies appear mauve, while non-O157 colonies appear blue. As with CT-SMAC, the agar is supplemented with cefixime and tellurite to prevent growth of non-*E. coli* species<sup>58</sup>. Similar to CHROMagar O157, Rainbow® Agar O157 can be used to aid in detection of STEC isolates. This agar is able to distinguish between four different STEC serotypes (O157, O26, O48, and O111) based on the presence of two *E. coli*-associated enzymes:  $\beta$ -galactosidase and  $\beta$ -glucuronidase. The resulting colonies range in colour, which allows for differentiation between the four above mentioned serotypes<sup>116</sup>.

Confirmatory testing is required no matter which type of agar has been used<sup>59</sup> and adds additional labour and cost to the testing. After the specified growth time, a well-isolated colony from the surface of the media is tested with O157-specific antiserum or O157 latex agglutination reagent. Up to three colonies should be analyzed. Isolates with presence of agglutination with one of the O157-specific reagents, but absence of agglutination with normal serum or control latex, are presumed to be O157 STEC<sup>60</sup>. Other bacterial species are able to cross-react with O157 antiserum; therefore, O157 colonies should be biochemically confirmed. Only after a STEC colony has been isolated, found to agglutinate with the O157 latex reagent, and been biochemically confirmed can a patient sample be deemed 'confirmed' as STEC positive<sup>61</sup>.

Epidemiological data exhibits a surge in STEC infections caused by non-O157 serotypes in the past few decades. The "Big 6" (serotypes O26, O45, O103, O111, O121, and O145) are the most common non-O157 serotypes implicated in human infection<sup>62</sup>. No specific media formulations yet exist for the

detection of non-O157 serotypes. A study by Kase *et al.* compared eight different culture media to determine which is most appropriate for detection of non-O157 isolates. They concluded that selectivity must be balanced; media that is too selective allows for false-negatives, while media that is not selective enough allows for growth of unwanted bacterial species. The authors recommend the simultaneous use of a combination of media to increase the likelihood of recovering non-O157 STEC<sup>62</sup>. The US CDC recommends a less selective media such as SMAC for non-O157 identification. As these isolates are usually able to ferment both lactose and sorbitol, well-isolated colonies with these characteristics should be selected. Further confirmation using O-specific antisera for the Big 6 serotypes or molecular methods such as polymerase chain reaction (PCR) and enzyme immunoassays should be performed. Isolates should be forwarded to local public health laboratories for further characterization<sup>59</sup>.

### **1.9.2. Molecular and antibody-based assays**

A rise in the incidence of non-O157 STEC has been reported<sup>6,9</sup>. This, in part, could be attributed to the introduction of non-culture assays for STEC detection as they do not rely on the use of differential or selective media<sup>9</sup>. Increased sensitivity and selectivity is associated with molecular and antibody-based assays, which generally are less laborious. Although not all of these assays require culturing of the bacterial isolate, the US CDC recommends simultaneous culture of all stool samples to allow for forwarding of the isolate to public health laboratories for further characterization or identification<sup>59</sup>, with Canada currently working on similar guidelines. Further characterization at reference laboratories may have little impact on patient care, but the information is necessary and critical for rapid outbreak detection and interventions to prevent more cases<sup>63</sup>. The assays described below can be used for both clinical detection and reference laboratory studies.

### **1.9.2.1. Vero cell assay**

Cell cytotoxicity assays are considered the gold standard for Shiga toxin detection. Vero cells, recovered from the African green monkey kidney (*Chlorocebus* sp.), are susceptible to Shiga toxin as they contain a high concentration of Gb3 and Gb4 receptors on the cell surface<sup>63</sup>. Vero cells are treated with filter-sterilized bacterial culture supernatants and examined for detachment, flocculation, rounding, and cytoplasmic granulation 48 to 72 hours post infection<sup>64</sup>. Other toxins are able to affect Vero cells in a similar fashion; therefore, antibody neutralization is required for confirmation. The antibody-dependent neutralization assay is also able to determine if the isolate is carrying Stx1, Stx2, or both<sup>63</sup>.

Cell cytotoxicity assays are known for their sensitivity (can reliably detect Stx at one colony forming unit (cfu) per 100), but are also time consuming, labour intensive, and require the knowledge of a trained technician for tissue culture. As well, the sensitivity of the VCA is affected by the cfu of STEC within the sample. As infection progresses, the cfu decreases making toxin detection from stool samples increasingly difficult<sup>63</sup>.

### **1.9.2.2. Enzyme immunoassays**

Enzyme immunoassays (EIAs) require the use of Stx-specific antibodies for detection. Currently, four Food and Drug Administration (FDA)-approved EIAs are commercially available ranging in format, target (Stx1, Stx2, or both), time required to perform, which specimen type they handle, and sensitivity and specificity. Most EIAs produce reportable results within 24 hours, compared to 72 hours for the VCA<sup>59</sup>.

There are currently two FDA-approved microplate EIAs; Premier<sup>®</sup> EHEC (Meridian Diagnostics, Cincinnati, Ohio) and ProSpecT<sup>™</sup> Shiga Toxin *E. coli* Microplate Assay (Remel, Lenexa, Kansas). Hands-on work for these assays can be completed within three to three and a half hours. Microplate EIAs use monoclonal or affinity-purified polyclonal antibodies coated on the bottom of 96-well plates. The antibodies are incubated with culture and if present, the Stx toxin binds to the antibody. In the Premier<sup>®</sup>

EHEC assay, bound toxin is detected with a second Stx-specific antibody and then by an appropriate anti-IgG-enzyme conjugate. The ProSpect™ assay does not use the second Stx-specific antibody and instead only applies the anti-IgG-enzyme conjugate. A substrate for the enzyme is added and, in the presence of Shiga toxin, a coloured reaction product will develop. In the absence of Stx no coloured reaction product will develop. Results can be read by a spectrophotometer or by the naked eye and compared with the positive and negative controls. Although these microplate assays are able to detect both Stx1 and Stx2, neither is able to differentiate between them<sup>65, 66</sup>.

Comparison of sensitivities between EIAs and other clinical diagnostic methods have been performed. Results show them to be as sensitive as the VCA without requiring cell culture expertise<sup>63</sup>. A study by Vallières et al. compared the performance of the Premier® EHEC EIA, an in-house PCR assay, and SMAC media using 21 confirmed STEC isolates. All 21 isolates were detected using PCR, while only six and five were detected using EIA and SMAC, respectively<sup>67</sup>. Schindler et al. compared the sensitivities of SMAC culture and EIA using 100 confirmed STEC isolates. They were able to identify 88% of O157 isolates using SMAC and EIA in combination, 9% by SMAC alone, and 3% by EIA alone. All non-O157 STEC isolates were detected using EIA alone<sup>54</sup>. Recommendations from both studies indicate culturing, in addition to at least one non-culture assay, must be performed on all stool samples, as neither alone is considered adequate<sup>54, 67</sup>.

In contrast to microplate EIAs, the Immunocard STAT!® EHEC (Meridian Diagnostics, Cincinnati, Ohio) and the Duopath® Verotoxins Gold-Labelled Immunosorbent Assay (GLISA) (Merck, Germany) are FDA-approved lateral flow immunoassays (LFIs). The advantage of these assays is their ability to differentiate between Stx1 and Stx2. They can be completed in only 20 minutes, but neither is able to test directly from stool. Both are immunochromatographic assays that use monoclonal antibodies labelled with red-coloured gold particles. Culture is applied to a circular port lined with chromatography paper and the

sample is absorbed through the reaction zone where it comes in contact with the gold-labelled Stx-specific antibodies. If toxin is present, an antibody-protein complex will form and travel through to the reaction zone until it comes into contact with the binding zones. The binding zones contain either Stx1- or Stx2-specific antibodies that immobilize the complex. A red line will appear in the binding zones of Stx-positive samples. A red line will always appear in the positive control zone<sup>68, 69</sup>. The US CDC reports a sensitivity and specificity for the Immunocard STAT!<sup>®</sup> EHEC of 92% and 100%, respectively. The Duopath<sup>®</sup> Verotoxins GLISA has a sensitivity of 100% for Stx1 and 99% for Stx2 and a specificity of 98% for Stx1 and 97% for Stx2<sup>59</sup>.

Park et al. compared the sensitivity of the Duopath<sup>®</sup> Verotoxins GLISA to the Premier EHEC assay using 41 STEC-positive samples. Both assays were reported to have a sensitivity of 100% and were able to positively identify all 41 samples<sup>70</sup>. Feng et al. compared the ability of these assays to detect a range of STEC subtypes. They determined that the Immunocard STAT!<sup>®</sup> was unable to detect Stx2b, Stx2c, Stx2e, Stx2f and Stx2g, while the Premier<sup>®</sup> EHEC and the ProSpecT<sup>™</sup> assays were unable to detect those subtypes in addition to Stx1c. Stx2a and Stx2d are most often associated with severe cases of STEC infection. Although both assays were able to detect those subtypes, it is important to have a diagnostic assay capable of detecting all subtypes as any can be implicated in human or animal outbreaks. For example, Stx2c was implicated in a severe human O157:H7 STEC disease outbreak caused by spinach in 2006. These isolates would not have been detected using the above assays<sup>71</sup>.

### **1.9.2.3. Polymerase chain reaction**

Polymerase chain reaction is used to detect the presence of the Shiga toxin genes, *stx1* and *stx2*. Sequencing of STEC genomes has allowed for the development of primers to amplify *stxAB* for Stx1 and Stx2<sup>63</sup>. A number of different PCR assays exist with most laboratories using in-house made primers and custom thermocycler programs. The most commonly used assays are conventional PCR and real-time

PCR. A small number of commercial PCR kits are available, but none are FDA-approved as of yet. For this reason, laboratories in the United States rarely use PCR as a confirmatory test for STEC diagnostics<sup>59</sup>.

Both conventional and real-time PCR involve DNA extraction from enriched stool samples or culture. The DNA template is combined with a mastermix of primers, DNA polymerase, and other required reagents. Samples analyzed by conventional PCR are placed in a thermocycler and exposed to a program of temperature changes. The amplified PCR products are then visualized on an agarose gel. In contrast, real-time PCR allows for monitoring of the reaction in real time. As samples are being cycled through the thermocycler program, a fluorescent signal is generated for the target amplicon and is recorded<sup>72</sup>. Assays can combine multiple primer sets for amplification of *stx1* and *stx2* in multiplex reactions or can use a single primer set for amplification of a consensus sequence<sup>59</sup>.

Chui *et al.* evaluated and compared four real-time PCR assays to a conventional assay to determine their effectiveness at detecting *stx1* and *stx2*. Analysis included O157 and non-O157 samples, either from enriched stool samples or culture. For enriched stool samples, two of the real-time PCR assays exhibited 100% sensitivity for *stx1* and *stx2*, while the conventional assay and other two real-time assays exhibited sensitivities below 100%. Using cultures, 100% sensitivity was observed for conventional PCR and two of the four real-time PCR assays, while one real-time assay exhibited 100% sensitivity for *stx2* but not *stx1*. Conventional PCR is more economical, but visualization of the amplified sequences on an agarose gel requires additional time. The real-time PCR assays varied in their time and cost requirements and after considerations of cost, turn-around time, and assay performance, the TaqMan™ real-time PCR assay was determined to be superior<sup>73</sup>.

### **1.9.3. Limitations of current diagnostic methods**

The multiple methods mentioned above are used throughout clinical and reference laboratories for detection of Stx, but there is no single assay that can provide sensitive, specific, low-cost, and time effective detection.

To summarize, culturing of bacterial species is a low-cost method of detecting bacterial isolates that produce Stx. A few different chromogenic media have been created to distinguish STEC from non-STEC isolates, but the specificity is still low, especially when trying to detect non-O157 STEC. To reduce the need for culturing, molecular and antibody-based assays have been developed, all with their own advantages and disadvantages. The VCA is a highly sensitive assay, but requires cell culture knowledge and is time-consuming. PCR is a time and cost-effective assay that is used to detect Stx genes and when combined with Sanger sequencing can provide molecular subtype information. An issue with detection of genes is that it does not imply the presence of the translated (expressed) protein. With PCR, one cannot assume that the protein has been translated from the gene that is present. Lastly, EIAs are an antibody-based detection method. Due to the fact that they require antibodies, cross-reactivity or non-specific binding can produce unreliable results. As well, antibodies to newly emerging subtypes require lengthy development time.

Using targeted proteomics, our goal is to improve upon the downfalls of techniques that are currently used for Stx detection. We believe that a mass spectrometry-based method would be equally sensitive, or have increased sensitivity, while reducing turnaround time and cost associated with testing. We are initially aiming towards detection from culture, but the long-term goal is to detect Stx directly from the specimen (stool).

## 1.10. Mass spectrometry for proteomic-based diagnostics

Proteomics can be described as the large-scale study of the structure and function of proteins. Mass spectrometry (MS) is a widely used technology in proteomics for the detection and quantitation of proteins<sup>74</sup>. Proteomics is complementary to the study of genomics and transcriptomics, but unlike an organism's genome, which is fairly constant, the proteome is dynamic between cell types, time points, and physiological situations<sup>75</sup> and, thus, more accurately represents the phenotype of the organism.

Prior to MS, Western immunoblots were the primary method used for identification and quantitation of proteins. Western blots require antibodies for detection of proteins that have been transferred from a gel to a membrane. They cannot distinguish between highly related homologues, do not provide reliable quantitation, and have limited dynamic range<sup>76</sup>.

As mass spectrometry technology has improved, it has begun to replace the use of Western blots. The popularity of MS and its applications in proteomics has rapidly grown within the past few decades. Originally, MS was a tool used in analytical chemistry of small molecules, but as the technology has improved, especially with the invention of "soft-ionization" methods such as matrix-assisted laser-desorption/ionization (MALDI) and electrospray ionization (ESI) in the late 1990's, so has its ability to identify increasingly complex biomolecules<sup>77</sup>. Mass spectrometry can be used to systematically characterize differences in protein structure and function. It allows for comparison of protein expression levels between samples under varying biological conditions. This information is essential for the understanding of protein regulatory pathways and a general knowledge of how cells work<sup>78</sup>.

Multiple types of MS systems exist and are used in many different applications, but all mass spectrometers have three basic components: an ion source that ionizes the molecular sample under analysis; a mass analyzer that separates ions based on their mass-to-charge ratio ( $m/z$ ) using electric or

magnetic fields, and a detector that provides a signal for relative abundance of ions present in the sample<sup>79</sup>.

Today, numerous MS systems and methods exist that have different proteomic applications within clinical and research laboratories. For example, shotgun proteomics methods are currently mainly used for research for the proteome-wide identification and characterization of proteins within a sample and are the link for identifying the relationship between genomics and proteomics. Shotgun proteomics enable sequence analysis of tryptic peptides (peptides acquired from the digestion of proteins with the enzyme trypsin) and provides a snapshot of the detectable proteins within a sample<sup>80</sup>.

Another example of an MS method is matrix-assisted laser-desorption/ionisation-time-of-flight mass spectrometry (MALDI-TOF MS), which is currently being used in clinical laboratories for whole-cell protein analysis for rapid identification of bacteria and other microorganisms. MALDI of undigested protein from cell lysate of an unknown microbe produces a unique TOF MS spectrum that can be compared to commercial or custom spectral libraries to identify the species or genus. This method is efficient and relatively inexpensive per sample, and it has been accepted by many diagnostic labs as the new gold-standard for clinical bacterial identification<sup>81</sup>. Currently, this whole-cell analysis method does not have the sensitivity required to detect lower abundance proteins, such as Stx from non-induced STEC strains and, therefore, is not feasible for Stx detection directly from clinical samples. As well, MALDI-TOF MS is not yet used for reliable antibiotic susceptibility testing<sup>81</sup> nor does it have the resolution to determine any isolates molecular subtype based on very small amino acid differences.

A third example of MS proteomic-based methods, which are more recently growing in interest, can be referred to as targeted proteomics. These methods target a small subset of proteins that are of interest. This can be accomplished using either triple quadrupole mass spectrometry (QqQ MS) using selected reaction monitoring mode (SRM) or quadrupole-orbitrap mass spectrometry (Qq-OT MS/MS) using

parallel reaction monitoring mode (PRM). These instruments are able to detect the presence of constituent peptides following proteolytic digestion. By focusing analysis on the peptides of interest, these mass spectrometers offer higher sensitivity and specificity and are able to process an increased number of samples<sup>76</sup>.

### **1.10.1. Targeted proteomics**

Targeted proteomic methods have become increasingly popular within the last few decades for both research within the proteomics field and clinical applications including assay development and clinical detection methods<sup>82</sup>. A small number of targeted assays have been developed for detection of pathogenic bacteria and viruses from a number of biological matrices such as plasma, urine, and cell lysate<sup>82</sup>. A PubMed search of “targeted proteomics” reveals a large increase in publications on the subject over the past few decades with less than 10 per year reported in the late 1990’s to almost 660 publications in 2015.

Targeted methods are based upon information initially acquired through discovery-based experiments, such as shotgun proteomics. Discovery experiments provide information such as protein identity and amino acid sequence, retention time, and  $m/z$  values. Once the discovery stage of the experimental workflow has determined the targeted proteins of interest, detectable peptides from the proteins (i.e., tryptic peptides) are selected to act as surrogates for the expressed intact proteins. The peptides have specific  $m/z$  and retention time windows, allowing methodology to be created for their specific detection<sup>83</sup>.

The most commonly used mass spectrometry systems for targeted proteomics are QqQ MS and Qq-OT MS/MS. The QqQ MS contains three quadrupoles, sometimes found in a horseshoe arrangement. Targeted proteomics using SRM with QqQ MS is carried out as follows: ionized sample enters the first quadrupole (Q1) where a target, predefined precursor ion ( $m/z$ ) is selected. The selected precursor ion

enters the second quadrupole (Q2) where it is fragmented. The fragments enter the third quadrupole (Q3) and only select, predefined fragments are then transmitted to the detector (Figure 5A). In contrast to QqQ MS, Qq-OT MS/MS systems, like the one used for this thesis (Figure 6A), contains one quadrupole, a higher-energy collision dissociation (HCD) cell (referred to as Q2 in Figure 5B), and an Orbitrap analyzer. Ionized sample enters the quadrupole where a predefined precursor ion is selected and is then transferred to the HCD cell via the C-trap. The ions are fragmented within the HCD cell and fragment ions are transferred to the Orbitrap mass analyzer via the C-trap for analysis (Figure 6B)<sup>83</sup>.

A comparative analysis between the Qq-OT MS/MS and the QqQ MS systems was performed by Peterson *et al.* using 25 isotopically heavy-labelled synthetic peptides spanning a large concentration range. The authors concluded that PRM was able to quantitate data over a wider dynamic range when compared to SRM. This is especially important when working with biological samples as they tend to be complex matrices with large dynamic ranges<sup>84</sup>. A large-scale metabolomics PRM assay was developed by Zhou *et al.* monitoring 237 metabolites. The authors claim that their PRM assay was more reproducible and was able to provide more accurate quantitation than when just measuring the precursor ions in data-dependent mode. As well, the PRM approach is less time-consuming than a SRM assay as all of the fragment ions are simultaneously monitored without having to pre-select them in the development stage<sup>82</sup>.

## PRM and SRM Targeted Approaches

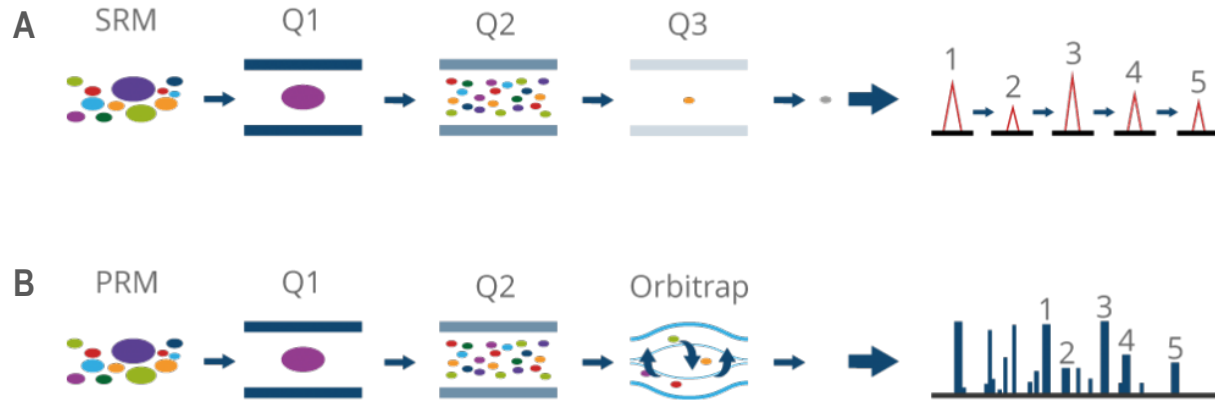


**Figure 5.** Comparing SRM and PRM targeted proteomics. SRM (A) used three quadrupoles for target detection, while PRM (B) uses two quadrupoles (the second being a HCD cell) and an Orbitrap mass analyzer<sup>113</sup>. Once discovery experiments have been completed and the targets are known, SRM or PRM methodologies can be used to detect those targets within complex matrices, such as bacterial cell components and biological fluids. Both methods allow for detection and quantitation of the targets, each with their own advantages and disadvantages<sup>113</sup> (Figure adapted from Titz *et al.*).

A



B

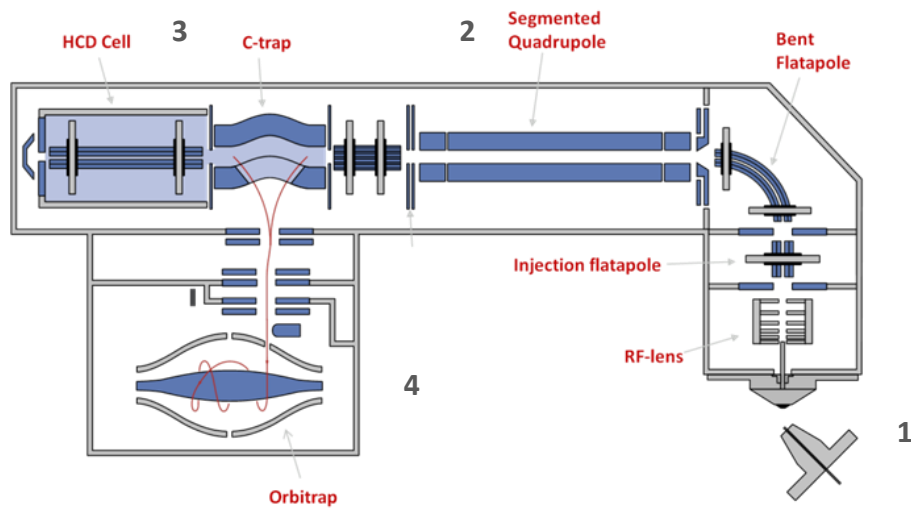


**Figure 6.** QExactive™ Plus (QE+) Hybrid Quadrupole-Orbitrap™ mass spectrometer. (A) The QE+ system used in the Mass Spectrometry and Proteomics Core Facility at the National Microbiology Laboratory (Winnipeg, Canada) for PRM analysis. (B) A schematic of the interior of the mass spectrometer. Sample is injected into the mass spectrometer (1) and ionized. Predefined precursor ions are selected (2) and fragmented (3). Fragment ions are then transferred to the Orbitrap for analysis (4).

(source: <http://planetorbitrap.com/q-exactive-plus#tab:schematic>)

During the development stage of a new targeted assay, a general accepted workflow is followed to ensure the mass spectrometer is tuned to detect the peptides of interest. The multiple development steps and optimizations provide the final assay with its increased sensitivity and specificity compared to other methods. The workflow, as described by Gallien *et al.*, includes determining the target proteins of interest and performing an *in silico* digestion to determine which potential target peptides exist for each expressed target protein. Peptides, which are used as proxy surrogates for the expressed protein, are then chosen for further analysis based on a specific set of criteria<sup>86</sup>. Fusaro *et al.* describe some features of good candidate peptides. For example, the peptides should provide the best signal when analyzed by MS and should be “proteotypic” (unique to the target protein). As well, the peptides chosen should have varied LC retention times, as peptides that are eluted around the same time could provide poor or confounded signals, and they should avoid including amino acids cysteine or methionine, as these amino acids are prone to oxidation<sup>85</sup>. Once the MS system has been optimized for detection of the target peptides, validation of the assay is completed using previously characterized samples<sup>86</sup>.

PRM and SRM methods provide high discriminatory power, allowing for sensitive and specific detection of disease and infection biomarkers. Development of targeted MS assays generally requires relatively short development time. Classical approaches, usually employing antibodies, typically require more time and cost to develop. Mass spectrometry-based assays tend to require less development time and use low-cost reagents, allowing for faster implementation and accessibility to a larger number of laboratories provided capital instrumentation is available<sup>87</sup>. As well, cross-reactivity remains an issue in the development of immunoassays and hinders the ability of these assays to be multiplexed. In contrast, MS-based assays can be highly multiplexed, which also reduces time and cost restraints<sup>87, 88</sup>.

Although SRM and PRM methods are similar, advantages and disadvantages exist. An SRM experiment monitors the precursor/product ion pairs that are mass filtered in Q1 and Q3, respectively. These pairs

are referred to as transitions. The monitoring of specific transitions provides high reproducibility and sensitivity. The analysis and identification of a peptide is dependent on the three to five most intense transitions<sup>84</sup>. To determine the best transitions, the method requires multiple iterations and optimizations, which could prolong the development stage<sup>83</sup>. Although it may require additional development time, the subsequent tuning of the mass spectrometer to the specific transitions does allow for the increased sensitivity seen in SRM assays relative to PRM<sup>84</sup>.

In contrast, PRM is able to co-detect all transitions at higher resolution and distinguish them from one another during the final mass analysis stage. This eliminates the need for prior knowledge of the target transitions and the multiple rounds of transition optimization, reducing assay development time. As well, the co-detection of all transitions increases specificity as there is an increased number of transitions to confirm the peptide identity, not just three to five as there is in SRM assays. This is especially important when analyzing sample in complex matrices since a large dynamic range could affect the mass spectrometers ability to detect the target analyte in high background. Another advantage to PRM is its ability to separate ions with similar  $m/z$  values through the use of the high resolution orbitrap, allowing for the assay to exhibit increased selectivity, especially in complex matrices. One disadvantage of a PRM assay is the reduction in sensitivity compared to SRM as the method has not been optimized to the same extent. Although this can be an issue in detecting lower abundant peptides, studies have shown that the increased specificity and selectivity can compensate for the reduced sensitivity<sup>84</sup>.

In summary, with the high risk of distribution within crucial food commodities, increasing prevalence of infections globally, and the severe long-term implications of infection, STEC continues to be a global public health concern. New means for rapid pathogen detection, identification and pathogen subtyping are of utmost importance to obtain a positive patient outcome. We find ourselves in a new 'omics era

where the advancement of high technology promises to accomplish this goal for the sake of public health.

## 2. Objectives

### 2.1. Objective 1: Stx induction optimization/characterization

The genes encoding Stx1 and Stx2 proteins are carried on lambdoid bacteriophages. Although spontaneous induction of the Stx-carrying phage produces a small amount of Stx, the concentration has been shown to be too low to detect using current MS technology without some form of enrichment, such as antibody-based affinity enrichment<sup>89</sup>. Studies with  $\lambda$  lysogens have shown that addition of agents that cause DNA damage (such as antibiotics or UV light) result in a sharp decrease in the cellular concentration of functional CI repressor resulting in temperate phage induction and increased Stx production *in vitro*<sup>89</sup>. Mitomycin C, a potent phage inducer, has been employed extensively in research studies to produce detectable amounts of toxin in STEC cultures. Although it is well known that MMC is able to actively induce Stx-carrying prophages, the exact time points in which the toxin becomes optimally detectable using MS has yet to be elucidated. A timeline providing the relative concentrations of Stx in STEC cultures is necessary to determine the shortest induction time in which toxin is produced in detectable amounts. By determining this optimal Stx expression time point, we can aim to create the most efficient induction procedure.

The first goal of this study was to measure relative toxin levels using a shotgun proteomics approach. The bacterial cultures of two serotypically distinct isolates (O157:H7 and O26:H11) were subjected to MMC induction over increasing amounts of time to determine if Stx concentrations increase as induction time increases. As well, previous in-house experiments failed to detect Stx toxin when analyzing only the cell pellet, which led us to believe that the toxin may be released into the culture supernatant. To compare relative Stx levels in order to infer an optimal induction time and sample fraction necessary to obtain detectable Shiga toxin expression levels, nano-flow liquid chromatography-tandem mass spectrometry (nLC/MS/MS) instrumentation and isobaric tag for relative and absolute

quantitation (iTRAQ®) methodology was applied. It was hypothesized that after induction with MMC, Stx would be released from the lysed bacterial cells into the culture supernatant at increasing concentrations compared to a non-induced control. As well, it was hypothesized that as duration of induction is lengthened, so too would the relative concentration of detectable toxin.

## **2.2. Objective 2: Evaluate PRM for Stx 1 & 2 detection from culture**

Patients infected with STEC can present to healthcare facilities with a broad range of common symptoms of GI infection. Previous research has shown that the administration of certain DNA-damaging antibiotics can induce the bacteriophage lytic cycle, increasing toxin production and causing increased damage to multiple organ systems of the human host. Patients who have been treated with antibiotics have higher incidences of HUS and can experience more severe long term consequences of infection<sup>1, 12, 51</sup>. To prevent the prescription of a broad-spectrum antibiotic, early and rapid detection of Shiga toxin from clinical specimens is of utmost importance. A variety of different methods for detection of Shiga toxin within clinical samples are currently available, each with their advantages and disadvantages, as laid out above in the introductory chapter.

The second goal of this project aimed to develop a single MS-based assay capable of detecting Shiga toxin 1 and 2 from clinical isolate cultures using targeted proteomics on a Qq-OT MS/MS mass spectrometer in PRM mode. The development of this assay is possible through multiple stages of method refinement that allow the Qq-OT MS/MS to detect unique peptides of the Stx protein. The optimal induction timeline, determined through shotgun proteomics in Objective 1, provides a robust sample preparation method to ensure that sufficient Stx peptides are available for detection. It was hypothesized that the development of a single assay for detection of unique Stx peptides using the Qq-OT MS/MS in PRM mode would allow for sensitive and specific detection of Shiga toxin. The goal of the detection assay is to not only provide a method that detects Stx with high sensitivity and specificity, but

also decreases the time and cost associated with performing STEC diagnostics. As well, it was hypothesized that the unique peptide pattern observed between subtypes of Stx2 would serve as a fingerprint allowing subsequent subtyping of Stx2-positive isolates by mass spectrometry.

## **3. Materials and Methods**

### **3.1. Shotgun Proteomics: Characterizing Stx induction**

The experimental work to elucidate the Stx production time course was part of a larger project aimed at uncovering the mechanisms of phage induction, performed by Dr. Clifford Clark and myself. The Stx data presented in this thesis represents a Stx-biased snapshot of the larger phage induction data set, in that only the collected data relevant to Stx production is presented. Not only did this time course experiment provide a workable sample preparation procedure for STEC isolates, it also added to our understanding of the effects that potent phage inducers have on global protein expression (Clifford Clark, personal communication). The investigations were accomplished using a shotgun proteomic approach to characterize a large proportion of the STEC proteome during MMC induction, looking at multiple, differently timed sample fractions over a time course experiment.

To test the hypothesis of Objective 1: Stx induction optimization/characterization, I performed four-plex iTRAQ® experiments using STEC cultures with no MMC induction, 1, 2, or 3 hr induction, analyzing both with the cell pellet and the culture supernatant. Each experiment was performed in triplicate using three biological replicates. Thereafter, relative Stx toxin levels were compared: 1) within the same time point and between sample fractions and 2) within the same sample fraction and between time points. A total of eight four-plex experiments were conducted. The relative amount of Stx protein in each fraction and at each time point, along with other sample and reagent considerations, was used to determine the optimal sample preparation procedure for further studies (Figure 7).

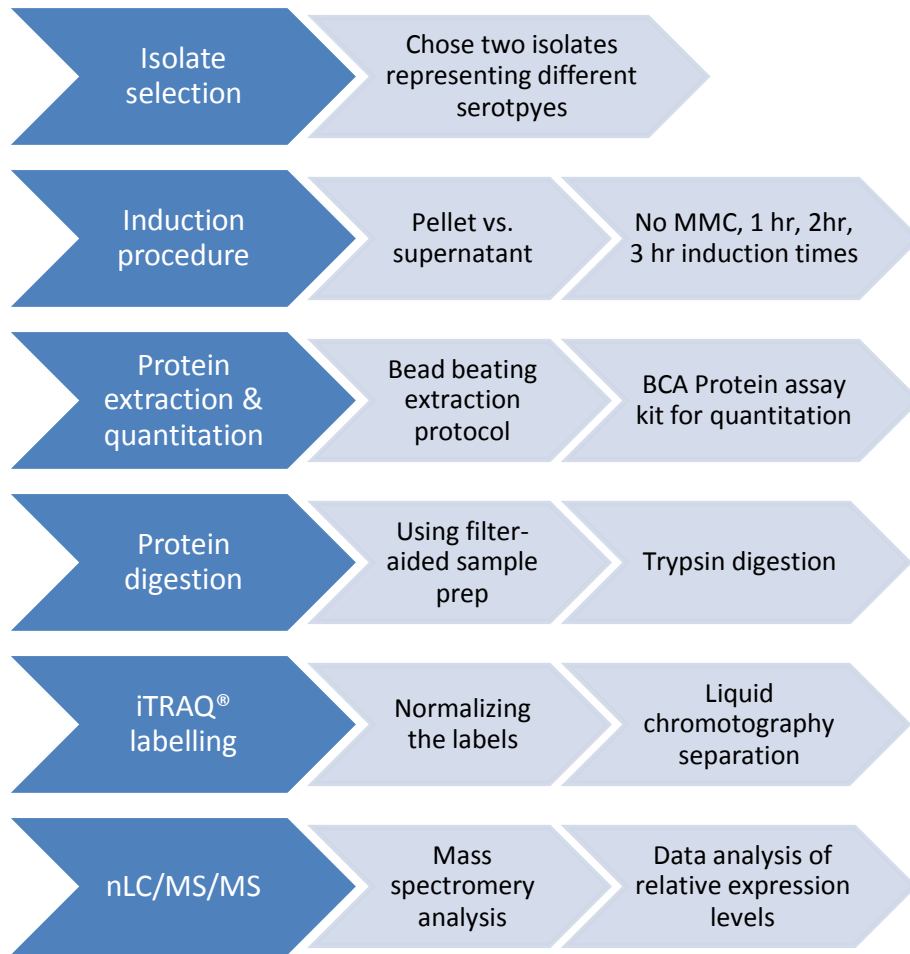


**Figure 7.** Workflow for characterization of Stx induction. The above steps were required to prepare the culture samples prior to mass spectrometry analysis on the LTQ Orbitrap Velos at the NML (Winnipeg). Two STEC isolates were chosen as representatives to determine an optimal length of induction and fraction to be used during the validation of the targeted PRM Stx detection assay. Each isolate was subjected to MMC induction of varying amounts of time (no induction, 1 hr, 2hr, and 3hr induction times) and MS analysis was performed on the peptides from both the cell pellets and culture supernatants at each time point. From a culture specimen, this procedure requires approximately nine days for sample preparation and mass spectrometry analysis.

### 3.1.1. Isolate selection

Historically, O157:H7 STEC was the predominant serotype routinely cultured from infected patients in Canada, but more recent studies have determined that non-O157 STEC incidence rates are on the rise<sup>6</sup>. Despite this change in Canadian STEC population distribution, hospitalization and case-fatality rates are still approximately 2-fold higher for patients infected with O157:H7 compared to those infected with non-O157 serotypes<sup>2</sup>. For the purpose of this study, two STEC isolates (one O157:H7 and one non-O157) were chosen as proxies for other STEC in order to determine the optimal induction timeline required to produce detectable amounts of Shiga toxin. Due to time and cost restraints we decided to pursue the testing of two isolates only, but realize that this may not be representative of the induction pattern of every STEC. Both isolates are reference strains belonging to the Genomics Research and Development Initiative (GRDI)-funded Food and Water Safety (FWS) project. They have been whole-genome sequenced and characterized for STEC specific genes using PCR. Isolates were archived at -80°C.

The O157:H7 isolate (designated GRDI FWS-EC004) contains both *stx1* and *stx2* genes and is LEE-positive. It was isolated from a human sample and logged as National Microbiology Laboratory (NML) Strain ID# 87-1215. In addition to whole-genome sequencing, the Enteric Diseases Division at the NML (Winnipeg, MB, Canada) confirmed the presence of virulence factor genes for intimin (*eae*) and a variety of non-enterocyte effacement effectors (*ent*, *nleA*, *nleB*, *nleE*, *nleF*, and *nleH*) using PCR. The second isolate (designated GRDI FWS-EC001) is serotype O26:H11, belonging to the “Big 6” group of non-O157 STEC. Similar to 87-1215, it contains both *stx1* and *stx2* genes and is LEE-positive. It was isolated from a human sample in British Columbia, Canada and logged as NML Strain ID# 02-6737. In addition to the virulence genes present in 87-1215, PCR confirmed the presence of enterohemolysin (*ehxA*) and EHEC hemolysin (*EHEC-hlyA*). These isolates will be distinguished by their NML Strain ID for the remainder of this thesis.

### 3.1.2. Induction procedure

Frozen bacterial cultures of 87-1215 and 02-6737 were removed from -80°C, streaked on Nutrient Agar + 1.5% NaCl plates, and grown at 37°C overnight (ON). The following induction procedure was performed in parallel on both isolates. After ON incubation, one isolated colony was subcultured into 11 ml trypticase soy broth (TSB) (17 g/L tryptone, 3 g/L phytone, 5 g/L NaCl, 2.5 g/L dipotassium phosphate, and 2.5 g/L glucose) in a 15-ml Falcon tube (BD Biosciences, Mississauga, ON, Canada). Inoculated broth was incubated with shaking at 37°C for approximately 16 hours. Additionally, 250 ml of uninoculated TSB was added to 500-ml screw-capped flasks (Thermo Fisher Scientific, Waltham, MA, USA). Uninoculated broth was incubated in parallel at 37°C for approximately 16 hours to assess sterility of the broth.

After incubation, 1 ml of bacterial cells was removed and placed in a cuvette for OD<sub>600</sub> reading using a BioRad SmartSpec™ Plus spectrophotometer (Life Science Research Division, Mississauga, ON, Canada). Uninoculated TSB was used as a blank. The remaining 10 ml of bacterial cells was added to the 250 ml of warmed TSB. Flasks were incubated at 37°C until an OD<sub>600</sub> of 0.5 was reached; at which time 0.5 ml of 0.5 mg/ml MMC (Sigma-Aldrich, Oakville, ON, Canada) was added (final concentration of 1 µg/ml). This time was noted as T=0. For control experiments without induction, 0.5 ml of sterile water was added in the place of MMC. The OD<sub>600</sub> was read every hour after T=0, continuing for 1, 2, or 3 hours (T=1, T=2, or T=3, respectively). Control experiments containing no MMC were incubated for 3 hours.

Once the specific number of time points for that experiment had been recorded (1, 2, or 3), the contents of the flasks were collected by pouring into a 250-ml centrifuge tube (Corning Incorporated, Corning, NY, USA). Tubes were centrifuged at 5000 x g for 15 minutes at 4°C. Next, 225 ml of supernatant was removed and placed in a fresh 250-ml centrifuge tube. Remaining supernatant was discarded. The cell pellet at the bottom of the original 250-ml centrifuge tube was resuspended in 5 ml sterile water and

aliquoted into 1.5-ml microcentrifuge tubes (Eppendorf Canada, Mississauga, ON, Canada). This was considered the cell pellet fraction. To the supernatant, 26 ml of trichloroacetic acid (TCA) (Sigma-Aldrich, Oakville, ON, Canada) (10% final concentration) was added, mixed by inverting, and placed at 4°C ON to precipitate proteins. The next day, the culture supernatants were centrifuged at 5000 x g for 30 minutes. The supernatant was removed and properly disposed into TCA waste containers. The remaining pellet was resuspended in 2 ml 100 mM HEPES buffer (pH 8.3) (in-house made) and aliquoted into 1.5-ml microcentrifuge tubes. This was considered the culture supernatant fraction. Aliquots were either kept at room temperature (RT) if continuing immediately to the protein extraction or frozen at -80°C until further processing.

### **3.1.3. Protein extraction and quantitation**

Prior to digestion, proteins are extracted from the cellular debris. A bead-beating procedure, based upon the methods of Adkins *et al.*<sup>90</sup>, was used for protein extraction. Aliquoted pellet and supernatant samples were used directly from the induction procedure or removed from the freezer and brought to RT. Samples were centrifuged in the 1.5-ml microcentrifuge tubes at 16,000 x g for 2 minutes. The supernatant was removed carefully by aspiration with a pipette. The resultant pellet was resuspended in 500 µl of phosphate buffered saline (PBS) and transferred to a screw-capped 1.5-ml microcentrifuge tube. The tube was centrifuged at 16,000 x g for 2 minutes and the supernatant removed. The pellet was resuspended in 250 µl of sterile water and approximately 100 µl of acid-washed glass beads (212-300 µm; Sigma-Aldrich, Oakville, ON, Canada) were added. Tubes were boiled in a boiling water bath for 5 minutes. Once the samples returned to RT, an additional 250 µl of sterile water was added and tubes were vortexed on high for 10 seconds. Tubes were “bead beaten” for 3 minutes using a bead-beating vortex attachment on a benchtop vortex (Scientific Industries, Inc., Bohemia, NY, USA) at low speed in order to disrupt the bacterial cell walls. The beads were allowed to settle and the cloudy supernatant was transferred to a 15-ml Falcon tube. Next, 500 µl of sterile water was added to the screw-capped

tube and vortexed on high for 10 seconds. The bead beating steps (bead beating, removal of supernatant, addition of water, and vortexing) were repeated, until the supernatant appeared clear on visible inspection (typically, this required five to six repeats). The crude protein was aliquoted into several 1.5-ml microcentrifuge tubes at 0.5 ml per tube.

The BCA Protein Assay Kit (Thermo Fisher Scientific, Waltham, MA, USA) was used to determine protein concentration of each sample. Bovine serum albumin (BSA) protein standards A-H (2,000, 1,500, 1,000, 750, 500, 250, 125, and 25 µg/ml) were made from a stock BSA solution according to kit protocols. A blank was made using MS-grade water. Protein samples were diluted 1 in 5 with MS-grade water. In a 96-well flat bottom plate (Corning Incorporated, Corning, NY, USA), 25 µl of each BSA standard was added per well in duplicate and 25 µl of each diluted STEC crude protein sample was added per well in triplicate. The working reagent was made by adding (200 µl Reagent A \* # of wells) + (4 µl Reagent B \* # of wells). Using a multichannel pipette, 200 µl of the working reagent was added to each well and pipetted up and down to mix. Plate was incubated at 37°C for 30 minutes for assay development. The absorbance of each well was measured using a BioRad xMark™ Microplate Absorbance spectrophotometer plate reader (Life Science Research Division, Mississauga, ON, Canada) at 562 nm. A standard curve was created in Microsoft Excel by plotting the 562 nm measurement minus the blank value of each BSA standard against its concentration in µg/ml. Interpolation of this standard curve was then used to determine the protein concentration of each sample from the absorbance measurement.

#### **3.1.4. Protein digestion**

Protein digestion was accomplished using a filter-aided sample preparation (FASP) cartridge trypsin digestion protocol adapted from Wisniewski *et al.*<sup>91</sup>. For each sample, 100 µg of protein was added to a 1.5-ml low-retention microcentrifuge tubes (Thermo Fisher Scientific, Waltham, MA, USA). Samples were concentrated by evaporation in a SpeedVac™ concentrator (Thermo Fisher Scientific, Waltham,

MA, USA). In all concentration steps, sample liquid was evaporated until approximately 1  $\mu\text{l}$  of liquid remained. To the 100  $\mu\text{g}$  dry protein pellet, 50  $\mu\text{l}$  of sodium dodecyl sulfate (SDS) solubilisation buffer (4% SDS, 50 mM HEPES buffer pH 8.3, 100 mM dithiothreitol (DTT) – prepared fresh) was added. Samples were heated in a ThermoMixer<sup>®</sup> temperature control device (Eppendorf Canada, Mississauga, ON, Canada) for 5 minutes at 95°C. After returning to RT, the samples were stored at -20°C ON.

Nanosep<sup>®</sup> 10K Omega cartridges (Pall Life Sciences, Port Washington, NY, USA) were prepared by adding 200  $\mu\text{l}$  MS-grade water to the cartridge and centrifuging at 10,000 x g for 1 minute. Flow through liquid was discarded after all centrifugation steps. Then, 200  $\mu\text{l}$  urea exchange buffer (UEB) (8 M urea in 50 mM HEPES buffer pH 8.3 – prepared fresh) was added to the cartridge and centrifuged at 10,000 x g for 2 minutes. Samples were removed from the freezer and brought to RT. UEB was added to the protein at 7x the sample volume (350  $\mu\text{l}$ ), bringing the total volume of sample to 400  $\mu\text{l}$ . Samples were left at RT for 10 minutes. Then, 200  $\mu\text{l}$  of sample was placed onto the cartridge and centrifuged at 10,000 x g for 10 minutes to load the sample onto the cartridge membrane. The membrane must remain moistened at all times and, therefore, centrifugation times are approximate at each step. The remaining 200  $\mu\text{l}$  of sample was placed on the cartridge and centrifuged at 10,000 x g for 10 minutes. Cartridges were washed by adding 250  $\mu\text{l}$  of UEB and centrifuging at 10,000 x g for 10 minutes. The wash step was repeated once more.

On-membrane modification of sulfhydryl groups was accomplished by adding 100  $\mu\text{l}$  iodoacetamide (IAA) solution (50 mM IAA in UEB – prepared fresh, light sensitive) to the cartridge membrane. Tubes were placed in the thermomixer for 1 minute with shaking (600 rpm) at RT. Tubes were incubated at RT in the dark for 20 minutes. After incubation, tubes were centrifuged at 10,000 x g for 10 minutes to elute the IAA reagent. The membranes were washed by adding 100  $\mu\text{l}$  UEB and centrifuging at 10,000 x g for 10 minutes. The wash step was repeated an additional two times for a total of three washes.

Membranes were prepared for benzonase treatment by adding 150  $\mu$ l of 50 mM HEPES buffer pH 8.3 to the cartridge and centrifuging at 10,000 x g for 10 minutes. This HEPES replacement step was repeated. To the cartridge membrane, 50  $\mu$ l of benzonase solution (50 mM HEPES pH 8.3, 25 mM  $MgCl_2$ , 250 U/  $\mu$ l benzonase (Sigma-Aldrich, Oakville, ON, Canada) – prepared fresh) was added. Tubes were placed in the thermomixer for 2 minutes with shaking (600 rpm) at RT and then incubated for 30 minutes at RT. The membranes were washed by adding 100  $\mu$ l of 50 mM HEPES buffer pH 8.3 to the cartridge and centrifuging at 10,000 x g for 10 minutes. The HEPES wash step was repeated an additional two times, for a total of three washes.

The content of one Promega™ Trypsin Gold MS grade (Promega North America, Madison, WI, USA) vial (100  $\mu$ g) was dissolved in 100  $\mu$ l of 0.1% formic acid (FA) (vol/vol) to give a final concentration of 1  $\mu$ g/ $\mu$ l. Cartridges were placed into a fresh collection tube. For each sample, 1.5  $\mu$ l of 1  $\mu$ g/ $\mu$ l trypsin was diluted in 48.5  $\mu$ l of 50 mM HEPES buffer pH 8.3 and all 50  $\mu$ l was added to the cartridge membrane. Samples were placed in the thermomixer for 1 minute with shaking (600 rpm) at RT. Tubes were placed in a moisture chamber (50-ml Falcon tube with 1 to 2 ml of MS-grade water) and incubated at 37°C for approximately 16 hours.

Peptide recovery was accomplished using the “flip and tap” method. This includes cutting off the top rim on the Nanosep® cartridge using a razor blade in order for the column to be flipped upside down in the collection tube. To the cartridge, 50  $\mu$ l of 50 mM HEPES buffer pH 8.3 was added and samples were placed in the thermomixer for 3 minutes with shaking (600 rpm) at RT. The cartridge was then inverted within the collection tube, and centrifuged at 10,000 x g for 1 minute to collect the eluted peptides. The collection step was repeated an additional two times for a total of three collection steps. The pooled peptide volumes were either frozen at -20°C until further processing or maintained at RT if immediately progressing with the iTRAQ® experiment.

### 3.1.5. iTRAQ® labelling

Samples stored at -20°C were brought to RT. The pooled peptides were concentrated in the SpeedVac then resuspended in 30 µl of 100 mM HEPES buffer pH 8.3. Samples were left for 10 minutes at RT and then shaken on the vortex for 10 minutes to ensure complete resuspension of peptides. The iTRAQ® Reagents Multiplex kit (SCIEX, Concord, ON, Canada) was used for labelling of peptides. iTRAQ® reagents were brought to RT then spun down in a VWR Galaxy Mini centrifuge (VWR Canada, Mississauga, ON, Canada) to collect. To each iTRAQ® label, 70 µl 100% ethanol was added; tubes were shaken on the vortex for 30 minutes, and then spun down in the mini centrifuge to collect. iTRAQ® labels were added to the corresponding sample, vortexed for 20 seconds, and then spun down in the mini centrifuge to collect. Tubes were incubated in the dark overnight at RT. The next day, 150 µl of MS-grade water was added to each tube to quench the labels. Samples were left for 30 minutes at RT, and then dried in the SpeedVac®. Samples could either be frozen at -20°C until further processing or maintained at RT if immediately moving forward with the experiment.

Dried down, labelled peptides were resuspended in 40 µl MS-grade water, shaken on the vortex for 30 minutes, and centrifuged at 16,000 x g for 2 minutes. In a 300 µl Polytetrafluoroethylene (PTFE)/Silicone Verex™ vial (Phenomenex, Torrance, CA, USA), 1 µl of each labelled peptide (labels 114, 115, 116, and 117) was added to 56 µl nano-flow LC running buffer A (2% Acetonitrile (ACN), 0.1% FA in MS-grade water) to achieve a final sample volume of 60 µl. Remaining sample was frozen at -20°C until further processing.

The unfractionated samples, mixed 1-to-1 by volume, were submitted to the Mass Spectrometry and Proteomics Core Facility (MSP Core) at the National Microbiology Laboratory in Winnipeg, Canada to measure the median intensity of the reporter ions. This was accomplished using tandem mass spectrometry (MS/MS) on a LTQ Orbitrap Velos mass spectrometer (Thermo Fisher Scientific, Waltham,

MA, USA). If the median intensity of the reporter ions is not 1-to-1, a correction is calculated and applied to the final mixing volume for each sample. Samples were stored at -20°C until further analysis.

Samples were brought to RT and centrifuged at 16,000 x g for 2 minutes. The appropriate volume of each labelled sample, determined by the isobaric label mixing calculator, was added to a 1.5-ml microcentrifuge tube. Combined labelled samples were dried down using the SpeedVac®, resuspended in 42 µl of liquid chromatography (LC) buffer A (20 mM NH<sub>4</sub>FA, pH 10 in MS-grade water), shaken on the vortex for 30 minutes, and centrifuged at 16,000 x g for 2 minutes. For LC analysis and peptide fractionation, the 42 µl of pooled peptides were transferred to a 300 µl PTFE/Silicone Verex™ vial. Samples were submitted for high-pH, C<sub>18</sub>-reverse phase LC on a micro-flow Agilent 1100/1200 series system (Agilent Technologies Canada Inc., Mississauga, ON, Canada) using a Waters XBridge™ C<sub>18</sub> guard column (10 mm long, 2.1 mm inner diameter, 3.5 µm particles) and a Waters XBridge™ C<sub>18</sub> analytical column (10 cm long, 2.1 mm inner diameter, 3.5 µm particles) (Waters Corporation, Milford, MA, USA). Resuspended samples were resolved by a gradient of LC buffer A (20 mM ammonium formate) and buffer B (90% ACN, pH 10). The gradient started at 3% B from 0–10 minutes, 8-11% B from 10–17 minutes; 11-60% B from 17–75 minutes; 95% B from 75–80 minutes; and 3% B from 80–170 minutes at a constant flow rate of 150 µl/minute. A total of 36 fractions were collected across the peptide elution profile that spanned approximately 65 minutes (Figure 8). Samples were dried in the SpeedVac® then resuspended in 80 µl of nano-flow LC running buffer A. Samples were left at RT for 10 minutes, shaken on the vortex for 30 minutes, and centrifuged at 16,000 x g for 2 minutes. To a 300 µl (PTFE)/Silicone Verex™ vial, 50 µl of labelled peptide was added and submitted for MS/MS analysis.

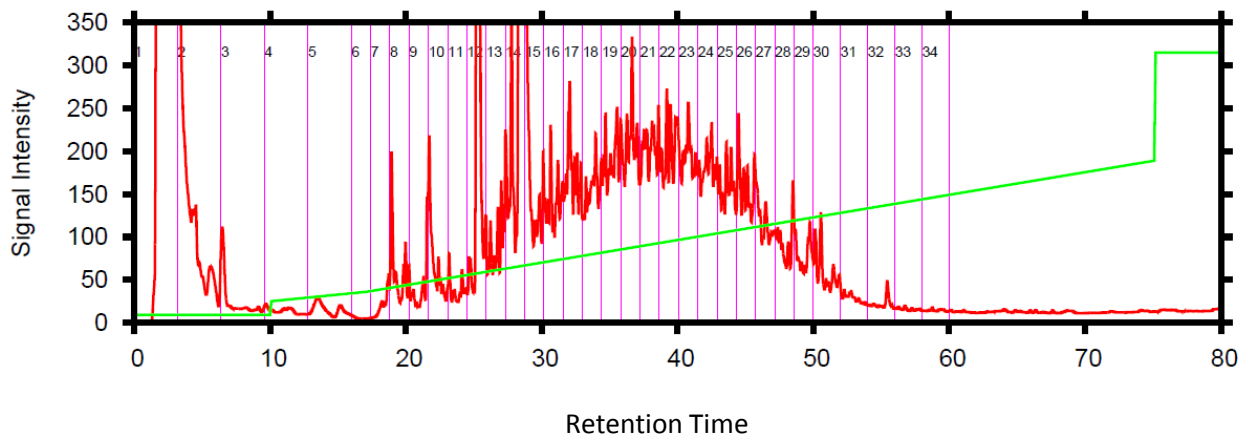


**Figure 8.** Representative 2D-LC chromatogram for fractionation of iTRAQ® samples. The chromatogram from one replicate of the 87-1215 pellet at T=2 is shown above. Combined iTRAQ® labelled samples were separated using liquid chromatography depending on their hydrophobicity. In reverse-phase LC, which was used for peptide separation in this thesis, the hydrophobic peptides were eluted through the column first, while the hydrophilic peptides were eluted later by increasing the polarity of the solution. LC separation prior to MS analysis is used to reduce sample complexity and provide higher proteome and sequence coverage.

### 3.1.6. Nano-flow liquid chromatography-tandem mass spectrometry (LC/MS/MS)

Each of the fractions were analysed using a methodology similar to that used by Clark *et al.*<sup>92</sup>, using a nano-flow Easy nLC II (Thermo Fisher Scientific, Waltham, MA, USA) connected in-line to a LTQ Orbitrap Velos™ mass spectrometer (Thermo Fisher Scientific, Waltham, MA, USA) with a nanoelectrospray ion source (Thermo Fisher Scientific, Waltham, MA, USA). Columns used in this experiment were packed in-house with ReproSil-Pur C<sub>18</sub>-AQ resin (Dr. Maisch). To begin MS analysis, 10 µl of each fraction was loaded onto a C<sub>18</sub>-reversed phase trap column (3 cm long, 100 µm inner diameter, 5 µm particles) (in-house packed) with 100% buffer A (2% ACN, 0.1% FA) at 4 µl /min for a total volume of 30 µl, then separated on a C<sub>18</sub>-reversed phase column (15 cm long, 75 µm inner diameter, 2.4 µm particles) (in-house packed). Peptides were eluted using a linear gradient of 2-32% buffer B (98% ACN, 0.1% FA) over 120 minutes at a constant flow rate of 250 nl/min. Total nLC/MS/MS run-time was 160 minutes.

Using data-dependent methodology, the top 10-most abundant precursor ions were isolated from each survey scan. The precursor ions were fragmented by higher-energy C-trap dissociation at 45% normalized collision energy. Survey scans in the Orbitrap were acquired at 300–1700 *m/z* using a target resolution of 60,000 at 400 *m/z*. Fragment ion scans in the iontrap were acquired over a dynamic *m/z* range using a target resolution of 7500 at 400 *m/z*. A lower threshold of 1000 counts was used for selecting precursor ions for fragmentation. Dynamic exclusion was enabled using a list size of 500 features, a *m/z* tolerance of 15 ppm, a repeat count of 1, a repeat duration of 30 s, and an exclusion duration of 15 s, with early expiration disabled.

### 3.1.7. Data analysis

Data analysis and processing method was similar to that used by Clark *et al.*<sup>92</sup>. The spectra resulting from MS analysis was processed using Mascot Distiller software V 2.5 (Matrix Science, Boston, MA, USA). Database searches were run against the draft genome data acquired from the two GRDI-FWS sequenced

isolates, EC0004 (87-1215) and EC0001 (02-6737) (Enteric Diseases Division, NML, Winnipeg, Canada) and used carbamidomethylation (C) and iTRAQ® (K and N-terminus) fixed modifications, as well as oxidations (M) variable modification. The search results from Mascot were imported into Scaffold Q+ software v. 4.4.3 (Proteome Software, Portland, OR, USA) where a protein threshold of 99% and a peptide threshold of 95% were chosen. Confirmation of the presence of a protein required identification of at least two peptides per protein. Scaffold Q+ allows for visualization of  $\log_2$  fold change (FC) between samples of different runs. The mean of the three replicates was calculated and used for comparison. Statistical analysis was performed within Scaffold Q+. The Permutation test was used to determine significant results with a  $p$ -value below 0.05 considered significant.

### **3.2. Targeted Proteomics: PRM detection of Shiga toxin**

The following methods were used to develop a targeted proteomic assay for the detection of Stx from bacterial cultures. The hypothetical tryptic peptides were determined through *in silico* digestion and were validated using both recombinant non-toxin Stx and intact Stx proteins. The lower limit of detection for each peptide was determined using synthesized peptides of the candidate target peptides. Optimal sample preparation, determined in the first objective, was applied to a cohort of clinical bacterial cultures to validate the detection assay (Figure 9).

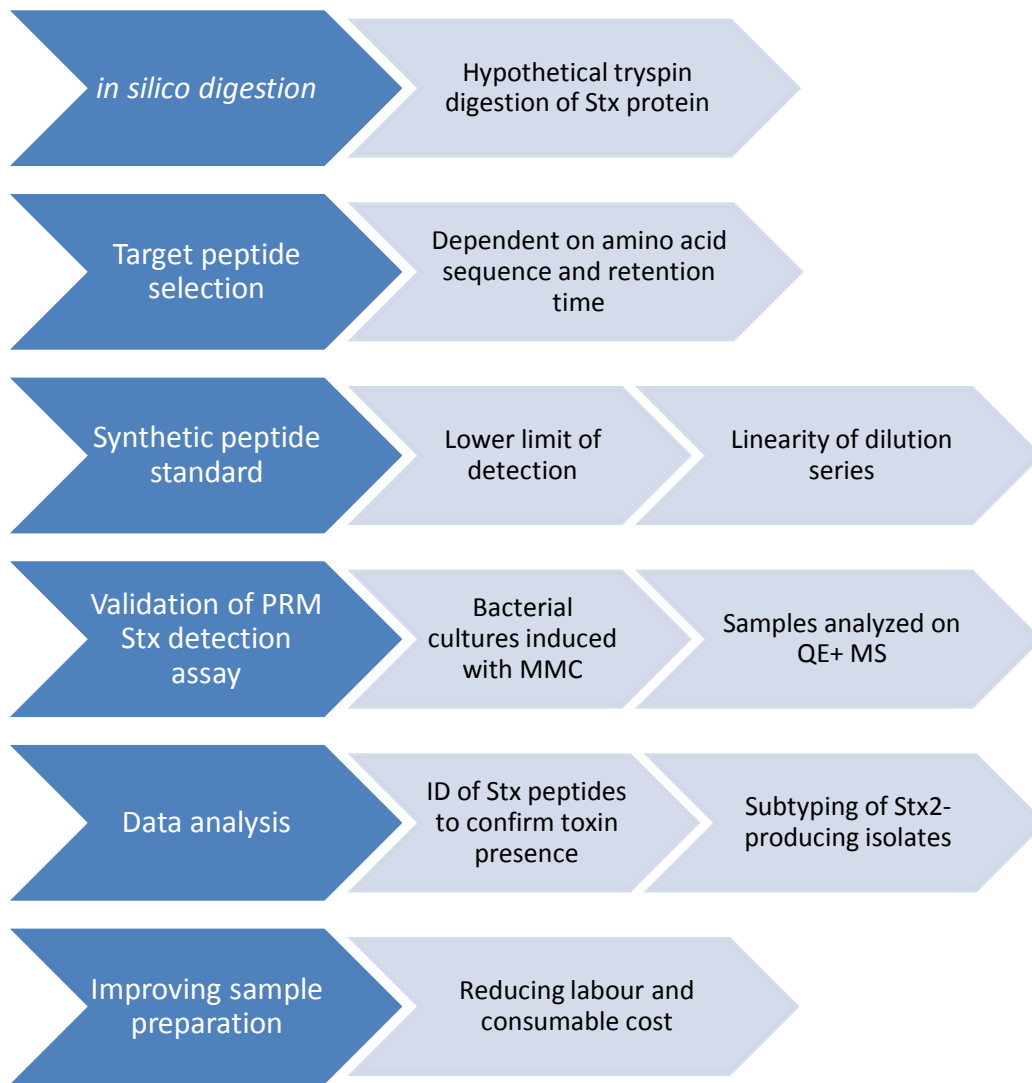


**Figure 9.** Workflow for developing and validating the PRM Stx detection assay. Target peptide selection was performed on the LTQ Orbitrap Velos™ at NML (Winnipeg) to analyze trypsin-digested Stx protein. Once the targets were chosen, the assay was developed and validated on the QExactive™ Plus (QE+) Hybrid Quadrupole-Orbitrap using bacterial cultures induced under the conditions determined in the first objective of this study.

### **3.2.1. Selecting target peptides for Shiga toxin detection**

#### **3.2.1.1. *in silico* digestion**

To begin the development of a targeted MS assay, the protein(s) of interest must be selected. The Shiga toxin A and B subunit proteins are the targets for this experiment because they are well established protein biomarkers associated with virulence of *E. coli*. Tryptic peptides are used in experimental procedures as surrogates for identification of the protein. To determine the trypsin enzyme cleavage sites available in the Stx proteins, an *in silico* digestion was performed using open source Skyline software v3.5 (MacCoss Lab Software, University of Washington, Seattle, WA, USA). Not all resulting peptides from the hypothetical digestion are appropriate targets for MS analysis. The list of candidate targets from the *in silico* digestion was analyzed to determine if they meet the specific criteria explained in 1.10.1 *Targeted proteomics*.

#### **3.2.1.2. Shiga toxin peptide identification**

To determine which tryptic peptides are suitable for targeted proteomics a purified or recombinant copy of the target protein is run. For our method development experiments, recombinant non-toxic Stx protein (1) and active, intact Stx protein (2) were used.

Peptides from the recombinant non-toxic Stx were obtained through an in-solution trypsin digestion. This was performed using 5 µg of toxoid protein of each Stx1 and Stx2. The toxoid proteins were resuspended in 30 µl in 100 mM ammonium bicarbonate (AB) buffer. To the protein, 5 µl of 200 mM DTT was added and incubated on a thermomixer at 60°C with shaking (900 rpm) for 1 hour. Next, 20 µl of 200 mM IAA solution was added, and samples were incubated at RT in the dark for 30 minutes. To neutralize the IAA, 11 µl of 200 mM DTT was added and samples were incubated at RT in the dark with shaking (900 rpm) for 1 hour. Trypsin was added at a 1:50 trypsin to protein ratio, and then samples were incubated at 37°C ON in a moisture chamber. The next morning, samples were removed from the

incubator and brought to room temperature. Peptides were dried down in the SpeedVac® and stored at -80°C until ready to use.

The procedure to obtain tryptic peptides from the active, intact Stx protein is as follows. For each Stx1 and Stx2, 10 µg of toxin protein was resuspended in 50 µl MS-grade water, boiled at 95°C for 5 minutes to inactivate, and aliquoted at 5 µg /tube. The lyophilized toxins we initially received in a mixture containing high sodium chloride concentration, which required salt removal. In-solution digestion and removal of salts was achieved through the help of Dr. Michael Carpenter (Viral Diseases Division, NML, Winnipeg, Canada) using the following protocol. One tube (5 µg) each of Stx1 and Stx2 was brought to a total volume of 100 µl in 6 M Urea/Tris buffer pH 8.0 (8 M urea, 0.5 M Tris pH 8.0, MS-grade water). To the protein, 5 µl of DTT/Tris (200 mM DTT, 50 mM Tris pH 8.0) was added and incubated at RT for 45 minutes. Then, 20 µl of IAA/Tris (200 mM IAA, 50 mM Tris pH 8.0) was added and incubated at RT for 45 minutes in the dark. To neutralize the IAA, another 20 µl DTT/Tris was added and incubated at RT for 45 minutes in the dark. Reduction of the urea concentration to 0.6 M was accomplished by adding 855 µl of 50 mM Tris/1 mM calcium chloride pH 7.5. Trypsin was added at a 1:50 ratio (w/w, trypsin:protein) and incubated ON at 37°C in a moisture chamber. The digestion was stopped by adding 100% FA until a pH of 3-4 was reached.

Salt removal was accomplished using an in-house made C<sub>18</sub> stage tip. The peptides, from the above in-solution digestion, were resuspended in 50 µl of Acid Solution (1x). To prime the stage tip, 50 µl of 100% methanol was loaded and the liquid aspirated by pipette, then 50 µl of 0.5% FA, 80% ACN in MS-grade water was loaded and aspirated, and finally 50 µl of 0.5% FA in MS-grade water was loaded and aspirated. Sample was loaded into the stage tip 50 µl at a time then aspirated. To elute the peptides, 50 µl of 0.5%FA, 80% ACN in MS-grade water was loaded and aspirated, then repeated. The peptides were

dried in the SpeedVac® and resuspended in 20 µl of MS-grade water. Peptides were frozen at -20°C until further processing.

To determine which of the hypothetical peptides from the *in silico* digestion was detectable on the mass spectrometer and confirm complete trypsin digestion, the toxin peptides were run on the LTQ Orbitrap Velos™ using a shotgun proteomics approach. The methods for this instrument are laid out below in

#### 3.2.5.1 Peptide identification.

### 3.2.2. Synthetic peptide standard

Synthetic copies of the target peptides were used to estimate the lower limit of detection since their exact concentration in solution is known. In addition to being used for method development, a mix of the synthetic peptides at a 1-to-1 molar ratio was used as a positive control when validating the assay with clinical bacterial cultures.

Custom-synthesized peptides (Sigma-Aldrich, Oakville, ON, Canada) of the candidate target peptides were purchased as surrogates for Stx target peptides. The synthetic peptides were amino acid analyzed with >95% purity and received lyophilized in 1 nmol aliquots. To solubilize the peptides, the contents of the vial were brought to RT and dissolved in 20 µl of 100% ACN. A stock solution of 5 pmol/µl was prepared by adding 180 µl of 0.1% FA and stored at -20°C.

#### 3.2.2.1. Determining lower limit of detection

A dilution series was prepared to determine the LLOD of the individual peptides in both nano-flow LC running buffer A and cellular peptide matrix. The bacterial isolate from which the peptide matrix was made was a lab-confirmed Stx-negative *E. coli* strain (ATCC 11775 or ATCC 25922) acquired from the Enteric Diseases Division (NML, Winnipeg, Canada). Frozen bacterial culture was plated on Nutrient Agar + 1.5% NaCl and incubated at 37°C ON. One colony was subcultured into 10 ml TSB incubated at 37°C ON with shaking. The next day, 1 ml of culture was added to 25 ml of TSB and grown to an OD<sub>600</sub> of 0.5.

Cultures were centrifuged at 5000 x g for 15 minutes at 4°C. The resulting pellet was treated as per section 2.1.3 *Protein extraction and quantitation*, and the proteins were trypsin digested using the in-solution digestion protocol as per section 2.2.1. *Selecting target peptides for Stx detection*. Peptides were diluted to 100 ng/μl for analysis.

The Stx1 and Stx2 peptides were combined at a one-to-one molar ratio by combining 1 μl of each stock peptide and diluted to 50 fmol/μl using nano-flow LC running buffer A or matrix peptides (at 100 ng/μl). The 50 fmol/μl concentration was used as the highest dilution and was serially diluted eight times using 1 in 3 dilutions, until a final concentration of 7.6 amol/μl was reached. Blanks were prepared with either Nano Running Buffer A or 100 ng/μl matrix. Each sample was run on the QExactive™ Plus Hybrid Quadrupole-Orbitrap™ (QE+) mass spectrometer (Thermo Fisher Scientific, Waltham, MA, USA). The method for this instrument is laid out below (3.2.5.2. *Parallel reaction monitoring*).

Results were manually interpreted using the transition with the largest peak area from each peptide and LLOD was defined as the dilution one higher than the sample where the Stx peptide was no longer detected. In addition to determining the LLOD, a qualitative assessment of linearity was performed by analyzing the dilution series for each peptide. This was done by plotting the amount of analyte (fmol) against the peak area and determining the goodness of fit of the trendline. The difference in  $r^2$  values between the samples in buffer and in matrix were used to evaluate changes in the linearity of the dilution series. Peptides with high  $r^2$  values and little change in  $r^2$  between the buffer and matrix were determined to be good candidates for the assay.

With the information gathered from the above exploratory experiments, a final list of 11 candidate target peptides was chosen to be included in the PRM detection assay (Table 6). With additional analysis, this list of 11 peptides had the potential to be further reduced to create an assay with only the optimal peptide and transition targets. The target peptides were used to search against the WGS data of

all GRDI-FWS STEC isolates to determine which of the genes encoding these peptides were present within the draft genomes of isolates carrying different subtypes of Stx. The information generated from these searches allowed us to create a map linking the specific peptides detected in each Stx2-carrying isolate to its subtype.

### **3.2.3. Validation of the PRM Shiga toxin detection assay**

To validate the PRM Stx detection assay developed on the QE+ mass spectrometer, 91 clinical bacterial isolates (62 previously characterized FWS STEC isolates, 27 non-STEC *E. coli* isolates, and 2 *stx*-positive *Shigella* isolates) were tested against the assay for validation. Isolates had been previously characterized by whole genome sequencing to determine if *stx* was present in their genome. Sample preparation for both STEC and non-STEC isolates followed the optimal induction methods determined in the first objective (2.1 *Induction procedure*).

The peptide solution appeared to be contaminated with cellular debris remaining from sample preparation. To avoid clogging of the column, Oasis® PRiME HLB (Waters, Milford, MA, USA) sample extraction columns were used to purify the digested peptides. Briefly, columns were conditioned with 100% methanol and equilibrated with 0.1% FA. Approximately 100 µg of peptide sample was loaded onto the column. The column was washed with MS-grade water and peptides were eluted with a 50% ACN/0.1% FA solution. The eluted peptides were quantitated using the Pierce™ Quantitative Colorimetric Peptide Assay (Thermo Fisher Scientific, Waltham, MA, USA).

To determine optimal concentration for analysis, five random samples were submitted for PRM analysis on the QE+ mass spectrometer at concentrations of 100 ng/µl, 200 ng/µl, and 400 ng/µl. It was determined that 200 ng/µl was the optimal concentration that allowed us to maximize the amount of total culture lysate we could load onto the column without causing clogging. Finally, 10 µl of peptides from the 91 clinical bacterial isolates was submitted in 300 µl (PTFE)/Silicone Verex™ vial at 200 ng/µl

for analysis on the QE+ mass spectrometer (run parameters can be found below in 3.2.5.2 *Parallel Reaction Monitoring*).

### **3.2.4. Improving sample preparation**

Using the induction timeline developed in 3.1. *Shotgun proteomics: Stx induction optimization/characterization* is time consuming and impractical in a clinical setting. From culture to mass spectrometry analysis, this method requires approximately 68 hours, with about 4.5 of those hours being hands-on time. In an attempt to reduce processing time, a modified sample preparation was investigated. In-house controls ATCC 11775 (*stx1/stx2* negative), H19 (*stx1* positive), and 90-2380 (*stx2* positive) were used in addition to a subset of the clinical culture samples tested in 2.2.3. *Isolate selection for PRM validation*.

Frozen bacterial cultures were removed from -80°C, streaked on Nutrient Agar + 1.5% NaCl plates, and grown at 37°C ON. A quarter of a loop of colonies were inoculated into Evan's toxins broth (20 g/L casamino acids, 6 g/L yeast extract, 2.5 g/L sodium chloride, 8.71 g/L dibasic potassium phosphate, 1 ml trace salts with iron, dissolved in 1 L water) and incubated with shaking for 24 hours. The next day, 1 ml of culture was removed and centrifuged at maximum speed for 1 minute. The supernatant was drawn into a 1-ml syringe (BD Biosciences, Mississauga, ON, Canada) and a 13 millimeter Acrodisc® syringe filter with 0.2 µm Supor® membrane (Pall Life Sciences, Port Washington, NY, USA) was placed onto the tip. The supernatant was expelled through the filter into a 1.5-ml microcentrifuge tube. The protein concentration was measured using the BCA™ Protein Assay Kit (2.1.3. *Protein extraction and quantitation*). An in-solution digestion was performed on 100 µg of protein (2.2.1.2. *Stx peptide identification*) and submitted for MS analysis on the QE+ mass spectrometer.

### **3.2.5. Nano-flow liquid chromatography-tandem mass spectrometry (LC/MS/MS)**

The following MS methods were employed throughout this section for sample analysis. The peptide identification method was used to determine the detectable Stx peptides from both the recombinant non-toxic Stx protein and active, intact Stx protein, while the PRM method was used when determining LLOD and validating the PRM assay using the clinical bacterial isolates.

#### **3.2.5.1. Peptide identification**

To prepare for MS analysis, the tryptic peptides were brought to RT and resuspended in 10  $\mu$ l of nano-flow LC running buffer A. Peptides were diluted to 50 fmol/ $\mu$ l and submitted for MS analysis in a 300  $\mu$ l PTFE/Silicone Verex™ vial. The LTQ Orbitrap Velos™ methods used for the second objective are the same as those used in 2.1.6 *nLC/MS/MS* with slight modifications. The peptides were eluted over a 60 minute gradient at a constant flow rate of 200 nl/min and a total run time of 100 minutes. The top 10-most abundant precursor ions were isolated from each survey scan.

#### **3.2.5.2. Parallel reaction monitoring**

Prior to MS analysis, samples were diluted to the appropriate concentration using nano-flow LC running buffer A. Determining the LLOD and evaluation of the PRM Stx detection assay utilized the QE+ mass spectrometer. Run parameters were as follows. Each sample was analyzed using a nano-flow Easy nLC 1000 (Thermo Fisher Scientific, Waltham, MA, USA) connected in-line to the QE+ mass spectrometer with a nanoelectrospray ion source. To begin, 5  $\mu$ l (for the clinical bacterial samples) or 2  $\mu$ l (for the synthetic peptide standards and matrix negatives) was loaded directly onto the PicoChip® analytical column (10.5 cm long, 75  $\mu$ m inner diameter, 1.9  $\mu$ m particles) (New Objective, Woburn, MA, USA) with 100% buffer A (2% ACN, 0.1% FA) at a pressure of 750 bar for a total volume of 15  $\mu$ l. Peptides were eluted using a linear gradient of 7-15% buffer B (98% ACN, 0.1% FA) over 15 minutes at a constant flow rate of 500 nl/min. Total LC/MS/MS run-time was 60 minutes. PRM analysis was performed on eleven peaks by higher-energy C-trap dissociation at 28% normalized collision energy, using an AGC target of

2e5 counts and a maximum injection time of 100 milliseconds with an isolation width of 1.5 *m/z*. Scans were acquired over a dynamic *m/z* range using a target resolution of 17,500 at 200 *m/z*.

### 3.2.6. Parallel reaction monitoring data analysis

The data generated from the QE+ mass spectrometer was analyzed using open source Skyline software (v3.5). A dot-product (dotp) value, which ranges from 0 and 1, is provided by Skyline to determine a peptide's presence or absence. The dotp value is a qualitative measure used to compare the similarity of spectra between the library entry and the fragment ion signal from the target peptide. The higher the dotp value, the more probable it is that the peptide identified is the corresponding library peptide<sup>93</sup>.

To confirm the presence of Stx, a dotp value of at least 0.85 must be observed in at least one target peptide. An isolate was considered Stx-positive if at least one peptide was with a dotp of 0.85 or greater was observed. In comparison, an isolate was considered Stx-negative if none of the targeted peptides had a dotp of at least 0.85. Sensitivity and specificity were calculated using the following equations:

$$\text{Sensitivity} = \frac{\text{\# of true positives}}{\text{\# of true positives} + \text{\# of false negatives}}$$

$$\text{Specificity} = \frac{\text{\# of true negatives}}{\text{\# of true negatives} + \text{\# of false positives}}$$

There is no distinguishable pattern in the Stx1 peptides that allows for subtyping. Unlike Stx1, the peptides found in Stx2 isolates vary by subtype. Isolates confirmed as Stx2-positive (at least one peptide with a dotp of 0.85 or greater) can potentially be subtyped by following the peptide map displayed in Table 6. This map was created by searching the WGS data (amino acid sequence) of each isolate to

determine if the peptide was present. Isolates were grouped by their subtype and the presence or absence of a target peptide in the subtype was noted. In the event that the peptides detected from a clinical isolate do not match any of those in the peptide map, the isolate cannot be subtyped using this method. Using the PRM assay, an isolate cannot be called a negative if no Stx peptides are detected, since we cannot determine if the isolate is truly Stx-negative or the Stx protein was not produced or detected.

### **3.3. Common Shiga toxin detection methods**

Common methods for detecting Stx were evaluated and compared to our PRM detection assay, which included the Vero cell assay (VCA) and Paton PCR. Both methods were performed following NML ISO 17025-accredited Standard Operating Procedures E-TT-PR-004 (Vero cell assay) and E-TT-PR-001-6 (General PCR for Toxin Gene Detection), respectively. The bacterial cultures used for both the VCA (36 isolates) and PCR (60 isolates) assays were chosen from the 91 isolates used to validate the PRM assay. As mentioned before, the validation isolates were previously characterized using whole genome sequencing to determine Stx-status.

#### **3.3.1. Vero cell assay**

Aseptic technique was maintained by performing all cell line work in a designated cell culture room within a biosafety cabinet and following all applicable procedures. A previously established Vero cell line, provided by the Enteric Diseases Division (NML, Winnipeg, Canada), was used to perform the assay. All reagents were brought to RT prior to use and remaining media and reagents adhered to proper disposal procedures.

Vero cells were passaged on Tuesdays and Fridays. To passage the cells, existing media in the cell flask was discarded, cells were rinsed with trypsin EDTA (Thermo Fisher Scientific, Waltham, MA, USA) for 30 seconds, trypsin EDTA was discarded, trypsin EDTA rinse was repeated, and the cell flask was incubated

at 37°C for 5 minutes. The cells were resuspended in 10 ml of Minimum Essential Media 1x with non-essential amino acids, L-glutamine, penicillin, streptomycin, and gentamycin added (Thermo Fisher Scientific, Waltham, MA, USA). To a new flask with 9 ml of fresh media, 1 ml of cells was added. Flasks were maintained at 37°C.

Cell line plates were set up and broths were inoculated on day one. Cells were trypsinized as per above and resuspended in 8 ml of media. To a 1.5-ml microcentrifuge tube, 10 µl of 0.4% trypan blue (Invitrogen, Carlsbad, CA, USA) and 10 µl of resuspended cells were added, and vortexed to mix. Using a Countess® Cell Counting chamber slide (Invitrogen, Carlsbad, CA, USA), 10 µl of the cell solution was placed in each chamber. Cells were counted using the Countess® Automated Cell Counter (Invitrogen, Carlsbad, CA, USA). The dilution factor required was determined by dividing the average count of the two chambers by 2.0E+5. The volume of cells was determined using  $(1/\text{dilution factor}) * 25 \text{ ml}$  and the total volume was brought to 25 ml with fresh media. To a 96-well plate, 200 µl/well of the diluted cells were added. The plate was incubated at 37°C overnight.

In-house bacterial controls for the Vero cells assay are ATCC 11775 (*stx1/stx2* negative), H19 (*stx1* positive), and 90-2380 (*stx2* positive). A small sweep of colonies from agar plates of the controls and STEC samples were inoculated in Evan's toxin broth and incubated at 37°C with shaking for 24 hours. The next day, 1 ml of culture was removed and centrifuged at maximum speed for 1 minute. The supernatant was drawn into a 1-ml syringe, a 13 millimeter Acrodisc® syringe filter with 0.2 µm Supor® membrane was placed onto the tip of the syringe, and the supernatant was expelled through the filter into a 1.5-ml microcentrifuge tube.

In the cell culture room, 100 µl of PBS was added to rows B, C, and D of the 96-well dilution plate. The controls and samples were added to row A at 100 µl, in duplicate. From row A, 25 µl of supernatant was serially diluted through rows B, C, and D. The cell culture plate was removed from the incubator and 20 µl

of supernatant was transferred from the dilution plate into the corresponding well of the cell culture plate. The cell culture plate was incubated at 37°C for 24 hours. Supernatants were stored at 4°C. The next day, cell culture plates were read using an Olympus IMT-2 microscope (Olympus Canada Inc., Richmond Hill, ON, Canada). Confluent cell growth covering the base of the well was considered a negative result. Evidence of cell death was characterized by rounding of the cells with nuclear condensation, increased cytoplasmic vacuolization, and detachment from the surface (Figure 10). Results were recorded as positive (+) if cell death was observed, negative (-) if no cell death was observed, or +/- if very weak cell death was observed. The plate was incubated for an additional 24 hours at 37°C, read again and any changes were recorded. If cell death was observed, the presence of Stx was confirmed using the Vero cell neutralization assay.

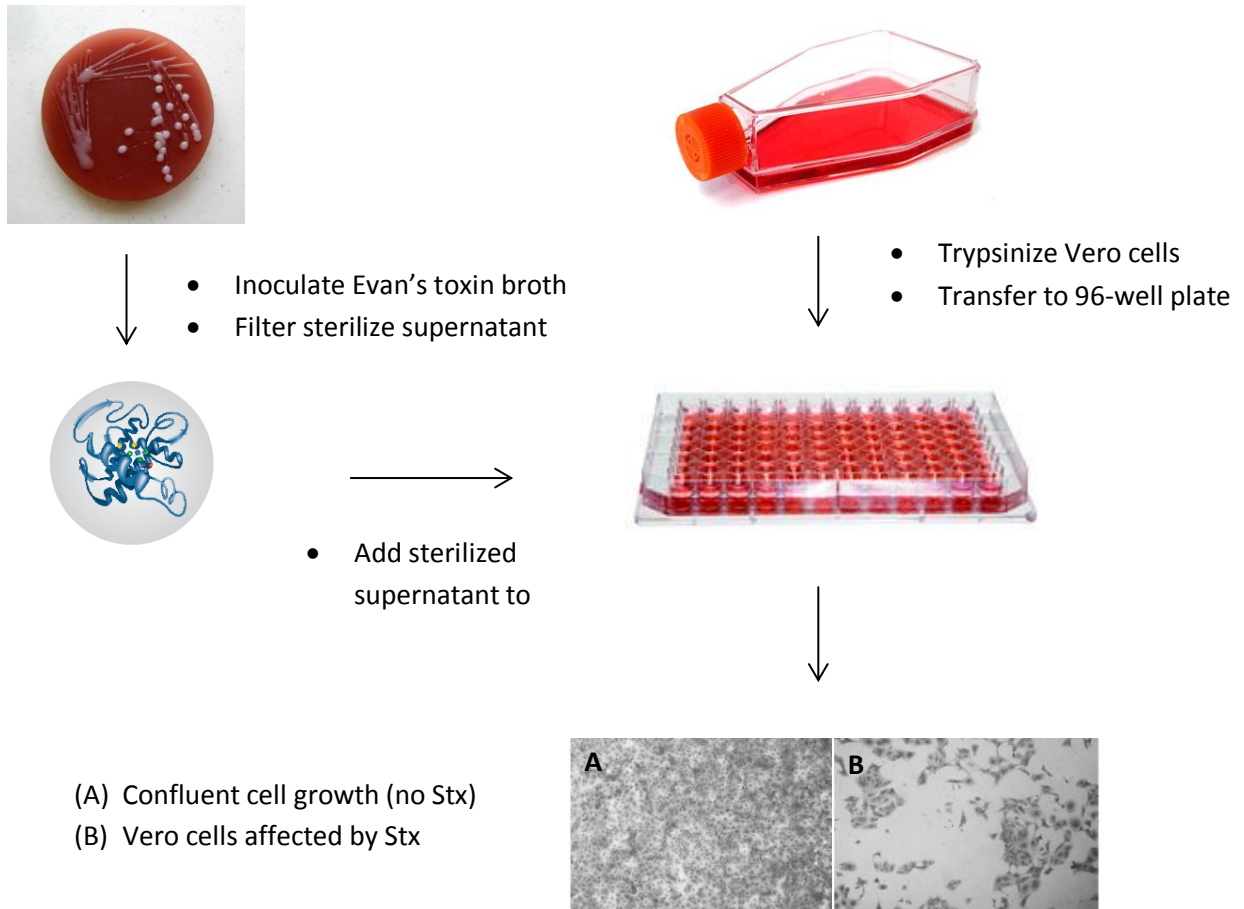


**Figure 10.** Vero cell assay procedure. Briefly, Evan's toxin broth was inoculated with bacterial culture, centrifuged, and syringe filtered. Vero cells were trypsinized and aliquoted into a 96-well cell culture plate. The filter-sterilized supernatant was added to the cells and incubated for 24 -48 hours. Cell death was recorded as evidence of Stx presence.

### 3.3.2. Vero cell neutralization assay

A Stx neutralization assay was performed to determine whether the isolate was producing Stx1, Stx2, or both. Stock solutions of anti-Stx1 and anti-Stx2 antibodies (Veterinary Technical Services, NML, Winnipeg, Canada) were diluted 1/100 in PBS and an anti-Stx1/anti-Stx2 mixture was made by combining 200 µl of each 1/100 antibody dilution. Normal rabbit serum (NRS) was diluted 1/10 with PBS. The dilution of the samples was dependent on the results from the VCA. Supernatants from samples that were positive to 1/5 were diluted 1/2.5 in PBS, those positive to 1/25 were diluted 1/12.5, those positive to 1/125 were diluted 1/62.5, and those positive past 1/125 were diluted 1/100.

A 96-well dilution plate was set up by adding 25 µl of PBS to row A, NRS to row B, anti-Stx1 to row C, anti-Stx2 to row D, and anti-Stx1/2 mixture to row E. Each control and sample was added to the plate (25 µl) with one sample being added to a single column. The plate was shaken for 2 minutes and incubated at 37°C for 2 hours.

A new flask of Vero cells was trypsinized and counted as previously stated in 2.3.1 VCA. The average cell count was divided by  $2.7E+5$  to determine the dilution factor. The volume of cells required was determined by  $(1/\text{dilution factor}) * 15 \text{ ml}$  and the total volume was brought to 15 ml with fresh media. To the plate containing the antibody/supernatant mixture, 150 µl of the diluted cells were added per well. The plate was incubated at 37°C for 24 hours.

The next day, cell culture plates were read using an Olympus IMT-2 microscope. Confluent cell growth covering the base of the well was considered antibody neutralization. In samples where the anti-Stx1 and anti-Stx1/2 wells had confluent cell growth, but the anti-Stx2 well showed cell death then the isolate was Stx1-positive. If the anti-Stx2 and anti-Stx1/2 wells had confluent cell growth, but the anti-Stx1 well showed cell death then the isolate was Stx2-positive. Samples that showed cell death in both anti-Stx1 and anti-Stx2 wells, but confluent cell growth in the anti-Stx1/2 well were Stx1- and Stx2-

positive (Figure 11). The plate was incubated for an additional 24 hours at 37°C, read again and any changes were recorded.

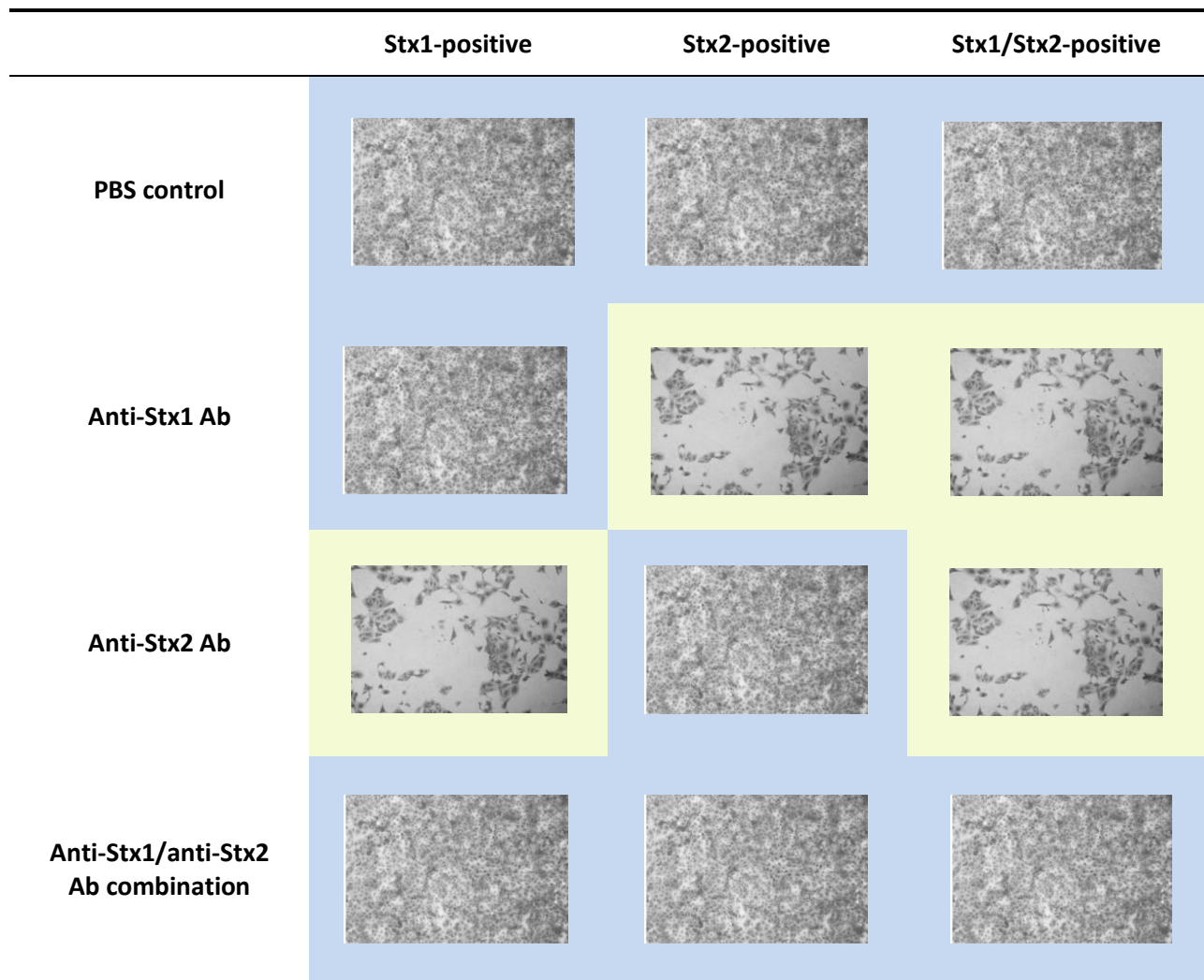


**Figure 11.** Vero cell neutralization assay methods. Briefly, trypsinized Vero cells were added to a 96-well cell culture plate and incubated with the anti-Stx1, anti-Stx2, and anti-Stx1/anti-Stx2 antibodies. The filter-sterilized supernatant was added to the cells and incubated for 24-48 hours. The above figure illustrates how the neutralization assay is interpreted. The pattern of cell death was indicative of which toxin was present. Boxes highlighted in light green indicate cell death (interpreted from the lack of a cell monolayer, clumping of cells and cellular debris) and therefore presence of active toxin, whereas images highlighted in blue indicate tissue monolayer confluency and therefore absence of active toxin.

### 3.3.3. Paton polymerase chain reaction

The Paton primer set<sup>118</sup> was used to amplify internal fragments the Shiga toxin genes (*stx1* and *stx2*), as well as other virulence factor genes (*hlyA* and *eaeA*) (Table 1). A master mix of PCR components was made in the PCR clean room. All components, excluding the FastStart Taq DNA polymerase (Roche Diagnostics, Laval, QC, Canada), were brought to RT, and vortexed to mix. The volume of master mix components (Table 2) required for one reaction was multiplied by 60 to make enough master mix for 60 PCR reactions. The final mix was vortexed and stored at -20°C in 300 µl aliquots.

Extraction of DNA from the positive bacterial control (#7, Division of Enteric Diseases, NML, Winnipeg, Canada) and STEC samples was performed using a whole-cell boil lysis method. The samples and control were plated on Nutrient Agar + 1.5% NaCl and incubated at 37°C for 16-18 hours. The next day, 500 µl of sterile water in 1.5-ml screw-capped cryovials was inoculated with approximately half of a loop full of bacterial culture from the agar plates. Tubes were placed in the thermomixer at 99°C for 10 minutes, brought to RT, then centrifuged at 14,000 rpm for 3 minutes. Supernatants were transferred to 1.5-ml microcentrifuge tubes and stored at -20°C until use.

To set up PCR reactions, template and master mix were brought to RT, vortexed, and spun in the mini centrifuge to collect. The appropriate amount of master mix ( $22.5 \mu\text{l} * \# \text{ of samples/controls} + 1$ ) and appropriate amount of FastStart Taq DNA polymerase ( $0.2 \mu\text{l Taq} * \# \text{ of samples/controls} + 1$ ) was added to a 1.5-ml microcentrifuge tube, lightly vortexed, spun in the mini centrifuge to collect, and aliquoted (23 µl) into 0.2 ml PCR reaction tubes. A negative control of 25 µl of sterile water was used. In the template CleanSpot™ PCR hood, 2 µl of template was added to the master mix tubes, mixed lightly by flicking the tube, and spun in the mini centrifuge to collect. The PCR reactions were carried out in a GeneAmp® PCR System 9700 (Thermo Fisher Scientific, Waltham, MA, USA) thermocycler following the run parameters set out in Table 3. Tubes maintained at 4°C until further processing.

**Table 1.** Primers for amplification of the Paton Multiplex genes. The Paton primer<sup>118</sup> set amplifies four nucleotide sequences corresponding to STEC virulence factors. An additional set of primers is required for amplification of Stx2f subtypes. The *stx1* primer set amplifies nt 454-633 of the A subunit coding region of *stx1*, the *stx2* primer set amplifies nt 603-857 of the A subunit coding region of *stx2* (including *stx2* variants), the *eaeA* primer set amplifies nt 27-410 of *eaeA*, and the *hlyA* primer set amplifies nt 70-603 of EHEC *hlyA*.

Amplified Gene	Size of Product (bp)	Primer	Primer Size (nt)	Sequence (5'-3')
<i>stx1</i>	180	P- <i>stx1</i> -f	23	5'-ATA AAT CGC CAT TCG TTG ACT AC-3'
		P- <i>stx1</i> -r	21	5'-AGA ACG CCC ACT GAG ATC ATC-3'
<i>stx2</i>	255	P- <i>stx2</i> -f	21	5'-GGC ACT GTC TGA AAC TGC TCC-3'
		P- <i>stx2</i> -r	22	5'-TCG CCA GTT ATC TGA CAT TCT G-3'
<i>eaeA</i>	384	P- <i>eaeA</i> -f	20	5'-GAC CCG GCA CAA GCA TAA GC-3'
		P- <i>eaeA</i> -r	20	5'-CCA CCT GCA GCA ACA AGA GG-3'
<i>hlyA</i>	534	P- <i>hlyA</i> -f	21	5'-GCA TCA TCA AGC GTA CGT TCC-3'
		P- <i>hlyA</i> -r	22	5'-AAT GAG CCA AGC TGG TTA AGC T-3'

**Table 2.** PCR reaction mix conditions for Paton multiplex PCR. All components excluding the FastStart™ Taq DNA Polymerase were combined into a mastermix and frozen until needed. The mastermix was brought to room temperature when needed and the DNA polymerase was added just prior to use. Total mastermix volume was 25 µl with 5 µl of template added for a total volume of 30 µl/reaction. A no-template control was run using 5 µl in place of the template.

<b>Stock Concentration</b>	<b>Volume Required for One Reaction (25 µl total volume)</b>	<b>Final Concentration</b>
10 X PCR Buffer	2.5 µl	1 X
2 mM dNTPs	2.5 µl	200 µM each dNTP
25 mM MgCl <sub>2</sub>	2.0 µl	2.0 mM
stx1-f Primer (20 µM)	0.31 µl	0.25 µM
stx1-r Primer (20 µM)	0.31 µl	0.25 µM
stx2-f Primer (20 µM)	0.31 µl	0.25 µM
stx2-r Primer (20 µM)	0.31 µl	0.25 µM
eaeA-f Primer (20 µM)	0.31 µl	0.25 µM
eaeA-r Primer (20 µM)	0.31 µl	0.25 µM
hlyA-f Primer (20 µM)	0.31 µl	0.25 µM
hlyA-r Primer (20 µM)	0.31 µl	0.25 µM
FastStart Taq DNA Polymerase (5 U/µl)	0.2 µl	1.0 U
Sterile, 18 MΩ dH <sub>2</sub> O	13.32 µl	

**Table 3. Run parameters for Paton Multiplex PCR.** The following run parameters were used, with the GeneAmp® PCR System 9700, to achieve amplification of the target genes.

Stage	Temperature (°C)	Time	Cycles
Initial denaturation	95	2 minutes	1
Dentaturation	95	1 minute	10
Annealing	65	2 minutes	
Extension	72	1.5 minutes	
Dentaturation	95	1 minute	5
Annealing	65-1/cycle	1 minute	
Extension	72	1.5 minutes	
Dentaturation	95	1 minute	10
Annealing	60	2 minutes	
Extension	72	1.5 minutes	
Dentaturation	95	1 minute	10
Annealing	60	2 minutes	
Extension	72	1.5 min. + 6 sec./cycle	
Final extension	72	5 minutes	1
Storage	4	Hold, Forever	1

Submarine gel electrophoresis and staining with GelRed™ (NML SOP# E-TT-PR-012) was used for analysis and visualization of the PCR products. To make the gel, approximately 1.5 g of 1.8% Ultrapure agarose (Invitrogen, Carlsbad, CA, USA) was combined in a 500-ml glass bottle with 100 ml 0.5 X Tris/Borate/EDTA buffer (prepared in-house). The bottle was microwaved at 30 second intervals until the agarose gel was completely dissolved, then poured into a gel cast with a 20-well comb and left to solidify.

The well comb was removed, the solidified gel was placed in an electrophoresis chamber (Bio-Rad, Hercules, CA, USA), and covered in 0.5 X TBE buffer. To wells 1, 10, and 20, 3.5 µl of TrackIt™ 100 bp DNA ladder (Invitrogen, Carlsbad, CA, USA) was loaded. Controls and samples were loaded by combining 8 µl PCR product with approximately 1 µl of BlueJuice™ Gel Loading Buffer (10X) (Invitrogen, Carlsbad, CA, USA) and pipetted into the wells. The electrophoresis chamber was plugged into the power pack (Bio-Rad, Hercules, CA, USA) and run at 120 volts for 60 minutes. The gel was transferred to a bucket containing GelRed™ Nucleic Acid Gel Stain (Biotium, Hayward, USA) for 30 minutes to 1 hour. A picture of the gel was taken using a GelDoc™ XR+ System (Bio-Rad Canada, Mississauga, Canada) in combination with ImageLab™ Image Capture and Analysis software (Bio-Rad Canada, Mississauga, Canada). The gel was disposed of as per standard procedure, in a GelRed™ bucket. Following confirmation of the PCR product, purified product was sent to the Genomics Core facility (NML, Winnipeg, Canada) for Sanger client sequencing service, using the primer sets for *stx1* and *stx2*.

## 4. Results

### 4.1. Shotgun Proteomics: Characterizing Stx Induction

In total, roughly 2000 proteins were detected in the STEC cell pellets and 800 in the culture supernatant. For this thesis, data analysis focused on relative amounts of the Stx1 and Stx2 A and B subunits in the cell pellet and culture supernatant of isolates 87-1215 (O157:H7) and 02-6737 (O26:H11). Each iTRAQ® experiment used the T=0 (no MMC induction) time point as a reference when evaluating the  $\log_2$  FC. Overall, we observed that the timing of Shiga toxin synthesis and release appears to be different between the two strains. The Permutation test was applied to determine statistical significance.

Analysis of the Stx1 data extracted from Scaffold software showed the presence of Stx1 subunits A and B in the cell pellet fractions from both 87-1215 and 02-6737 (Figure 12). The relative amount of A and B subunits from the cell pellet fraction of 87-1215 steadily increased as induction time increased ( $p < 0.05$ ). Resuspending the cell pellet of 87-1215 at T=3 was challenging as it had become gelatinous and sticky. In comparison to 87-1215, the A and B subunits in the 02-6737 cell pellet showed a different expression pattern, where little change in toxin production was observed over time ( $p=0.6$  for both A and B subunits). No issues occurred for resuspending the 02-6737 cell pellets. The 02-6737 B subunit was present in the culture supernatant fractions, but only in two of the three replicates. Both replicates exhibit only small deviations from zero  $\log_2$  FC ( $p=0.52$ ).

In contrast to the Stx1 data, Stx2 was detected at varying levels in all cell pellet and culture supernatant fractions tested (Figure 13). In the cell pellet, the 87-1215 A and B subunits followed a similar pattern, with negligible  $\log_2$  fold increases at T=1 but large increases at both T=2 and T=3 ( $p < 0.05$ ). The A and B subunits of the 02-6727 cell pellet showed  $\log_2$  fold increases at all time points. The results for 02-6737 were not significant for either subunit (A subunit  $p=0.17$ , B subunit  $p=0.14$ ). Of all Stx2 fractions tested, the 02-6737 cell pellet B subunit saw the largest average  $\log_2$  fold increase compared to T=0. A constant

average  $\log_2$  fold increase was observed in the 87-1215 A subunit in culture supernatant, whereas the 87-1215 B subunit and 02-6737 A and B subunits exhibited a small increase at T=1, a sharp increase at T=2, and then a small plateau at T=3. All results for the Stx2 culture supernatants are considered significantly different from T=0 with p-values below 0.05.

After consideration of the iTRAQ<sup>®</sup> data, along with the observations made throughout processing of the samples, we concluded that the cell pellet after two hours of MMC induction would be used for future experiments. Due to the hazardous nature of TCA and the additional time required to process the culture supernatant, the cell pellet was chosen. As well, the gelatinous, sticky pellet that resulted from three hours of MMC induction in 87-1215 lead us to choose the two hour induction time. At this time-point, toxin was detectable but the pellets remained easy to process.

The iTRAQ<sup>®</sup> experiments were also set up to allow the comparison of Stx production between the cell pellets and culture supernatants at each time point. In summary, the relative Stx protein levels found in each fraction varied. For example, after 2 hours of induction, the 87-1215 pellet contained the highest levels of the Stx1 A and B subunits and the Stx2 B subunit ( $p < 0.0001$ ), while the Stx2 A subunit was found at the highest levels in the 87-1215 supernatant ( $p=0.4$ ). This portion of the experiment further increased our confidence in choosing the cell pellet as the appropriate fraction for the remainder of our experiments.

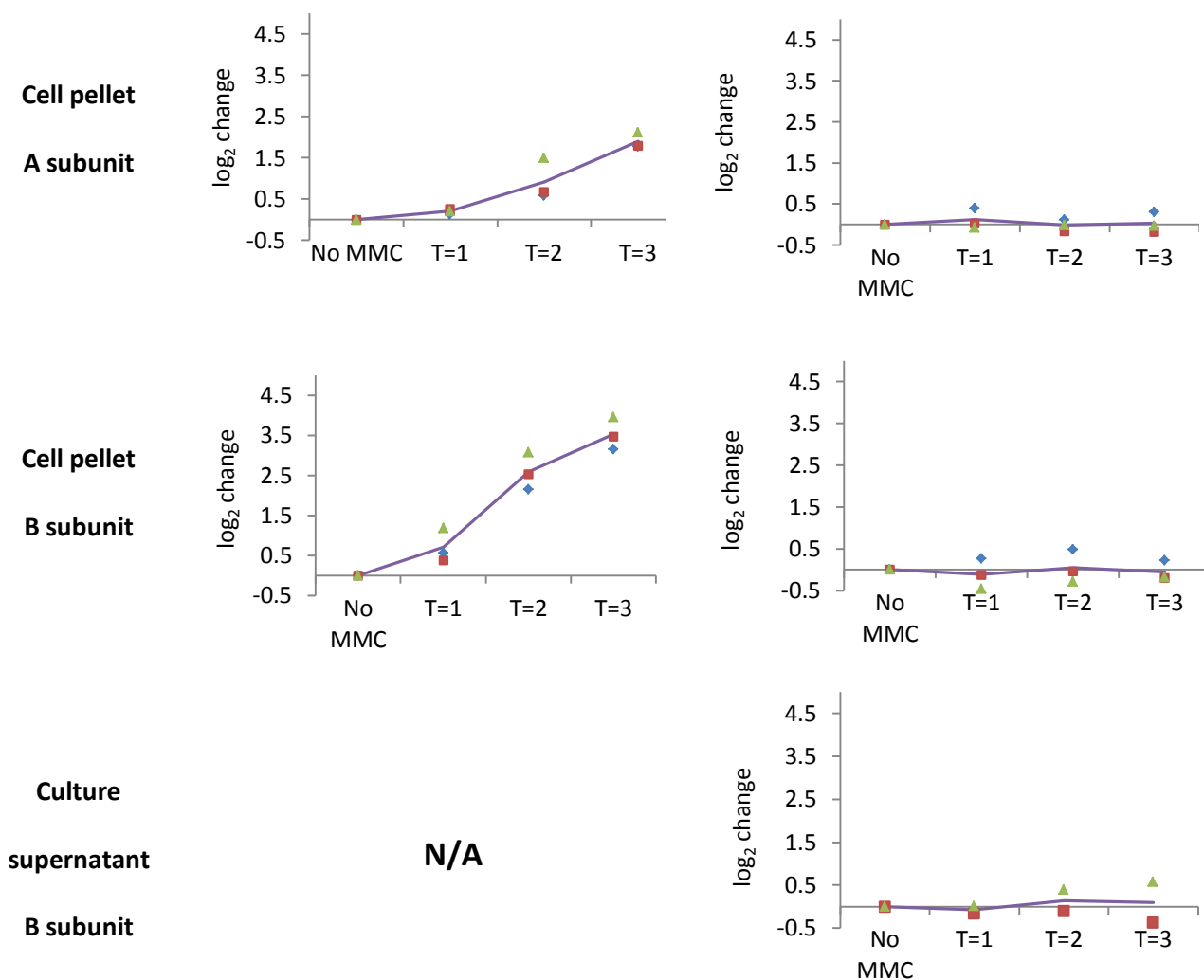


**Figure 12.** Stx1 induction timeline results. Each graph displays the  $\log_2$  changes observed over the four time points, no MMC (reference), T=1, T=2, and T=3 for the fractions where Stx1 was detected. The blue diamonds, red squares, and green triangles represent replicates 1, 2, and 3, respectively. The purple line represents the average of the three replicates. The 02-6737 B subunit was not detected in replicate 1 in culture supernatant; therefore, the analysis was performed using only two replicates.

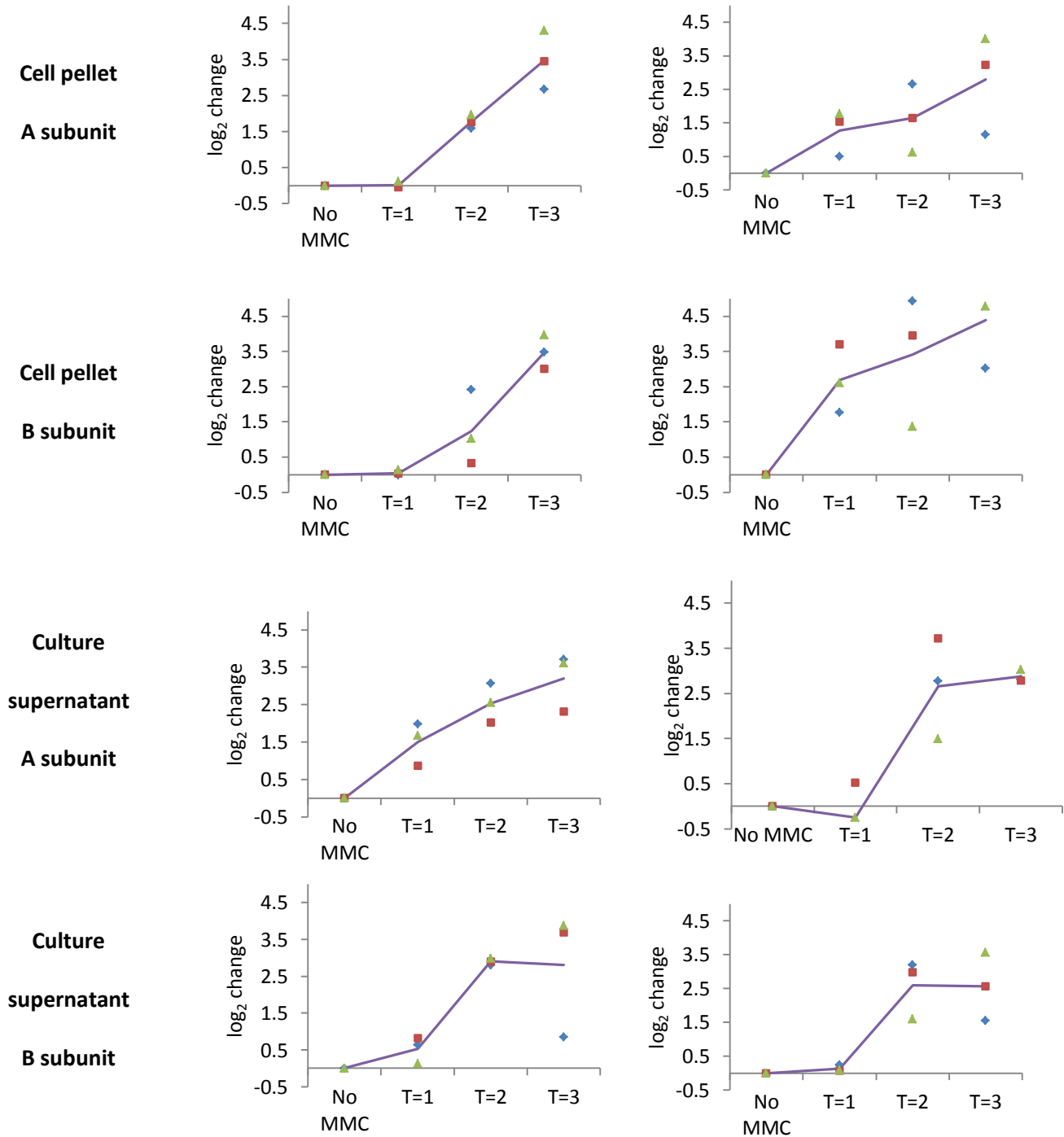


**Figure 13.** Stx2 induction timeline results. Each graph displays the  $\log_2$  changes observed over the four time points, no MMC (reference), T=1, T=2, and T=3 for the fractions where Stx2 was detected. The blue diamonds, red squares, and green triangles represent replicates 1, 2, and 3, respectively. The purple line represents the average of the three replicates.

## **4.2. Targeted Proteomics: PRM detection of Shiga toxin**

### **4.2.1. Selecting target peptides for Shiga toxin detection**

The *in silico* digestion of the Stx1a and Stx2a amino acid sequences from the recombinant, non-toxic Stx revealed 29 and 26 candidate tryptic peptides, respectively. The tryptic digested Stx peptides from the recombinant, non-toxic Stx and active, intact Stx protein we analyzed using the LTQ Orbitrap Velos™. In summary, we were able to identify seven peptides for both Stx1 (dotp values ranging from 0.80 to 0.99) and Stx2 (dotp values ranging from 0.49 to 0.98), providing a total of 14 candidate target peptides. After manual analysis of the 14 candidate target peptides, three peptides were removed as they did not meet at least one of the target peptide criteria (listed in 1.10.1 *Targeted Proteomics*). The final 11 peptides were chosen based on their signal intensity and their ability to be routinely identified by the mass spectrometer with high dotp values (*i.e.*, consistent matches to library spectra). The list of these peptides, and the subtype in which they are present in, can be seen in Table 4. After further analysis and optimization, the list of 11 peptides had the potential to be reduced further.

The amino acid sequences of the 11 candidate target peptides were cross referenced with the WGS data acquired for all FWS STEC strains to determine which of the peptides mapped to each Stx subtype. Unique peptide fingerprints were not available for the Stx1 subtypes, but unique peptide fingerprints could be observed for the Stx2 subtypes (Table 6). We also observed that each Stx2-carrying isolate produced only one of two variant Stx2 subunit B peptides (YNENDTFTVK or YNEDDTFTVK), but never both.

### **4.2.2. Determining lower limit of detection**

The synthetic peptide standards were spiked into buffer and Stx-negative *E. coli* cell lysate matrix and analyzed on the QE+ mass spectrometer to determine the LLOD of each peptide. Stx peptides were not

detected in the blanks of either dilution series. Results for the LLOD and linearity analysis are summarized in Table 4. The LLOD ranged from 69 to 1850 amol/ $\mu$ l. Plotting the dilution series values allowed us to assess the goodness of fit of the trendline for each peptide. Overall, only small variations in linearity could be observed between the buffer and matrix samples. Figure 14 provides an example of the dilution series plot for peptide ISNVLPEYR. At the same amount of analyte, the peptide in matrix is producing more signal than in buffer, which becomes more exaggerated as the amount of analyte increases. A 1.6-fold difference is observable at 40 fmol. The buffer trendline does not fit the data as well as the matrix trendline, as is reflected by the  $r^2$  value. The other target peptides each displayed unique plots, but no observable differences in  $r^2$  values between the buffer and matrix dilution series were large enough to exclude them as targets.

**Table 4. Evaluation of LLOD for Stx peptides.** The QE+ mass spectrometer was used to determine the LLOD of each Stx target peptide using synthetic standards. The values in parentheses under Signature Target Peptides correspond to the amino acid location of the peptide within its associated protein. The values reported are for the dilution series performed in Stx-negative *E. coli* matrix (derived from either ATCC 11775 or ATCC 25922). The FVTVTAEALR peptide is found in the A subunit of both Stx1 and Stx2, but the LLOD was only assessed once. The linearity of the dilution series of each peptide was assessed by plotting the amount of analyte against the peak area. The smaller the LLOD value, the more likely it is that the peptide can be detected at low concentrations. The resulting trendline provided a goodness of fit value ( $r^2$ ) to evaluate how linear the data was. The more linear the data, the closer the  $r^2$  value is to 1.

Toxin	Signature Target Peptides	LLOD (amol/ $\mu$ l)	Linearity			
			$r^2$ Buffer	$r^2$ Matrix		
Stx1	A subunit	K.TYVDSLNVIR.S [33, 42]	69	0.897	0.9559	
		R.NNLYVTGFVNR.T [95, 105]	620	0.9692	0.9582	
		R.FVTVTAEALR.F [182, 191]	1850	0.9409	0.9546	
		R.TTLDDLSGR.S [201, 209]	23	0.9855	0.8851	
	B subunit	K.YNDDDTFTVK.V [33, 42]	210	0.9802	0.9845	
Stx2	A subunit	R.GLDVYQAR.F [77, 84]	69	0.9977	0.9606	
		R.FVTVTAEALR.F [182, 191]	1850	0.9409	0.9546	
		R.ISNVLPEYR.G [226, 234]	69	0.956	0.9781	
		K.SQFLYTTGK.- [310, 318]	69	0.9855	0.9355	
		B subunit	K.YNENDTFTVK.V [31, 40]	69	0.9785	0.9843
			K.YNEDDTFTVK.V [31, 40]	210	0.9545	0.9924
		K.EYWTSR.W [45, 50]	210	0.9881	0.9861	

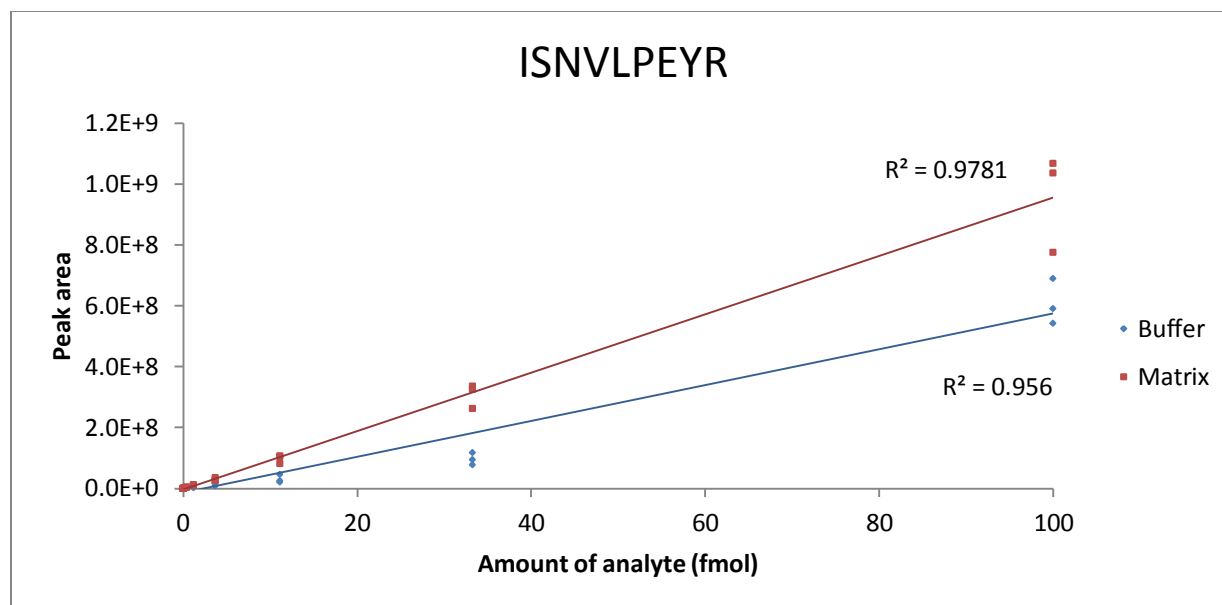


**Figure 14.** Dilution series plot for peptide ISNVLPEYR. The dilution series for each peptide in buffer and matrix was analyzed using the QE+ mass spectrometer then plotted and assessed for linearity. Differences in linearity in the ISNVLPEYR peptide between the buffer and matrix samples were observed. As the amount of analyte increased, the variation between replicates at one x-value became more pronounced. Although there were observable differences within the plot, the goodness of fit between the buffer and matrix samples remained small.

#### 4.2.3. Validation of the PRM Shiga toxin detection assay

Using the induction procedure determined in the first objective and the PRM Stx detection assay developed on the QE+ mass spectrometer, a total of 91 clinical bacterial cultures were analyzed for the presence of Stx peptides. As indicated in the Materials and Methods, the samples were run at 200 ng/μl with a 5 μl injection for a total of 1 μg of peptide on column. The results are summarized in Table 5A.

Overall, the assay was able to distinguish between Stx-positive and Stx-negative isolates in 85 of 91 samples, with Stx-positive isolates exhibiting a dotp value of at least 0.85 in one or more target peptides. The assay exhibited an overall sensitivity of 90% and a specificity of 100%. Broken down further, Stx was not detected in all 29 non-STEC isolates, including the two toxin-positive *Shigella* isolates, providing no false-positive results. Of the 62 STEC isolates, 56 were identified as Stx-positive. In 52 of the 56 positive identifications (93%), we also were able to ascertain whether the isolate produced Stx1, Stx2, or both. The remaining four isolates had dotp values of at least 0.85 in only the common FVTVTAEALR peptide, confirming the presence of Stx but not discriminating which toxin (Stx1 or Stx2) the isolate was producing. Of the six Stx-positive isolates where toxin was not detected by PRM assay, one isolate encoded Stx1 genes and five isolates encoded Stx2 genes. None of the STEC isolates in which Stx was undetectable shared the same O-serotype and none belonged to the O157 serotype or to the “Big 6” non-O157 serotypes. There also does not appear to be any discernable pattern in the subtypes found in these isolates, with isolates carrying the following subtypes: Stx1c (isolate ID# 12-3003), Stx1c/Stx2b (10-2726), Stx2a (09-1765, 12-3002), Stx2b (09-0529), and Stx2e (06-3440). In 10-2726, the isolate producing Stx1c/Stx2b, Stx1c was detected but not Stx2b.

The subtype of Stx2-carrying isolates was determined using the peptide fingerprinting pattern map (Table 6). The isolates analyzed carried either one or two Stx2 subtypes, either alone or in combination with Stx1. Of the 45 Stx2-carrying isolates, Stx2 peptides were not detected in six of the isolates,

therefore, those isolates were impossible to subtype. The PRM assay was able to correctly identify 32/39 (82%) subtypes using the peptide fingerprint scheme. Results broken down by subtype are recorded in Table 7. The seven non-typable isolates were identified as Stx2 by PRM but did not have a peptide pattern matching any of those in Table 6. The draft genomes for one isolate simultaneously carried two Stx2 subtypes (10-8268, Stx2a and 2b); making it impossible to subtype this isolate as all Stx2 peptides were detected.

A time and cost analysis was performed for each of the detection assays (PRM, VCA, and PCR) to compare feasibility. Completing the PRM assay, beginning from a STEC bacterial culture grown to stationary phase, required approximately 68 hours total time with 4.5 hours of that being hands-on. The mass spectrometer requires around 1.5 hours to complete analysis including washes; the remainder of time is for pre-MS preparation of the sample. The cost per sample to run the PRM assay was approximately \$27.45 per sample. This cost estimate does not take into account the cost of capital infrastructure. This high cost and labour time is associated with the lengthy MMC induction procedure that is required to produce detectable amounts of Stx from culture. Further investigations to potentially reduce the number of steps involved in PRM sample preparation may drastically reduce both the time and cost requirements.

**Table 5.** Analysis of clinical STEC and non-STEC samples using PRM, VCA, and PCR. The PRM Stx detection assay (A) was assessed using 91 clinical bacterial culture samples (62 Stx-positive and 29 Stx-negative). The results were then compared to current STEC identification techniques: VCA (B; 36 isolates tested) and Paton PCR (C; 60 isolates tested). The PRM assay had a sensitivity of 90% and a specificity of 100%. The VCA and PCR had sensitivities of 100% and 97%, respectively. The isolates tested were previously characterized through whole genome sequencing to determine Stx status.

Table 5A		PRM Results	
		Stx +	Stx -
<b>WGS results</b>	Stx +	56	6 †
	Stx -	0	29

† Isolates 06-3440, 09-0529, 09-1765, 10-2726, 12-3002, 12-3003

Table 5B		VCA Results	
		Stx +	Stx -
<b>WGS results</b>	Stx +	36	0
	Stx -	0	0

Table 5C		PCR Results	
		Stx +	Stx -
<b>WGS results</b>	Stx +	58	2*
	Stx -	0	0

\* Isolates 10-8265, 10-8279

**Table 6.** Stx1 and Stx2 subtype fingerprint map. The QE+ mass spectrometer was used to analyze trypsin-digested Stx protein to obtain the target peptides for the PRM assay. The values in parentheses under Signature Target Peptides correspond to the amino acid location of the peptide within its associated protein. The target peptides were searched against the WGS data previously obtained for all FWS isolates to determine which peptides could be detected in the genome of each Stx subtype. From this information, a peptide fingerprint map was created. Stx1 subtypes cannot be distinguished using this scheme, but the Stx2 subtypes exhibit unique fingerprints that can be used to assign a subtype to Stx2-carrying isolates without additional assays.

Toxin		Signature Target Peptides	Stx subtype distribution									
			1a	1c	1d	2a	2b	2c	2d	2e	2f	2g
Stx1	A subunit	K.TYVDSLNVIR.S [33, 42]	■	■								
		R.NNLYVTGFVNR.T [95, 105]	■	■	■							
		R.FVTVTAEALR.F [182, 191]	■	■	■							
		R.TTLDDLGR.S [201, 209]	■	■	■							
	B subunit	K.YNDDDTFTVK.V [33, 42]	■	■	■							
Stx2	A subunit	R.GLDVYQAR.F [77, 84]				■	■	■	■			
		R.FVTVTAEALR.F [182, 191]				■	■	■	■	■		■
		R.ISNVLPEYR.G [226, 234]				■	*				■	■
		K.SQFLYTTGK.- [310, 318]				■	*					
	B subunit	K.YNENDTFTVK.V [31, 40]					■	■	■			
		K.YNEDDTFTVK.V [31, 40]				■		†	†		*	
		K.EYWTSR.W [45, 50]				■	*		■			

\* only detected in some isolates

† may be detected instead of YNEND

**Table 7. Subtype analysis of Stx2-carrying isolates using the PRM assay.** The isolates were previously characterized and subtyped through additional PCR and sequencing. Of the 91 isolates tested, 45 isolates were previously determined to carry Stx2, with one isolate carrying two Stx2 subtypes. Of the 45 Stx2-positive isolates, there were six instances where Stx2 was not detected by PRM. The PRM assay was able to correctly classify 32 of the 39 (82%) Stx2 subtypes in isolates where Stx2 was detected.

<b>Subtype</b>	<b>Subtype distribution (# of subtypes)</b>	<b>Stx2 not detected by PRM</b>	<b>Correct subtype ID by PRM</b>
Stx2a	24	2	19
Stx2b	8	2	4
Stx2c	2	0	0
Stx2d	7	0	7
Stx2e	2	1	0
Stx2f	2	0	2
Stx2g	1	1	0
<b>Total</b>	<b>46 †</b>	<b>6*</b>	<b>32^</b>

† One isolate was carrying more than one Stx2 subtype

\* Isolates 06-3440, 09-0529, 09-1765, 10-2726, 10-8267, 12-3002

^ Isolates incorrectly subtyped: 06-7270, 09-1250, 10-8262, 10-8263, 10-8268, 10-8273, 11-2646

### 4.3. Common Shiga toxin detection methods

#### 4.3.1. Vero Cell Assay

A total of 36 FWS STEC isolates were tested for the presence of Stx using the VCA. Three controls, ATCC 11775 (-), H19 (*stx1+*), and 90-2380 (*stx2+*), were used on each 96-well plate. The VCA is able to determine the presence of functional toxin, but does not discriminate between Stx1 and Stx2. All wells containing supernatant from ATCC 11775 (negative control) showed confluent cell growth, indicating no cytopathic effect as a result of the absence of Stx. Wells containing supernatant from H19 and 90-2380 showed rounding of the cells with nuclear condensation, increased cytoplasmic vacuolization, and detachment from the surface, all indicative of cell death owing to the presence of functional Stx. The presence of Stx was confirmed in all 36 of 36 STEC isolates tested with a sensitivity of 100% (Table 5B).

The neutralization assay was used to determine if an isolate is producing Stx1, Stx2, or both. A well containing confluent cell growth is indicative of the presence of that toxin type, while cell death is indicative of the absence of that toxin type. All wells containing the neutralizing antibodies against both Stx1 and Stx2 should show confluent cell growth. Of the 36 isolates tested, only 24 (sensitivity of 67%) were correctly identified by neutralization assay as Stx1, Stx2, or Stx1/Stx2 carrying isolates. Of the remaining 12 isolates, 10 carried *stx2* genes but were incorrectly identified as Stx1+/Stx2+ by VCA, while two carried *stx1* and *stx2* genes with one being incorrectly identified as Stx1+ and the other incorrectly identified as Stx2+ by VCA.

The time and cost requirements were combined for the VCA and neutralization assay as both tests were run for each sample. A total of approximately 96 hours was required to complete the two assays, of which approximately 4.5 hours were hands-on time; the remainder was required for host cell confluence development and/or development of measurable cytopathic effects. The cost per sample was approximately \$24.78, which does not take into account the cost of capital infrastructure.

#### 4.3.2. Polymerase chain reaction

A total of 60 FWS STEC isolates were tested using PCR for detection of Stx genes, including the 36 isolates tested using the VCA. The results show that the Paton primer set was able to produce amplicons of the expected size: *hlyA* (534 bp), *eaeA* (384 bp), *stx2* (255 bp), and *stx1* (180 bp). Analysis of the agarose gels showed the positive control strain #7 (*hlyA*+, *eaeA*+, *stx2*+, *stx1*+; obtained from the NML Division of Enteric Diseases) has bands of the required base pair size (lane 2, Figures 15A, 15B, 15C, and 15D). As well, the no template control (NTC) did not yield any bands (lane 17, Figure 15D).

Previous laboratory testing-based characterization of the 60 isolates did not include information regarding the presence of *hlyA* and *eaeA*; therefore the isolates were only analyzed for the presence of *stx1* and *stx2* genes. Of the 60 isolates tested, 58 were correctly identified (Table 5C). The assay exhibited a sensitivity of 97%. The isolates chosen for PCR testing were previously characterized as Stx-positive using whole genome sequencing. Further investigation determined that the two false-negative isolates were of the subtype Stx2f. Samples of this subtype cannot be detected with the Paton primer set and require amplification with an additional set of Stx2f-specific primers (not done).

PCR detection of Stx genes requires substantially less time and money compared to the VCA and PRM assays. From culture, Paton PCR testing of one isolate requires approximately 8.5 hours total time, with 1.5 hours of that being hands-on; the remainder was for instrument and submarine gel electrophoresis run time. The cost per sample of running the Paton PCR assay is \$2.88 per sample. This is due to the simple sample preparation and low-cost reagents. As well, PCR requires only a small investment in capital compared to what is required to run the VCA and PRM assays.

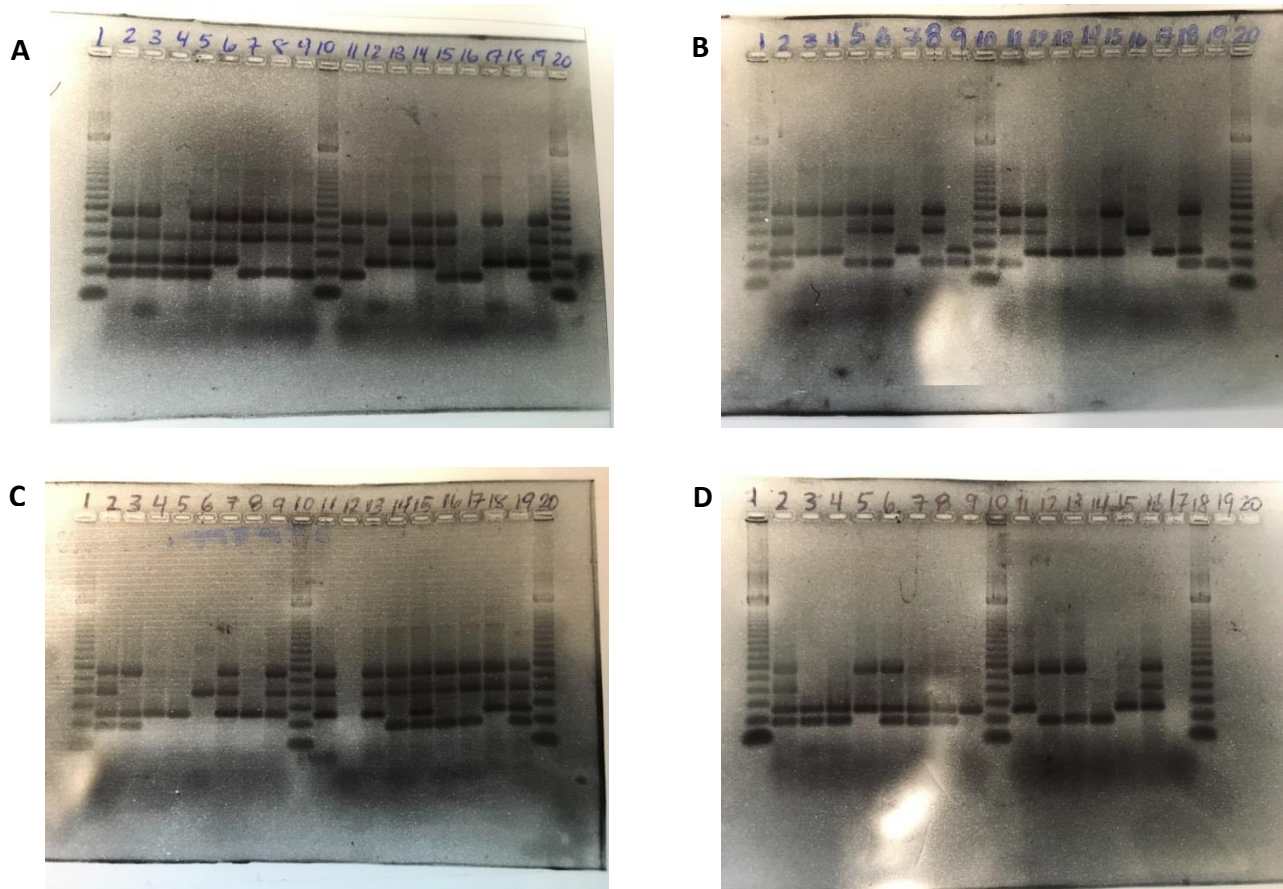


**Figure 15.** Submarine agarose gel electrophoresis analysis of Paton PCR products. Above are the results from PCR analysis of the 60 Stx-positive isolates. A 1.8% agarose gel with GelRed™ was used to visualize the Stx PCR products. Lanes 1, 10, and 20 (lane 18 in gel D) contain the 100 bp DNA ladder. Lane 2 contains positive control strain #7 (*stx1* is 180 bp, *stx2* is 255 bp, *eaeA* is 384 bp, and *hlyA* is 534 bp in size). Lane 17 in gel D contains the no template (negative) control. Lane 16 in gel B and lane 6 in gel D contain the two Stx2f isolates that were falsely identified as negative for Stx (10-8265, 10-8279).

## 5. Discussion

This thesis leveraged two popular and current proteomic approaches, shotgun and targeted proteomics, to create an assay that was capable of detecting Shiga toxin from clinical bacterial cultures. Diagnostic testing requires a fine balance between providing the sensitivity and specificity required for confidence in the results and ensuring there is high enough throughput for efficiency of testing. Mass spectrometry-based approaches have previously been implemented for detection of metabolites, disease markers, and bacterial diagnostics, but never before using a targeted PRM approach for rapid, laboratory-based bacterial diagnostics to our knowledge. Although the mortality rate for STEC infections is low, the long term complications that arise can affect the long term health and wellbeing of the patient long after the acute infection has cleared<sup>1, 48</sup>, and treatment of STEC infections with antibiotics is contraindicated as they can lead to worsened patient outcomes and progression to HUS<sup>1</sup>. The goal of this research project was to generate the groundwork for developing a targeted MS-based Stx detection assay and examine its feasibility to improve upon the limitations of current Stx characterization techniques used in laboratories today.

### 5.1. Shotgun Proteomics: Characterizing Shiga toxin Induction

The regulation of Shiga toxin production is complex. As with any biological system, many factors play a role in Stx production and distribution of toxin within the host. The first objective of this study was to employ iTRAQ® methodology coupled with LC/MS/MS analysis to determine the appropriate induction timeline and fraction for optimal detection of Stx. This iTRAQ® approach was the first step in building a targeted mass spectrometry assay for detection of Stx from cultured bacteria, as assembly of a workable sample preparation method is a critical requisite towards the larger thesis goal of MS-based Stx detection. Without first optimizing the sample preparation procedures, it would be unclear whether the proper sample fraction (cell pellet or culture supernatant) and the appropriate duration of phage

induction (1hr, 2 hrs, or 3 hrs) was being used. As anticipated, the results confirmed that these experimental parameters significantly alter Stx production and detection, thereby impacting the performance and the potential outcome of the final assay. The iTRAQ® experiment was used to provide primary in-depth proteomic analysis of the MMC induction timeline, and ultimately determined that at two hours post-induction, the cell pellet fraction would provide the best opportunity to detect Stx. Affected by numerous other influencing factors (e.g. complex bacterial protein matrix) and constraints (such as laboratory consumables, equipment, and workflows), sample preparation represents a dynamic laboratory procedure that likely requires further refinement(s) for optimization.

### **5.1.1. Methodology and analysis**

iTRAQ® direct labeling methodology was used for the optimization of STEC sample preparation because it conveniently allowed side-by-side comparative assessments of Stx protein levels. iTRAQ® reagents label peptides by directly reacting with primary amines of amino-termini or lysine residues. During MS/MS, the iTRAQ® reporter ions (specific to each sample) are released upon collision-induced dissociation, and their relative intensities are measured by the detector. Compared to other labelling methods, application of the iTRAQ® direct labelling approach allows sets of up to four samples to be run in parallel, promoting decreased instrument run-times and limiting run-to-run variability<sup>94</sup>. Studies comparing iTRAQ® to other isotope labelling methods, including differential gel electrophoresis and isotope-coded affinity tags, have determined that iTRAQ® is the most sensitive isotope-based method<sup>94</sup>.

Compared to label-free methods, isotope labelling is generally thought to offer higher reproducibility in quantitation, although studies comparing label-free and labelled quantitative proteomic analysis have provided mixed results<sup>94</sup>. Trinh and colleagues determined that there was no difference between the distinct labelling methods; yet they concluded that there was a slight advantage in quantifying significantly regulated proteins using the label-free methods<sup>94</sup>. The thesis iTRAQ® experiment was

originally designed to assess global proteomic changes occurring in STEC following MMC induction. As we expected wide-ranging proteomic changes in response to induction, iTRAQ® labelling was chosen for comprehensive comparison and relative quantitation since it provides opportunity for in-depth analysis of global proteomic variation<sup>94</sup>.

In addition to the different labelling methods, multiple analysis tools are available for secondary analysis to infer, visualize, and assess both labelled and label-free MS/MS results. Scaffold Q+ uses Bayesian statistics in combination with the outputs from search programs to estimate peptide and protein identification probabilities<sup>94</sup>. It has been reported that Scaffold Q+ software is able to reduce false-positive protein identifications and improve confidence in the protein identification process<sup>95</sup>. Scaffold Q+ is used for secondary analysis of iTRAQ® experiments in the MSP Core (NML, Winnipeg, Canada) as it provides a user-friendly interface with reliable quantitation and statistics (Garrett Westmacott, personal communication).

### **5.1.2. Appropriate fraction and induction time**

Initial pre-MSc. experiments, performed by Dr. Clifford Clark (Division of Enteric Diseases, NML), used iTRAQ® and 2D-LC/MS/MS for detection of global proteome changes, which included assessments of Stx1 and Stx2 (data not shown). At the time, the procedure was designed to look only at bacterial cell pellet fractions without using a phage lytic cycle inducer, such as MMC. As well, no set guidelines were known regarding which point of the bacterial growth phase should be used for MS analysis. Repeatedly, Stx could not be detected from cell pellets in the course of these prior experiments. This knowledge led to the hypothesis that toxin would be detectable if the cultures were treated prior with MMC for the purpose of inducing phage and Stx production. We elected to investigate this in cultures grown to OD<sub>600</sub> of 0.5 to ensure the bacteria were in logarithmic growth phase, which is the optimal phase for production of proteins. Protein production decreases as the cell enters the stationary phase and protein

degradation can begin to occur. Finally, since Stx seemed to not be detectable in cell pellets, it was hypothesized that the toxin may be detectable in MMC-induced culture supernatants.

The data acquired via 2D-LC/MS/MS for two representative but distinct serotypes of STEC after MMC induction has determined the sample fraction and induction time parameters appropriate and necessary for optimum detection of Shiga toxin using MS. Although distinct induction timelines were observed depending on the fraction analyzed (cell pellet vs. culture supernatant), the duration of induction time (no MMC, T=1, T=2, or T=3 hours), and the toxin subunit (subunit A vs. subunit B) (Tables 5 and 6), we successfully derived a set of parameters to reproducibly detect Stx peptides by MS.

The Stx1 A and B subunits were reproducibly detected in the cell pellets of both 87-1215 and 02-6737, but aside from the B subunit of 02-6727, Stx1 was not detectable in the culture supernatants under any of the tested conditions (Figure 12). Previous research determined that expression of Stx1 does not involve significant lysis of the bacterial cells and that Stx1 is not excreted into culture supernatants<sup>41, 98</sup>. Our data (Stx1 not detected in TCA-precipitated culture supernatants; Results section) concurs with this observation. We concluded that Stx1 would not be detectable in future planned experiments if culture supernatants were employed. We also decided to continue with the cell pellets since precipitating proteins from culture supernatant required large volumes (26 ml) of TCA, plus an additional 24 hours. Given the difficulty of working with hazardous TCA (considered an irritant by ingestion, and inhalation; additionally corrosive in the case of skin and eye contact) and the prohibitive additional time required, cell pellets were deemed the appropriate fraction to use for future experiments, and culture supernatants were not used in later experiments.

In contrast to Stx1, the research literature states that Stx2 is released from bacterial cells and is found in higher concentrations in culture supernatants than in cell pellets<sup>98</sup>. Our data did not support this claim

as the relative amount of Stx toxin peptides were higher in the pellet when compared to the supernatant at T=2.

We observed a plateau in the culture supernatant from the Stx2 B subunit (87-1215) and the Stx2 A and B subunits (02-6737) between T=2 and T=3. We hypothesize that for 87-1215, where complete cell lysis produced a gelatinous pellet at T=3, the Stx2 proteins may have re-associated with the rather sticky pellet simultaneously accounting for the plateau of Stx2 toxin peptide levels detected in the 87-1215 culture supernatants and for the cumulative increase in toxin measured in the pellets at T=3. This theory did not apply to the 02-6737 cell pellet as there was no gelatinous pellet observed. We hypothesize that for this isolate there simply was no more Stx being released from the lysed bacterial cells and the Stx levels remained constant.

Although there were often higher Stx levels after three hours of MMC induction, this time point produced gelatinous pellets that required additional time and materials to complete the sample processing workflow. As one of the main goals of laboratory testing is to promote efficiency by reducing the complexity and turnaround time of sample preparation, and in a manner that is universally applicable to all strains, the 3-hour induction time point was deemed too cumbersome. Hence, a shortened, two-hour MMC induction timeframe was deemed likely sufficient for robust Stx toxin detection (sufficient toxin production to provide detection by MS) without such problematic cell lysis.

In general, higher relative amounts of Stx2 peptides were observed compared to Stx1 peptides at the 2-hour induction time point (data not shown). Studies have shown that patients infected with isolates expressing Stx2 are at higher risk for developing HUS and tend to experience more severe infections<sup>2, 25, 34</sup>. As well, *in vitro* studies have demonstrated that purified Stx2 is 1,000 times more toxic to human renal endothelial cells than is Stx1<sup>34</sup>. Higher levels of Stx2 were detected relative to Stx1 in our tested strains, which may explain why infections with Stx2-producing STEC are associated with more severe

disease. There is also evidence to suggest the level of toxin production is influenced by which subtype of Stx2 is harboured within the phage. Ogura *et al.*<sup>34</sup> measured the difference in toxin production via reversed passive latex agglutination between different Stx2 subtypes and determined that higher Stx levels were seen for toxin subtype Stx2a<sup>34</sup>, the subtype encoded by 87-1215. Ogura and colleagues did observe highly variable Stx2 production levels for O157 STEC strains (i.e. large strain-to-strain variation exists)<sup>34</sup>. This could mean that if our experiments were repeated with multiple Stx2a-producing isolates, the results may vary. With that being said, we still hypothesize that Stx2-producers would have higher toxin expression levels compared to Stx1-producers when studied with an expanded panel of STEC isolates.

### **5.1.3. Limitations**

Cumulative technology improvements over the past decades have allowed a deeper look into the proteomes of complex bacterial samples, but as with many shotgun proteomic experiments, detection and characterization of every single expressed protein is difficult. Often only the most highly abundant proteins are identifiable from samples, overwhelming the lower abundance proteins and the ability of the mass spectrometer to detect them. Another substantial drawback of shotgun proteomics is the common occurrence of “missing data” between replicate runs, where lower-abundant peptides may be detected in some replicates but not others. This type of situation can complicate the statistical analysis and make it hard to compare between replicates<sup>76</sup>. We also observed complicating variability in our iTRAQ® data set, with several large log<sub>2</sub> FC inconsistencies between replicates and run-to-run variability (lack of reproducibility) resulting in peptides being identified in one run, but not another. Not only does this cause a problem for quantitation, but it also complicates statistical analysis and interpretation between replicates of the same run<sup>76</sup>.

The statistical analysis represented another limitation of the study. As reported in 4.1. *Shotgun Proteomics: Characterizing Stx Induction*, many of the Stx1 and Stx2 results were not considered statistically significant by Scaffold Q+ software (including the Stx1 A and B subunits in the 02-6737 cell pellet, the Stx1 B subunit in the 02-6737 culture supernatant, and the Stx2 A and B subunits of the 02-6737 cell pellet). The lack of significance could be due to variation in  $\log_2$  FC between biological replicates. iTRAQ<sup>®</sup> has been known to have high relative variability between replicates, especially in low-abundant proteins<sup>99</sup>. Tertiary analysis using technical replicates would be required to determine how much variability exists between runs. Although our results were deemed not statistically significant using Scaffold Q+ software, we did consider them to be biologically significant. Our reasoning is that the data exhibited Stx detection trends that are complementary to those previously described in the literature for STEC isolates induced using MMC<sup>97, 100</sup>.

#### **5.1.4. Future considerations for sample preparation**

Sample preparation is one of the most integral steps in laboratory testing. The most sensitive and specific assays can be undermined if pre-detection sample processing is not optimized. Additionally, appropriate sample preparation is pivotal to ensuring assay repeatability and robustness. As important as sample preparation is, sample workflows can be time consuming. The bare minimum requirements for MS sample preparation are: extracting the protein, enzymatically digesting the proteins into predictable peptides, and, for complex samples, separating/purifying the peptides, each potentially achievable by several distinct methods. Sample preparation needs to be rapid, but also must ideally retain maximal amounts of targeted peptides. This is especially important in STEC samples, as some isolates naturally produce only small amounts of Stx.

Sample preparation and data analysis remain the rate-limiting steps within these thesis experiments. With an ever-growing number of commercial kits and in-house made reagents, several steps could

potentially be shortened, or even combined, to reduce the turnaround time between sample submission and reporting of results. For example, Charretier *et al.* were able to perform bacterial cell lysis and trypsin digestion within approximately one hour. In their method, suspended bacterial cells were collected by centrifugation for 15 minutes, the resultant pellets were resuspended in a reducing solution containing DTT with glass beads and rapidly disrupted using an ultrasonic probe for 5 minutes, proteins were alkylated for 5 min using IAA, and the alkylated peptides trypsin digested at 50°C for 15 minutes<sup>81</sup>. The downside of the Charretier *et al.* protocol is that digestion with trypsin for short amounts of time can reduce the digestion efficiency and lead to variable or in-complete digestion. As well, the Charretier *et al.* experiment was performed on *Staphylococcus aureus*, which does not require any form of induction prior to detection of the target peptides. Despite the fact that the iTRAQ® experiment is not the basis for the final PRM-based MS assay, it highlighted that requisite Stx induction complicates our sample preparation approach.

The first objective of this thesis experiment provided data that aided in the development of a sample preparation procedure that could be used to detect Stx1 and Stx2 from clinical cultures. Although it may not have been optimal in regards to efficiency, it provided a robust method required to continue moving forward with the development of a targeted MS-based PRM detection approach (Objective 2). Analysis of the MS-detectable proteome allowed us to compare and contrast the induction timeline and fractions for the two tested isolates. The MMC induction timeline for Stx is just one example of many differences that should be observed between two isolates differing in serotype (hence their genomic context) within the same bacterial species.

## **5.2. Targeted Proteomics: Characterizing Stx induction**

The results from our small-scale study show promise for a MS-based Stx detection assay. Others have used targeted MS for detection of metabolites in blood and urine<sup>88</sup>, as well as a study similar in concept

that used Selected Reaction Monitoring (SRM) to detect *S. aureus* peptides for identification, resistance, virulence, and type profiling from bacterial colonies or positive blood cultures<sup>81</sup>. These foundational studies, particularly that of Charretier *et al.*, were used as proof-of-concept material to guide the development of our Stx PRM assay.

The second objective of this study was to create a Stx detection assay using targeted MS methodology. Primary analysis was performed using the QE+ mass spectrometer. We were able to detect the targeted Stx peptides from the majority of the tested STEC clinical bacterial isolates, which were chosen to represent a large number of STEC serotypes and toxin subtypes from the NML Division of Enteric Diseases collection. It is also important to point out that the assay did not detect any Stx peptides in all Stx-negative isolates, providing solid evidence that this assay should not generate false-positive results. Our proof-of-concept approach targeting Stx indicates that MS-based detection methods are a viable option that could be useful for future reference laboratory testing, and potentially for clinical diagnostic testing.

### **5.2.1. Shiga toxin peptide identification**

Prior to development of the targeted Stx detection assay, data-dependent mass spectrometry analysis of Stx1a and Stx2a trypsin-digested proteins was performed to determine which Stx peptides could be detected by the mass spectrometer. This prerequisite assessment was essential in the development of the targeted MS assay as it provided valuable information on the uniqueness of the sequence and retention time of the peptides. As listed in the thesis Introduction, the targeted peptides must meet certain minimal criteria. None of the selected peptides contained a methionine or a cysteine. The peptides chosen to develop the Stx PRM detection assay were checked for specificity by searching them against the public Protein BLAST database containing all known protein sequences. The sensitive BLASTP analysis revealed that the amino acid sequences of the chosen peptides matched only to Shiga toxin,

and therefore we could conclude that at the time of the search they were proteotypic. A few of the peptides had similar observed retention times, especially three Stx B subunit peptides (namely YNDDDTFTVK, YNENDTFTVK, and YNEDDTFTVK), which differ from each other by only a single amino acid. Despite this, we elected to retain all three of these peptides as all isolates produce at least one of them.

Once the list of target peptides was determined, multiple method development runs (Supplementary Tables S1, S2, and S3) using both trypsin-digested Stx proteins (which are relatively pure, actual proteins) and synthetic peptides were performed to refine both the MS methods and the sample preparation methods. For example, it was determined that the TNNVFYR peptide provided weak signal when run in cellular matrix; for this reason, TNNVFYR was removed from all of the subsequent PRM assay development work.

The synthetic (surrogate) peptides were used to estimate the relative lower limit of detection (LLOD) for each target peptide. This LLOD information was important when assessing the sensitivity of the assay and determining its dynamic range (measure of the detection range of the detector)<sup>101</sup>. The lower the LLOD value for each peptide, the more sensitive the assay and the higher the probability that Stx it will be detected in samples where Stx production is low. It is ideal to have a large dynamic range as there will most likely be a very small amount of Stx target analyte and a large amount of other cellular proteins within the typical digested STEC samples. By comparing our LLOD values to those found in the literature, we determined that our Stx peptides exhibit similar reported LLODs to others data, which is into the attomole range<sup>114</sup>.

The PRM assay was derived using the interim information generated from the iTRAQ® and other method development runs, and by leveraging available draft genome data. A total of 11 peptides were included in the PRM assay for follow up assessment; experiments with clinical bacterial samples were expected to

reveal which additional target peptides might be removed from the final assay configuration. The process of creating an assay such as this is dynamic and refinement or adjustments are common as more information becomes available.

A recent publication by Silva *et al.* explored the use of SRM proteomics to detect Stx1 and Stx2 from bacterial cultures<sup>119</sup>. As mentioned in the Introduction, SRM assays tend to be more sensitive than PRM assays, but require longer development time since the MS system needs to be tuned to detect the targeted peptides. In contrast, PRM development requires less time and the assays are generally able to quantitate data over a larger dynamic range and provides more reproducible and accurate quantitation. This is an important feature when analyzing complex samples such as serum or stool. The SRM assay developed by Silva *et al.* looks to quantitate the different Stx subtypes by targeting only one B subunit peptide per subtype<sup>119</sup>. In comparison, our PRM assay has been developed to target peptides that are both common to all subtypes and distinguishable between subtypes. We believe that having multiple targets allows for better confirmation of Stx presence as some peptides may not always be detected in all samples.

### **5.2.2. Shiga toxin detection**

It was hypothesized that our PRM detection assay targeting 11 Stx peptides would be capable of detecting Stx within clinical bacterial isolates. The hypothesis was tested using a cohort of 91 clinical bacterial samples (62 STEC isolates and 29 non-STEC isolates). The data acquired from the QE+ mass spectrometer supported our hypothesis, with the assay detecting Stx in 56 of 62 (sensitivity and specificity of 90 % and 100%, respectively) Stx-positive isolates and not detecting Stx in all 29 Stx-negative isolates. To reiterate, secondary analysis was performed by manually analyzing the data using Skyline software. A Stx peptide was interpreted as “present” if it produced a dotp value of 0.85 or greater.

One of the Stx-identifying peptides, FVTVTAEALR, was found to be conserved in the A subunit of both Stx1 and Stx2. Of the 56 Stx-positive tested isolates, four had a dotp value of 0.85 or greater in this conserved peptide, but not in any of the other peptides. This result determined that these were Stx-positive isolates, but such a result did not provide further information regarding which toxin subtype was being expressed. Under such circumstances, these isolates would need to be sent for further characterization by other methods such as Paton PCR or the VCA neutralization test. At a clinical level, further characterization may not be as important, but public health laboratories and epidemiologists may require this additional toxin characterizing information for the tracking of outbreaks and sporadic cases. It also would give public health officials a better overview of STEC infections in Canada.

Of the six Stx-positive isolates where toxin was not detected by PRM, none of the isolates belonged to the same serotype and they covered a broad range of Stx subtypes (Stx1c (12-3003), Stx1c/Stx2b (10-2726), Stx2a (09-1765, 12-3002), Stx2b (09-0529), and Stx2e (06-3440)). Of these six isolates, five were run in parallel using the Vero cell assay, the gold standard for Stx functional assessment. In all five of those isolates, Stx was detectable via VCA detecting host cellular pathological effects. From this information, we hypothesized that these 6 false-negatives by PRM could have resulted from a limited or failed MMC induction, as we were relying on the induction procedure to produce MS-detectable amounts of Stx. Another hypothesis was that the isolates were carrying non-functional phages that could not be induced using MMC. The WGS data would have reported the presence of *stx* genes, but there would be no protein expression for MS detection.

The induction procedure was only optimized on two STEC isolates, both of which were different serotypes than the observed six false-negative isolates. Differences in genomic content and thereby toxin production have been observed between STEC isolates of differing serotypes<sup>4</sup>. Admittedly, the MMC induction procedure we devised may not be optimal for all STEC serotypes and strains; moreover

it may not be optimal for Stx-carrying non-*E. coli* isolates such as *Shigella*. It is possible that some strains or serotypes will require a different duration of MMC induction, which was not investigated beyond three hours in this work. Additionally, the difference in amount of toxin proteins found in cell pellets could be due to the observed gelatinous and problematic pellet generated for some isolates following longer term MMC induction. Given that the sticky pellet was not observed for all isolates, we speculate that the amount of toxin proteins remaining as detectable (owing to variation in their association with the cell pellet) will differ between isolates.

Additionally, five of the six PRM-assayed false-negative isolates were confirmed Stx2-producers. The experiments from the first objective led us to choose cell pellets for Stx detection, as per reasons outlined in 5.1.2. *Appropriate fraction and induction time*. Given that Stx2 is known to be released from the cells during lysis<sup>41</sup> it is possible that most, if not all, of the Stx2 proteins were released into the supernatant for these strains. We did not explore further to support or refute this issue.

We determined that the devised sample induction procedure is specific to STEC isolates, by including two *Shigella* isolates in the 29 non-STEC clinical cultures. The two *Shigella* isolates were previously characterized as *stx*-positive but Stx was not detected when they were induced under the same conditions as the STEC isolates and analyzed by PRM. As stated in the Introduction, the Stx produced by *Shigella* isolates is closely related to the Stx1 produced by STEC isolates, but is encoded on the bacterial chromosome rather than within an integrated bacteriophage. We have concluded that this additional PRM specificity has both advantages and disadvantages. Specificity is important if the goal of this assay is to detect Stx from STEC isolates only. For example, *Shigella* infections are routinely treated with antibiotics, specifically, those that are contraindicated for treatment of patients with STEC infections<sup>102</sup>. Stx is not produced in *Shigella* under MMC induction conditions as the *stx* genes are chromosomally encoded and not under control of the phage. We believe that with this induction procedure it is likely

that when Stx is detected in an isolate by PRM it is because it is due to STEC infection and not due to infection caused by another bacterial species. This idea would have to be further validated with a larger cohort of non-STEC samples to confirm the hypothesis. On the other hand, since Stx is found on mobile genetic elements, it can be transferred between different species, as observed with the new Stx1e subtype. This could pose a problem if the goal of the PRM assay is to simply detect Stx regardless of the bacterial species harbouring the genes. When designing a sample preparation procedure for Stx detection from all bacterial species, it may not be possible to induce toxin production in all Stx-carrying isolates using a generic MMC induction time course combined with alternate culturing conditions (media).

### **5.2.3. Shiga toxin 2 subtyping**

Without performing any additional testing, the PRM Stx detection assay was designed to provide subtyping information on the Stx2-carrying isolates. Evidence shows that isolates carrying Stx2 subtypes are more likely to cause severe disease in humans<sup>103</sup>. Infections caused by Stx2 subtypes tend to have a higher risk of the patient progressing to HUS, as well as experiencing severe long-term sequelae. Differences in toxicity between Stx2 subtypes also have been noted<sup>103</sup>, emphasizing the importance of rapid subtype determination. Certainly, toxin subtyping is important from the perspective of bacterial disease surveillance. It was hypothesized that Stx2-carrying isolates could be subtyped using the same PRM assay created for Stx detection. Subtyping (as we proposed by PRM) relied on both the detection of Stx2 peptides (dotp of 0.85 or greater) and the mapping of those peptides to a subtype using its unique peptide fingerprint. A total of six unique peptide fingerprints can be used for Stx2 subtyping by PRM, five fingerprints are unique to only one subtype (Stx2a, 2b, 2c, 2d, and 2f); whereas Stx2e and 2g share identical fingerprints that are distinct from the others. Hence, a total of six toxin subtype determinations can be made (Stx2a, 2b, 2c, 2d, 2f, and 2e/2g) based on PRM peptide fingerprint detection. Fortunately

Stx2e and 2g are rarely implicated in human infections to date; consequently, distinguishing these subtypes may remain less crucial from a human public health perspective<sup>29, 104, 105</sup>.

In contrast to our hypothesis, not all Stx2-carrying isolates could be subtyped using the PRM peptide fingerprint scheme. Stx2 peptides were not detected in six of the Stx2-carrying isolates, which is a prerequisite for typing. Reasons for these six false-negative results are not known at this time, although we suspect it may be attributed to MMC induction complications. As subtypes 2a, 2c, and 2d are most often linked to the development of bloody diarrhea and HUS<sup>105</sup>, identification of these subtypes is important. Importantly, our PRM method was successful at subtyping most 2a isolates and all 2d isolates, but was unable to subtype the two isolates carrying Stx2c. Unfortunately, for some subtypes only a small number of isolates were available for testing using the PRM assay, making it difficult to ascertain the underlying reason(s). An expanded strain test panel is required to assess whether the PRM approach will be capable of confidently identifying all Stx2 subtypes in a majority of isolates.

There were seven Stx2 isolates where Stx2 subtyping was unsuccessful because their fingerprints did not match any of those in the scheme. One of the tested isolates carried two Stx2 subtypes, which created a situation where all peptides were detected. It is unlikely that isolates carrying two subtypes will be typeable using this scheme. The remaining six isolates were not matched with the incorrect subtype, but instead their pattern simply did not match any of those from Table 6. There was never a case where peptides were detected when they should not have been, there were only instances where peptides were not detected when they should have been. Undetected peptides could be caused by having a concentration below the LLOD, or that peptide may not have been sampled since we were only injecting 5 µl from a large volume of sample. Consequently, while these samples would be correctly reported by PRM as Stx2-positive, they would lack further sub-classification into a toxin subtype. Despite this PRM subtyping shortcoming (having less than 100% typability), we feel that PRM remains promising and is

worth further exploration. Perhaps PRM cannot subtype every single strain; however, Paton PCR and subsequent *stx* gene subtyping may only be required when PRM subtyping was inconclusive. If used in this manner, PRM may serve to reduce the bulk requirement for other Stx2 molecular subtyping volumes, thereby improving laboratory operations.

One study found that of 132 STEC isolates found in fresh produce, 20 of them carried multiple Stx2 subtypes. Of the 20 isolates, 17 of them carried a combination of Stx2a and Stx2d, while the other three isolates carried a combination of Stx2a and Stx2c<sup>120</sup>. In contrast, only two of the 350 FWS STEC isolates from the NML contained multiple Stx2 subtypes (one isolate carrying Stx2a and Stx2b, the other carrying Stx2a and Stx2g). Our subtyping scheme is not able to distinguish between Stx2 subtypes in isolates carrying more than one Stx2 subtype. Further investigation into the true prevalence rate of STEC isolates carrying two Stx2 subtypes would be required to determine if our subtyping scheme would be of value in a real-world situation.

#### **5.2.4. Comparison to common Shiga toxin detection methods**

Overall, this targeted MS-based PRM assay has been able to provide an alternative to traditional serological and molecular detection techniques, such as cell culture assays, PCR, and enzyme immunoassays. According to Fusaro *et al.*, antibodies are only available for a very small number of proteins, limiting the number of targets that can be used for certain detection assays and alternative diagnostic approaches must fill the void that immunoassays cannot address<sup>85</sup>. Mass spectrometry is a promising approach that allows for detection of almost any expressed protein of interest without the extensive time and costs associated with development of antibodies. To continue the evaluation of our PRM assay, a subset of the Stx-positive clinical cohort samples were run in parallel using the VCA and Paton PCR for a comparison of overall performance, specificity, and assessment of their labour requirements and cost.

The Vero cell assay coupled with the neutralization assay has historically been considered the “gold standard” for functional Stx detection<sup>63</sup>. The VCA correctly detected functionally active toxin with a sensitivity of 100% in all Stx-positive samples tested, whereas the PRM assay detected expressed Stx with a sensitivity of 90%. Given that other bacterial products or toxins within the sample supernatant aside from Stx could produce the observed cell cytotoxicity during the VCA, positive VCAs are always followed up with an anti-Stx antibody-based neutralization assay to confirm the presence of Stx toxin<sup>63</sup>. Use of Stx1- and Stx2-specific antibodies alone or in combination allows the lab technician to determine whether the tested isolate is carrying Stx1, Stx2, or both. Of the 36 isolates tested with the neutralization assay, the Stx type present was only correctly identified in 24 (sensitivity of 67%) samples, with no subtype determinations.

A downfall of the neutralization assay is its reliance on specific antibodies and functional Antigen:Antibody interactions for Stx toxin confirmation. Development of specific antibodies is time consuming and costly, and decreases the feasibility of routinely performing this assay as a rapid turnaround diagnostic test. It was previously mentioned that the newly discovered Stx1 subtype, Stx1e, was not neutralized by existing anti-Stx1 monoclonal antibodies; thus isolates carrying Stx1e would show VCA cytopathic effects but the toxin would be unconfirmed. Developing new antibodies every time another Stx subtype is discovered is not practical. As well, costly maintenance of antibody stocks will continually be required. With the PRM detection assay, once a new subtype is discovered and sequenced, it can quickly undergo an *in silico* digestion to determine if the novel amino acid sequence contains a unique peptide sequence or a more conserved peptide, such as FVTVTAEALR. Synthetic peptide(s) can be quickly ordered to determine the retention time on the mass spectrometer and the LLOD. After one determines that the new target peptide(s) can reliably be detected, it should easily be incorporated into any existing PRM assay. This process can be completed as many times as needed, as

PRM assays can be multiplexed for 100's of targets<sup>82, 84, 88</sup>. This degree of PRM assay flexibility is advantageous in detecting an evolving pathogen such as STEC.

When we conducted the Paton PCR assay, we determined that the PCR assay was able to detect Stx with a sensitivity of 97% in Stx-positive isolates tested, versus the PRM assay, which had a sensitivity of 90%. Hence, PCR was able to correctly detect a higher percentage of Stx-positive isolates. No false-positive results were obtained with either Paton PCR or the PRM approach. Advantageously, with the Paton primer set there are no additional tests required to determine if the tested isolate is producing Stx1, Stx2, or both. However, additional PCR testing reactions with a subtype-specific primer set and gel electrophoresis is required to determine the isolate subtype, with additional time and cost for subtype results. In contrast, the PRM assay conducts both toxin detection and subtyping.

Gene-based detection methods, such as PCR, can create issues for phenotypic characterization of bacterial isolates since the presence of a gene does not always result in the presence of functional protein<sup>119</sup>. Overall, isolates can display variations between their genotypes and their phenotypes. An infected patient may have Stx genes, *stx1* and *stx2*, both present within their infecting organism's genome, but that does not necessarily mean that the toxin has been transcribed and translated into a functional protein. The detection of *stx* genes may lead to false-positive predictions of actual toxin protein presence or function. As well, presence of DNA within laboratory environments and on instruments used to prepare the samples has been shown to produce false-positive pathogen detection results<sup>106</sup>. One benefit of using MS-based detection, such as the PRM assay, is its ability to infer the presence of the expressed Stx protein through the detection of its digested peptides.

Commonly used Stx detection assays have been extensively optimized and field tested for decades, but there is still no single assay that is yet able to accomplish rapid, inexpensive detection with high sensitivity. In comparison, our PRM assay development is still in its infancy. As the results show, PRM

was unable to identify Stx in all STEC isolates tested, something that the VCA and PCR (with exception of isolates carrying Stx2f) were able to accomplish. With additional refinement of the MS methods (such as including stable isotopically labelled peptides), along with optimization of the sample preparation, we believe that the PRM Stx detection assay will be able to outperform the techniques currently used in both clinical and reference testing laboratories.

#### **5.2.5. Limitations of the PRM detection assay**

As development and assessment of the Stx assay progressed for this thesis, it was clear that the laborious sample preparation and high cost associated with preparing STEC samples were not going to be a good fit within a clinical setting in which speed and ease of use are of utmost importance. At this point, we now believe that the PRM assay would be a better fit for federal or provincial reference testing laboratories, where more epidemiological studies, surveillance, and characterization of isolates is performed. Future technology advancements and improvements in laboratory workflows may later allow for the transition of a future iteration of this PRM assay or approach in a clinical setting.

Overall, the issues experienced in the development of this Stx-detecting PRM assay had little to do with the mass spectrometer itself, but with the preparation needed to get the STEC samples ready for analysis. In simplest terms, the biology of Stx toxin production was the issue. Owing to the need for MMC induction of the phage, sample preparation for STEC isolates is not straightforward. Toxin production is dependent on many factors, including the isolate serotype and toxin subtype. As mentioned above, it has been shown that the amount of toxin produced is variable. Together these pose problems when designing a standard method for preparing the samples. As was observed with the *stx*-positive *Shigella* samples that underwent the sample preparation but did not produce detectable Stx toxin, one universal method may not exist that is going apply to all Stx-positive isolates. There may not be a one-size-fits-all approach for preparing samples from Stx-positive isolates.

In addition to the limitations imposed by the PRM assay itself, one must also consider the expensive capital that is required to perform an assay such as this. Smaller or underfunded laboratories would not be able to afford a mass spectrometer that is capable of performing PRM. It may be easier to justify the cost of a mass spectrometer if there are multiple assays that it can be used for. As more assays or highly multiplexed assays become more common, laboratories may be able to consider replacing multiple systems with one instrument that is capable of doing more kinds of analyses.

## **5.2.6. Future steps**

### **5.2.6.1. Sample preparation**

The described experiments and results provide evidence that a MS-based Stx detection assay has the potential to replace standard means of lab testing currently in use. Our PRM assay was able to detect Stx peptides and provide Stx2 subtyping results for most isolates within a single assay, reducing the number of samples requiring further Stx2 subtype testing. With additional optimization within the different workflow areas of the PRM assay, such as sample preparation to determine optimal induction conditions, PRM may be able to provide sensitivity and specificity that rivals what current assays offer, yet with increased throughput.

Through the validation of the PRM assay, we discovered that there were six previously characterized Stx-positive isolates that could not be identified using the PRM assay. These samples were not repeated or further examined to determine the reasoning behind the false-positive result, which should be further looked into. As well, the assay should be validated with a larger cohort of bacterial samples to ensure the induction sample preparation is applicable to varying subtypes and serotypes. This would also help us determine if the Stx2 subtyping scheme can be applied.

In order to provide a rapid diagnostic test, sample preparation should be performed in the shortest amount of time. A bottleneck in STEC sample processing is obtaining the bacterial culture from a stool

sample. It requires overnight incubation on agar plates, delaying detection. Testing directly from stool can reduce the time between receiving the sample and beginning testing. Unfortunately, STEC detection from stool can be difficult. Overall, presence is confirmed in approximately 30-69% of patients with clinical signs and symptoms, as STEC cfu decreases rapidly after symptom onset<sup>59, 107</sup>. As well, the concentration of free fecal Shiga toxin is generally low<sup>59</sup>, making it difficult to directly test from stool without concentrating the protein. With that being said, after initiation of this thesis project, quantitative analysis of Stx concentrations in stool from an EHEC outbreak in Japan revealed that Stx was detectable in patient stool samples without pre-treatment using a bead enzyme-linked immunosorbent assay (bead-ELISA) immunoassay<sup>108</sup>. This Yamasaki proof-of-concept experiment suggests that Stx proteins are present in detectable amounts in stool; however, the feasibility for detecting Stx toxins by MS directly from stool has not yet been tested and was beyond the scope of this thesis. We suspect that for low Stx-producing isolates, Stx capture (e.g. with antibodies) or prior processing of complex stool specimens by other means will likely be necessary.

The FDA still recommends simultaneous culturing in addition to molecular methods of detection; therefore, we may never get away from culturing the isolate. Further molecular characterization can then be performed for epidemiological data at a reference laboratory.

The future of laboratory diagnostics is likely heading in the direction of microfluidics, or “lab-on-chip” technologies. These devices will be able to automate sample preparation by performing all of the steps on one chip, reducing labour and contamination concerns<sup>106</sup>. Our PRM may be able to take advantage of microfluidics to help automate the long PRM sample preparation.

#### **5.2.6.2. Absolute peptide quantitation**

PRM mass spectrometry is a dynamic discipline that allows an investigator to easily expand a developed assay to perform additional duties. The Stx detection assay that was developed herein was used simply

to determine the presence or absence of Stx within a sample. However, targeted proteomics is able to do much more than that, including quantifying the amount of target present within the sample. Quantifying toxin concentrations is important because isolates producing large amounts of toxin tend to cause the most damage on the host, and those patients also have a higher chance of progressing to HUS and having severe sequelae, such as end-stage renal disease. To accomplish this, stable isotopically labelled (SIL) internal standards would need to be incorporated into the assay to provide toxin expression levels. This would appropriately extend the PRM assay as a lab test that also infers the relative “degree of pathogen risk”.

Not only do SIL internal standards allow for quantitation of the targets, they are also important in method development. For example, during the development of the PRM Stx detection assay the LLOD was determined by serial diluting a known concentration of synthetic peptide and manually analyzing the minimum concentration in which the peptide could reliably be detected. A more accurate LLOD measurement could have been acquired with the use of SIL internal standards, allowing for a more reliable evaluation of the sensitivity of the assay. In addition, SIL internal standards allow for the measurement of the lower limit of quantitation (LLOQ), which is the lowest concentration that a target can be reliably quantitated at. Incorporating SIL internal standards not only will compensate for inefficiencies and losses during sample preparation, but also compensates for matrix effects during the quantitation of target peptides. According to Taylor *et al.*, matrix effects occur when an endogenous peptide co-elutes with the target peptide. The matrix effect can be measured using post-extraction addition, which compares the peak area of the targets spiked into a pure solution and a matrix background. If no difference in peak area is observed then a value of 100% is obtained. Any values above or below 100% imply the presence of ion enhancement or suppression, respectively. By incorporating an internal SIL standard, the matrix effect on both the target peptides and SIL peptide will be consistent, allowing for precise quantitation even in the presence of a large amount of background peptides<sup>109</sup>.

### 5.3. Broader applications

Mass spectrometers are versatile instruments that are being applied in many different disciplines, not just infectious disease diagnostics and molecular subtyping. The possibility of assays, such as the one developed in this thesis, that can and will likely be applied to multiple disciplines is almost endless. Described below are a few examples in which PRM is being applied or can be potentially applied for targeted proteomics.

For example, targeted proteomics can be used in a food safety capacity where it is used to detect pathogens in our food sources to prevent human illness<sup>110</sup>. Rapid testing in these situations is important to prevent or reduce the severity of outbreaks, but also prevents economic losses that could be incurred as a result of contaminated food products. In addition to food safety, targeted proteomics also can be used as a measure of food identity. One of many studies applying targeted proteomics was used to detect horse or pork meat disguised in beef products<sup>110</sup>. In another example, a PRM assay was developed to quantify the concentration of xenobiotics in honey. Researchers were able to create a simple sample preparation protocol to screen honey samples for 157 compounds in less than 15 minutes. Unlike conventional methods, this PRM assay was able to provide quick and high-throughput analysis of multiple contaminants in complex matrices<sup>111</sup>.

The use of targeted proteomics in the veterinary field also has expanded in the last few years. Although the proteomes of very few animal species have been studied, the benefit of proteomics within the field is becoming much more appreciated. Assays can be developed to detect animal pathogens, in a manner similar to assays being developed to detect human pathogens. Additionally, targeted assays have been developed to detect growth-promoting proteins and peptides in animals. Large-scale abuse of growth promoters has been reported to enhance muscle growth and milk production in cattle, as well as

performance enhancers in race horses. The goal of these targeted proteomic detection assays is to reduce the administration of growth promoters for health of both the animals and humans<sup>112</sup>.

## 6. Conclusion

The goal in developing any new diagnostic approach or applied technology is to improve upon what is currently in use for the betterment of human health diagnostics or laboratory operations. To the best of our knowledge, this is the first report of a targeted MS-based detection assay for Stx. Using a 91-isolate validation panel, our PRM assay was able to detect Stx proteins with a sensitivity of 90% and a specificity of 100%. In comparison, the Vero cell and PCR assays were able to identify Stx with sensitivities of 100% and 97%, respectively.

Although this MS-based detection assay is far from ready for implementation within a clinical laboratory setting, it is leading the way to improved detection of Stx from clinical bacterial cultures. At this point, it is more applicable in high throughput reference laboratories for the purpose of detection and surveillance of Stx toxin subtypes. In the future, MS-based techniques will be relied upon for their highly sensitive, reproducible, and accurate results.

As was mentioned previously, the PRM assay that we have developed to detect Stx has not been refined to a point where it yet has sufficient robustness to be introduced into a laboratory workflow. The PRM assay was able to detect Stx, determine if Stx1, Stx2, or both were present, and subtype most of the Stx2-carrying isolates, something that is not possible using either the VCA or PCR. We were unable to detect Stx in all STEC samples, but hypothesize that this may be due to limited phage induction rather than an issue of sensitivity of the mass spectrometer. This thesis has not only been valuable in the development of MS-based detection, but has also added to the fundamental understanding of Shiga toxin induction patterns, as well as contributed to the ever-expanding body of diagnostic research. Continuing research into optimal STEC sample preparation will be pivotal to developing a more robust PRM assay, particularly, for determining induction differences for strains of different serotypes and toxin subtypes.

## 7. References

1. Ho, N. K., Henry, A. C., Johnson-Henry, K. & Sherman, P. M. Pathogenicity, host responses and implications for management of enterohemorrhagic *Escherichia coli* O157:H7 infection. *Can. J. Gastroenterol.* **27**, 281-285 (2013).
2. Croxen, M. A. *et al.* Recent advances in understanding enteric pathogenic *Escherichia coli*. *Clin. Microbiol. Rev.* **26**, 822-880 (2013).
3. Durso, L. M., Bono, J. L. & Keen, J. E. Molecular serotyping of *Escherichia coli* O26:H11. *Appl. Environ. Microbiol.* **71**, 4941-4944 (2005).
4. Franz, E. *et al.* Exploiting the explosion of information associated with whole genome sequencing to tackle Shiga toxin-producing *Escherichia coli* (STEC) in global food production systems. *Int. J. Food Microbiol.* **187**, 57-72 (2014).
5. Majowicz, S. E. *et al.* Global incidence of human Shiga toxin-producing *Escherichia coli* infections and deaths: a systematic review and knowledge synthesis. *Foodborne Pathog. Dis.* **11**, 447-455 (2014).
6. Public Health Agency of Canada. *E. coli* fact sheet – Surveillance. <http://www.phac-aspc.gc.ca/fs-sa/fs-fi/ecoli-eng.php>. Accessed 2016-01-21.
7. Hazen, T. H., Kaper, J. B., Nataro, J. P. & Rasko, D. A. Comparative Genomics Provides Insight into the Diversity of the Attaching and Effacing *Escherichia coli* Virulence Plasmids. *Infect. Immun.* **83**, 4103-4117 (2015).
8. Wang, X. *et al.* Etiology of Childhood Infectious Diarrhea in a Developed Region of China: Compared to Childhood Diarrhea in a Developing Region and Adult Diarrhea in a Developed Region. *PLoS One* **10**, e0142136 (2015).
9. Crim, S. M. *et al.* Preliminary incidence and trends of infection with pathogens transmitted commonly through food - Foodborne Diseases Active Surveillance Network, 10 U.S. sites, 2006-2014. *MMWR Morb. Mortal. Wkly. Rep.* **64**, 495-499 (2015).
10. Lee, M. S., Koo, S., Jeong, D. G. & Tesh, V. L. Shiga Toxins as Multi-Functional Proteins: Induction of Host Cellular Stress Responses, Role in Pathogenesis and Therapeutic Applications. *Toxins (Basel)* **8**, 10.3390/toxins8030077 (2016).
11. Whitney, B. M. *et al.* Socioeconomic Status and Foodborne Pathogens in Connecticut, USA, 2000-2011(1). *Emerg. Infect. Dis.* **21**, 1617-1624 (2015).
12. Kavanagh, D., Raman, S. & Sheerin, N. S. Management of hemolytic uremic syndrome. *F1000Prime Rep.* **6**, 119-119. eCollection 2014 (2014).
13. Smith, J. L., Fratamico, P. M. & Gunther, N. W., 4th. Shiga toxin-producing *Escherichia coli*. *Adv. Appl. Microbiol.* **86**, 145-197 (2014).
14. Beutin, L. Emerging enterohaemorrhagic *Escherichia coli*, causes and effects of the rise of a human pathogen. *J. Vet. Med. B Infect. Dis. Vet. Public Health* **53**, 299-305 (2006).
15. Etcheverria, A. I. & Padola, N. L. Shiga toxin-producing *Escherichia coli*: factors involved in virulence and cattle colonization. *Virulence* **4**, 366-372 (2013).
16. Nguyen-The, C. *et al.* Agrifood systems and the microbial safety of fresh produce: Trade-offs in the wake of increased sustainability. *Sci. Total Environ.* **562**, 751-759 (2016).
17. Lewis, L., Corriveau, A. & Osborne, R. Independent Review of XL Foods Inc. Beef Recall 2012. (2013).
18. Bolton, D. J. Verocytotoxigenic (Shiga toxin-producing) *Escherichia coli*: virulence factors and pathogenicity in the farm to fork paradigm. *Foodborne Pathog. Dis.* **8**, 357-365 (2011).
19. Bielaszewska, M., Aldick, T., Bauwens, A. & Karch, H. Hemolysin of enterohemorrhagic *Escherichia coli*: structure, transport, biological activity and putative role in virulence. *Int. J. Med. Microbiol.* **304**, 521-529 (2014).

20. DiRienzo, J. M. Uptake and processing of the cytolethal distending toxin by mammalian cells. *Toxins (Basel)* **6**, 3098-3116 (2014).
21. Stevens, M. P. & Frankel, G. M. The Locus of Enterocyte Effacement and Associated Virulence Factors of Enterohemorrhagic Escherichia coli. *Microbiol. Spectr.* **2**, EHEC-0007-2013 (2014).
22. Vogeleeer, P., Tremblay, Y. D., Mafu, A. A., Jacques, M. & Harel, J. Life on the outside: role of biofilms in environmental persistence of Shiga-toxin producing Escherichia coli. *Front. Microbiol.* **5**, 317 (2014).
23. Chen, C. Y. *et al.* Phenotypic and genotypic characterization of biofilm forming capabilities in non-O157 Shiga toxin-producing Escherichia coli strains. *PLoS One* **8**, e84863 (2013).
24. Woerner, D. R. *et al.* Determining the prevalence of Escherichia coli O157 in cattle and beef from the feedlot to the cooler. *J. Food Prot.* **69**, 2824-2827 (2006).
25. Lee, J. E. *et al.* Phylogenetic analysis of Shiga toxin 1 and Shiga toxin 2 genes associated with disease outbreaks. *BMC Microbiol.* **7**, 109 (2007).
26. Mukhopadhyay, S. & Linstedt, A. D. Retrograde trafficking of AB(5) toxins: mechanisms to therapeutics. *J. Mol. Med. (Berl)* **91**, 1131-1141 (2013).
27. Russo, L. M., Melton-Celsa, A. R., Smith, M. J. & O'Brien, A. D. Comparisons of native Shiga toxins (Stxs) type 1 and 2 with chimeric toxins indicate that the source of the binding subunit dictates degree of toxicity. *PLoS One* **9**, e93463 (2014).
28. Pacheco, A. R. & Sperandio, V. Shiga toxin in enterohemorrhagic E.coli: regulation and novel anti-virulence strategies. *Front. Cell. Infect. Microbiol.* **2**, 81 (2012).
29. Scheutz, F. Taxonomy Meets Public Health: The Case of Shiga Toxin-Producing Escherichia coli. *Microbiol. Spectr.* **2**, 10.1128/microbiolspec.EHEC-0019-2013 (2014).
30. Scheutz, F. *et al.* Multicenter evaluation of a sequence-based protocol for subtyping Shiga toxins and standardizing Stx nomenclature. *J. Clin. Microbiol.* **50**, 2951-2963 (2012).
31. Sandvig, K., Bergan, J., Dyve, A. B., Skotland, T. & Torgersen, M. L. Endocytosis and retrograde transport of Shiga toxin. *Toxicon* **56**, 1181-1185 (2010).
32. Magwedere, K. *et al.* Incidence of Shiga toxin-producing Escherichia coli strains in beef, pork, chicken, deer, boar, bison, and rabbit retail meat. *J. Vet. Diagn. Invest.* **25**, 254-258 (2013).
33. Probert, W. S., McQuaid, C. & Schrader, K. Isolation and identification of an Enterobacter cloacae strain producing a novel subtype of Shiga toxin type 1. *J. Clin. Microbiol.* **52**, 2346-2351 (2014).
34. Ogura, Y. *et al.* The Shiga toxin 2 production level in enterohemorrhagic Escherichia coli O157:H7 is correlated with the subtypes of toxin-encoding phage. *Sci. Rep.* **5**, 16663 (2015).
35. Melton-Celsa, A. R. Shiga Toxin (Stx) Classification, Structure, and Function. *Microbiol. Spectr.* **2**, 10.1128/microbiolspec.EHEC-0024-2013 (2014).
36. Muniesa, M. *et al.* Shiga toxin 2-converting bacteriophages associated with clonal variability in Escherichia coli O157:H7 strains of human origin isolated from a single outbreak. *Infect. Immun.* **71**, 4554-4562 (2003).
37. Gamage, S. D., Patton, A. K., Hanson, J. F. & Weiss, A. A. Diversity and host range of Shiga toxin-encoding phage. *Infect. Immun.* **72**, 7131-7139 (2004).
38. Mauro, S. A. & Koudelka, G. B. Shiga toxin: expression, distribution, and its role in the environment. *Toxins (Basel)* **3**, 608-625 (2011).
39. Calderwood, S. B. & Mekalanos, J. J. Iron regulation of Shiga-like toxin expression in Escherichia coli is mediated by the fur locus. *J. Bacteriol.* **169**, 4759-4764 (1987).
40. Kimmitt, P. T., Harwood, C. R. & Barer, M. R. Toxin gene expression by shiga toxin-producing Escherichia coli: the role of antibiotics and the bacterial SOS response. *Emerg. Infect. Dis.* **6**, 458-465 (2000).
41. Schuller, S. Shiga toxin interaction with human intestinal epithelium. *Toxins (Basel)* **3**, 626-639 (2011).

42. Brigotti, M. *et al.* Interactions between Shiga toxins and human polymorphonuclear leukocytes. *J. Leukoc. Biol.* **84**, 1019-1027 (2008).
43. Obrig, T. G. & Karpman, D. Shiga toxin pathogenesis: kidney complications and renal failure. *Curr. Top. Microbiol. Immunol.* **357**, 105-136 (2012).
44. Karve, S. S. & Weiss, A. A. Glycolipid binding preferences of Shiga toxin variants. *PLoS One* **9**, e101173 (2014).
45. Johannes, L. & Romer, W. Shiga toxins--from cell biology to biomedical applications. *Nat. Rev. Microbiol.* **8**, 105-116 (2010).
46. Lee, M. S., Cherla, R. P. & Tesh, V. L. Shiga toxins: intracellular trafficking to the ER leading to activation of host cell stress responses. *Toxins (Basel)* **2**, 1515-1535 (2010).
47. Obata, F. & Obrig, T. Role of Shiga/Vero toxins in pathogenesis. *Microbiol. Spectr.* **2**, 10.1128/microbiolspec.EHEC-0005-2013 (2014).
48. Batz, M. B., Henke, E. & Kowalcyk, B. Long-term consequences of foodborne infections. *Infect. Dis. Clin. North Am.* **27**, 599-616 (2013).
49. Tironi-Farinati, C. *et al.* A translational murine model of sub-lethal intoxication with Shiga toxin 2 reveals novel ultrastructural findings in the brain striatum. *PLoS One* **8**, e55812 (2013).
50. Matussek, A. *et al.* Molecular and functional analysis of Shiga toxin-induced response patterns in human vascular endothelial cells. *Blood* **102**, 1323-1332 (2003).
51. Davis, T. K., McKee, R., Schnadower, D. & Tarr, P. I. Treatment of Shiga toxin-producing *Escherichia coli* infections. *Infect. Dis. Clin. North Am.* **27**, 577-597 (2013).
52. Page, A. V. & Liles, W. C. Enterohemorrhagic *Escherichia coli* Infections and the Hemolytic-Uremic Syndrome. *Med. Clin. North Am.* **97**, 681-95, xi (2013).
53. Kehl, K. S., Havens, P., Behnke, C. E. & Acheson, D. W. Evaluation of the premier EHEC assay for detection of Shiga toxin-producing *Escherichia coli*. *J. Clin. Microbiol.* **35**, 2051-2054 (1997).
54. Schindler, E. I., Sellenriek, P., Storch, G. A., Tarr, P. I. & Burnham, C. A. Shiga toxin-producing *Escherichia coli*: a single-center, 11-year pediatric experience. *J. Clin. Microbiol.* **52**, 3647-3653 (2014).
55. Tang, Y. *et al.* Light scattering sensor for direct identification of colonies of *Escherichia coli* serogroups O26, O45, O103, O111, O121, O145 and O157. *PLoS One* **9**, e105272 (2014).
56. BD. BBL Sorbitol MacConkey II Agar with Cefixime and Tellurite: Quality control procedures. , 1 (2012).
57. Sallam, K. I., Mohammed, M. A., Ahdy, A. M. & Tamura, T. Prevalence, genetic characterization and virulence genes of sorbitol-fermenting *Escherichia coli* O157:H- and *E. coli* O157:H7 isolated from retail beef. *Int. J. Food Microbiol.* **165**, 295-301 (2013).
58. BD. BBL CHROMagar O157: Quality control procedures. (2012).
59. Gould, L. H. *et al.* Recommendations for diagnosis of shiga toxin--producing *Escherichia coli* infections by clinical laboratories. *MMWR Recomm Rep.* **58**, 1-14 (2009).
60. March, S. B. & Ratnam, S. Latex agglutination test for detection of *Escherichia coli* serotype O157. *J. Clin. Microbiol.* **27**, 1675-1677 (1989).
61. Borczyk, A. A., Harnett, N., Lombos, M. & Lior, H. False-positive identification of *Escherichia coli* O157 by commercial latex agglutination tests. *Lancet* **336**, 946-947 (1990).
62. Kase, J. A., Maounounen-Laasri, A., Son, I., Lin, A. & Hammack, T. S. Comparison of eight different agars for the recovery of clinically relevant non-O157 Shiga toxin-producing *Escherichia coli* from baby spinach, cilantro, alfalfa sprouts and raw milk. *Food Microbiol.* **46**, 280-287 (2015).
63. Paton, J. C. & Paton, A. W. Methods for detection of STEC in humans. An overview. *Methods Mol. Med.* **73**, 9-26 (2003).
64. Bhunia, A. & Wempler, J. in *Foodborne Pathogens: Microbiology and Molecular Biology* (eds Fratamico, P., Bhunia, A. & Smith, J.) 15 (Caister Academic Press, 2005).

65. Meridian Bioscience, I. Premier EHEC: EIA for the detection of the Toxins Produced by Enterohemorrhagic *E. coli* in Stool Specimens or Culture Systems. , 1 (2008).
66. Remel Microbiology Products. ProSpecT Shiga Toxin *E. coli* (STEC) Microplate Assay. , 1 (2012).
67. Vallieres, E., Saint-Jean, M. & Rallu, F. Comparison of three different methods for detection of Shiga toxin-producing *Escherichia coli* in a tertiary pediatric care center. *J. Clin. Microbiol.* **51**, 481-486 (2013).
68. Merck. in *Merck Microbiology Manual 623* (Christian Denk, 2012).
69. Meridian Bioscience, I. ImmunoCard STAT! EHEC: Rapid test for Shiga toxins 1 and 2 in human stool., 1 (2013).
70. Park, C. H., Kim, H. J., Hixon, D. L. & Bubert, A. Evaluation of the duopath verotoxin test for detection of shiga toxins in cultures of human stools. *J. Clin. Microbiol.* **41**, 2650-2653 (2003).
71. Feng, P. C., Jinneman, K., Scheutz, F. & Monday, S. R. Specificity of PCR and serological assays in the detection of *Escherichia coli* Shiga toxin subtypes. *Appl. Environ. Microbiol.* **77**, 6699-6702 (2011).
72. Paton, J. C. & Paton, A. W. Pathogenesis and diagnosis of Shiga toxin-producing *Escherichia coli* infections. *Clin. Microbiol. Rev.* **11**, 450-479 (1998).
73. Chui, L. *et al.* Comparison of Shiga toxin-producing *Escherichia coli* detection methods using clinical stool samples. *J. Mol. Diagn.* **12**, 469-475 (2010).
74. Cox, J. & Mann, M. Quantitative, high-resolution proteomics for data-driven systems biology. *Annu. Rev. Biochem.* **80**, 273-299 (2011).
75. Forler, S., Klein, O. & Klose, J. Individualized proteomics. *J. Proteomics* **107**, 56-61 (2014).
76. Liebler, D. C. & Zimmerman, L. J. Targeted quantitation of proteins by mass spectrometry. *Biochemistry* **52**, 3797-3806 (2013).
77. Waaijer, C. J. & Palmlblad, M. Bibliometric Mapping: Eight Decades of Analytical Chemistry, With Special Focus on the Use of Mass Spectrometry. *Anal. Chem.* (2015).
78. Gstaiger, M. & Aebersold, R. Applying mass spectrometry-based proteomics to genetics, genomics and network biology. *Nat. Rev. Genet.* **10**, 617-627 (2009).
79. Dass, C. in *Fundamentals of Contemporary Mass Spectrometry* (Wiley, 2007).
80. Hu, Q. *et al.* The Orbitrap: a new mass spectrometer. *J. Mass Spectrom.* **40**, 430-443 (2005).
81. Charretier, Y. *et al.* Rapid Bacterial Identification, Resistance, Virulence and Type Profiling using Selected Reaction Monitoring Mass Spectrometry. *Sci. Rep.* **5**, 13944 (2015).
82. Zhou, J. *et al.* Development and Evaluation of a Parallel Reaction Monitoring Strategy for Large-Scale Targeted Metabolomics Quantification. *Anal. Chem.* (2016).
83. Rauniyar, N. Parallel Reaction Monitoring: A Targeted Experiment Performed Using High Resolution and High Mass Accuracy Mass Spectrometry. *Int. J. Mol. Sci.* **16**, 28566-28581 (2015).
84. Peterson, A. C., Russell, J. D., Bailey, D. J., Westphall, M. S. & Coon, J. J. Parallel reaction monitoring for high resolution and high mass accuracy quantitative, targeted proteomics. *Mol. Cell. Proteomics* **11**, 1475-1488 (2012).
85. Fusaro, V. A., Mani, D. R., Mesirov, J. P. & Carr, S. A. Prediction of high-responding peptides for targeted protein assays by mass spectrometry. *Nat. Biotechnol.* **27**, 190-198 (2009).
86. Gallien, S., Duriez, E. & Domon, B. Selected reaction monitoring applied to proteomics. *J. Mass Spectrom.* **46**, 298-312 (2011).
87. Bozovic, A. & Kulasingam, V. Quantitative mass spectrometry-based assay development and validation: from small molecules to proteins. *Clin. Biochem.* **46**, 444-455 (2013).
88. Domon, B. & Gallien, S. Recent advances in targeted proteomics for clinical applications. *Proteomics Clin. Appl.* **9**, 423-431 (2015).
89. Livny, J. & Friedman, D. I. Characterizing spontaneous induction of Stx encoding phages using a selectable reporter system. *Mol. Microbiol.* **51**, 1691-1704 (2004).

90. Adkins, J. N. *et al.* Analysis of the Salmonella typhimurium proteome through environmental response toward infectious conditions. *Mol. Cell. Proteomics* **5**, 1450-1461 (2006).
91. Wisniewski, J. R., Zougman, A., Nagaraj, N. & Mann, M. Universal sample preparation method for proteome analysis. *Nat. Methods* **6**, 359-362 (2009).
92. Clark, C. G. *et al.* DNA sequence heterogeneity of Campylobacter jejuni CJIE4 prophages and expression of prophage genes. *PLoS One* **9**, e95349 (2014).
93. Sherwood, C. A. *et al.* Correlation between y-type ions observed in ion trap and triple quadrupole mass spectrometers. *J. Proteome Res.* **8**, 4243-4251 (2009).
94. Trinh, H. V. *et al.* iTRAQ-Based and Label-Free Proteomics Approaches for Studies of Human Adenovirus Infections. *Int. J. Proteomics* **2013**, 581862 (2013).
95. Searle, B. C. Scaffold: a bioinformatic tool for validating MS/MS-based proteomic studies. *Proteomics* **10**, 1265-1269 (2010).
96. Kruger, A., Lucchesi, P. M. & Parma, A. E. Verotoxins in bovine and meat verotoxin-producing Escherichia coli isolates: type, number of variants, and relationship to cytotoxicity. *Appl. Environ. Microbiol.* **77**, 73-79 (2011).
97. Wagner, P. L. *et al.* Bacteriophage control of Shiga toxin 1 production and release by Escherichia coli. *Mol. Microbiol.* **44**, 957-970 (2002).
98. Rahal, E. A., Kazzi, N., Nassar, F. J. & Matar, G. M. Escherichia coli O157:H7-Clinical aspects and novel treatment approaches. *Front. Cell. Infect. Microbiol.* **2**, 138 (2012).
99. Fuller, H. R. *et al.* Valproate and bone loss: iTRAQ proteomics show that valproate reduces collagens and osteonectin in SMA cells. *J. Proteome Res.* **9**, 4228-4233 (2010).
100. Los, J. M., Los, M., Wegrzyn, G. & Wegrzyn, A. Differential efficiency of induction of various lambdoid prophages responsible for production of Shiga toxins in response to different induction agents. *Microb. Pathog.* **47**, 289-298 (2009).
101. Armbruster, D. A. & Pry, T. Limit of blank, limit of detection and limit of quantitation. *Clin. Biochem. Rev.* **29 Suppl 1**, S49-52 (2008).
102. Bowen, A. *et al.* Elevated Risk for Antimicrobial Drug-Resistant Shigella Infection among Men Who Have Sex with Men, United States, 2011-2015. *Emerg. Infect. Dis.* **22**, 1613-1616 (2016).
103. Kruger, A. & Lucchesi, P. M. Shiga toxins and stx phages: highly diverse entities. *Microbiology* **161**, 451-462 (2015).
104. Kruger, A., Lucchesi, P. M. & Parma, A. E. Verotoxins in bovine and meat verotoxin-producing Escherichia coli isolates: type, number of variants, and relationship to cytotoxicity. *Appl. Environ. Microbiol.* **77**, 73-79 (2011).
105. Baranzoni, G. M. *et al.* Characterization of Shiga Toxin Subtypes and Virulence Genes in Porcine Shiga Toxin-Producing Escherichia coli. *Front. Microbiol.* **7**, 574 (2016).
106. Lauri, A. & Mariani, P. O. Potentials and limitations of molecular diagnostic methods in food safety. *Genes Nutr.* **4**, 1-12 (2009).
107. Wijnsma, K. L. *et al.* Fecal diagnostics in combination with serology: best test to establish STEC-HUS. *Pediatr. Nephrol.* (2016).
108. Yamasaki, E. *et al.* Quantitative Detection of Shiga Toxins Directly from Stool Specimens of Patients Associated with an Outbreak of Enterohemorrhagic Escherichia coli in Japan--Quantitative Shiga toxin detection from stool during EHEC outbreak. *Toxins (Basel)* **7**, 4381-4389 (2015).
109. Taylor, P. J. Matrix effects: the Achilles heel of quantitative high-performance liquid chromatography-electrospray-tandem mass spectrometry. *Clin. Biochem.* **38**, 328-334 (2005).
110. Piras, C., Roncada, P., Rodrigues, P. M., Bonizzi, L. & Soggiu, A. Proteomics in food: Quality, safety, microbes, and allergens. *Proteomics* **16**, 799-815 (2016).

111. Li, Y. *et al.* Hybrid quadrupole-orbitrap mass spectrometry analysis with accurate-mass database and parallel reaction monitoring for high-throughput screening and quantification of multi-xenobiotics in honey. *J. Chromatogr. A* **1429**, 119-126 (2016).
112. van den Broek, I., Blokland, M., Nessen, M. A. & Sterk, S. Current trends in mass spectrometry of peptides and proteins: Application to veterinary and sports-doping control. *Mass Spectrom. Rev.* **34**, 571-594 (2015).
113. Titz, B. *et al.* Proteomics for systems toxicology. *Comput. Struct. Biotechnol. J.* **11**, 73-90 (2014).
114. Silva, C. J. *et al.* Safe and effective means of detecting and quantitating Shiga-like toxins in attomole amounts. *Anal. Chem.* **86**, 4698-4706 (2014).
115. Public Health Agency of Canada. National Enteric Surveillance Program (NESP) 2013 Annual Report Executive Summary. <https://www.nml-inm.gc.ca/NESP-PNSME/surveillance-2013-eng.html>. Accessed November 22, 2016.
116. Biolog. Ranbow® Agar O157 Technical Information. (2008).
117. Thomas, M. K. *et al.* Estimates of the burden of foodborne illness in Canada for 30 specified pathogens and unspecified agents, circa 2006. *Foodborne Pathog. Dis.* **10**, 639-648 (2013).
118. Paton, A. W. & Paton, J. C. Detection and characterization of Shiga toxigenic *Escherichia coli* by using multiplex PCR assays for *stx1*, *stx2*, *eaeA*, enterohemorrhagic *E. coli* *hlyA*, *rfbO111*, and *rfbO157*. *J. Clin. Microbiol.* **36**, 598-602 (1998).
119. Silva, C. J., Erickson-Beltran, M. L., Skinner, C. B., Patfield, S. A. & He, X. Mass Spectrometry-Based Method of Detecting and Distinguishing Type 1 and Type 2 Shiga-Like Toxins in Human Serum. *Toxins (Basel)* **7**, 5236-5253 (2015).
120. Feng, P. C. & Reddy, S. Prevalences of Shiga toxin subtypes and selected other virulence factors among Shiga-toxigenic *Escherichia coli* strains isolated from fresh produce. *Appl. Environ. Microbiol.* **79**, 6917-6923 (2013).

## 8. Supplementary Data

**Supplementary Table S1.** Method development runs using recombinant, non-toxic Stx peptides. The following submissions for MS analysis were performed on multiple MS systems for development and refinement of the Stx detection assay.

Sub #	Sample description	Concentration	Injection volume	Instrument
2745	In-solution digested Stx peptides in buffer - Assuming 1:5 A to B subunit ratio - Determine detectible peptides	50 fmol/ $\mu$ l	2 $\mu$ l	QqQ in MRM mode
2749	In-solution digested Stx peptides in buffer - Confirm trypsin peptide cleavage	10 ng/ $\mu$ l	2 $\mu$ l	LTQ Orbitrap XL
2755	In-solution digested Stx peptides in buffer - Assuming a 1:1 A to B subunit ratio	50 fmol/ $\mu$ l	2 $\mu$ l	QqQ in MRM mode

**Supplementary Table S2.** Method development runs using Stx peptides from active, intact Stx. The following submissions for MS analysis we performed on multiple MS systems for development and refinement of the Stx detection assay.

Sub #	Sample description	Concentration	Injection volume	Instrument
2813	In-solution digested Stx peptides in buffer <ul style="list-style-type: none"> <li>- Confirm trypsin peptide cleavage</li> <li>- Ensure successful salt removal</li> </ul>	500 pg/ $\mu$ l	10 $\mu$ l	LTQ Orbitrap Velos
2814	In-solution digested Stx peptides in buffer <ul style="list-style-type: none"> <li>- Determine detectible peptides</li> </ul>	50 fmol/ $\mu$ l	2 $\mu$ l	QqQ in MRM mode
2851	In-solution digested Stx peptides in buffer <ul style="list-style-type: none"> <li>- Continued method development and refinement</li> </ul>	50 fmol/ $\mu$ l	2 $\mu$ l	QqQ in MRM mode
2868	In-solution digested Stx peptides in buffer <ul style="list-style-type: none"> <li>- Determine if higher concentration gives better signal</li> </ul>	500 fmol/ $\mu$ l	2 $\mu$ l	QqQ in MRM mode
3024	In-solution digested Stx peptides spiked into buffer and matrix <ul style="list-style-type: none"> <li>- Dilution series to determine LLOD</li> <li>- 1 in 5 dilutions – blank containing no Stx peptides</li> </ul>	25 ng/ $\mu$ l to 0.128 pg/ $\mu$ l	2 $\mu$ l	QqQ in MRM mode

**Supplementary Table S3.** Method development runs using synthetic Stx peptides. The following submissions for MS analysis we performed on the QE+ mass spectrometer for development and refinement of the Stx detection assay.

Sub #	Sample description	Concentration	Injection volume	Instrument
3271	Synthetic peptides spiked into buffer and matrix (ATCC 11775) - 1:1 molar ratio	50 fmol/ $\mu$ l	2 $\mu$ l	QExactive Plus
3281	Synthetic peptides spiked into buffer and matrix (ATCC 11775) - Dilution series to determine LLOD - 1 in 3 dilutions – blank containing no Stx peptides	50 fmol/ $\mu$ l to 7.6 amol/ $\mu$ l	2 $\mu$ l	QExactive Plus
3307	Synthetic peptides spiked into buffer and matrix (ATCC 25922 and ATCC 11775) - Stx1 peptides, Stx2 peptides, Stx1 and Stx2 peptides, and blanks	50 fmol/ $\mu$ l	2 $\mu$ l	QExactive Plus
3327	Synthetic peptides spiked into matrix (ATCC 25922) - Dilution series to determine LLOD - 1 in 3 dilutions – blank containing no Stx peptides	50 fmol/ $\mu$ l to 7.6 amol/ $\mu$ l	2 $\mu$ l	QExactive Plus

**Supplementary Table S4.** Validation of the PRM Stx detection assay using bacterial cultures. The following submissions for MS analysis we performed on the QE+ mass spectrometer to determine if the PRM Stx detection assay was capable of distinguishing between STEC and non-STEC isolates.

Sub #	Sample description	Concentration	Injection volume	Instrument
3372	In-solution digested clinical STEC peptides - Determine optimal concentration for sample analysis - 5 samples at each concentration	100 ng/ $\mu$ l 200 ng/ $\mu$ l 400 ng/ $\mu$ l	5 $\mu$ l	QExactive Plus
3379	In-solution digested clinical STEC peptides - Assay validation with 91 clinical samples - Buffer and matrix blanks - Dilution series using synthetic peptide mix at beginning and end - Positive control using synthetic peptide mix	<i>Dilution series:</i> 50 fmol/ $\mu$ l to 7.6 amol/ $\mu$ l <i>+ve control:</i> 5 fmol/ $\mu$ l <i>Clinical samples:</i> 100 ng/ $\mu$ l	<i>Dilution series/positive control:</i> 2 $\mu$ l <i>Clinical samples:</i> 5 $\mu$ l	QExactive Plus
3428	In-solution digested clinical STEC peptides - Post-cleanup test run	<i>Clinical samples:</i> 0.2 ug/ $\mu$ l <i>Controls:</i> 0.1 ug/ $\mu$ l	5 $\mu$ l	QExactive Plus
3456	In-solution digested peptides from clinical bacterial cultures - Assay validation with 91 clinical samples - Buffer and matrix blanks - Dilution series using synthetic peptide mix at beginning and end - Positive control using synthetic peptide mix	<i>Dilution series:</i> 50 fmol/ $\mu$ l to 7.6 amol/ $\mu$ l <i>+ve control:</i> 50 fmol/ $\mu$ l <i>Clinical samples:</i> 0.2 ug/ $\mu$ l	<i>Dilution series/positive control:</i> 2 $\mu$ l <i>Clinical samples:</i> 5 $\mu$ l	QExactive Plus

**Supplementary Table S5.** Summary of the STEC isolates used for evaluation of Stx detection. The following isolates were used as STEC positive isolates to determine the sensitivity and specificity of the VCA, PCR, and PRM Stx detection assays.

NML lab number	FWS number	Serotype	Stx subtype	VCA	PCR
87-1215	FWS_EC_0004	O157:H7	stx1a, stx2a		✓
00-4748	FWS_EC_0005	O111:NM	stx1a, stx2a		✓
02-6737	FWS_EC_0001	O26:H11	stx1a, stx2a		✓
03-2832	FWS_EC_0006	O121:H19	stx2a		✓
03-4699	FWS_EC_0002	O145:NM	stx1a		✓
04-2446	FWS_EC_0007	O103:H2	stx1a		✓
05-6544	FWS_EC_0075	O26:H11	stx1a		✓
05-6545	FWS_EC_0003	O45:H2	stx1a, stx2a		✓
06-1595	FWS_EC_0076	O1:H20	stx2a		✓
06-3440	FWS_EC_0078	O51:H49	stx2e	✓	✓
06-7270	FWS_EC_0081	O(untypeable):HNM	stx2c	✓	✓
07-5698	FWS_EC_0084	O26:H11	stx1a		✓
09-0526	FWS_EC_0090	O107:H7	stx1a		✓
09-0529	FWS_EC_0092	O91:H14	stx2b	✓	✓
09-0530	FWS_EC_0093	O146:H28	stx2b	✓	✓
09-1250	FWS_EC_0094	O26:H11	stx1a, stx2a		✓
09-1765	FWS_EC_0097	O130:H11	stx2a		✓
09-2555	FWS_EC_0008	O91:H21	stx2d		✓
09-4076	FWS_EC_0100	O26:H11	stx1a		✓
09-5073	FWS_EC_0102	O98:H29	stx1a		✓
10-2157	FWS_EC_0107	O79:H7	Stx2c	✓	
10-2400	FWS_EC_0110	O103:H2	stx1a		✓
10-2726	FWS_EC_0111	O174:H8	stx1c, stx2b	✓	✓
10-2734	FWS_EC_0112	O41:H26	stx1d	✓	✓
10-3993	FWS_EC_0153	O121:H19	stx2a		✓
10-8262	FWS_EC_0114	O139:H1	stx2e	✓	✓
10-8263	FWS_EC_0115	O171:H2	stx2b	✓	✓
10-8264	FWS_EC_0116	O91:H21	stx2d	✓	✓
10-8265	FWS_EC_0117	O145:H34	stx2f	✓	✓
10-8267	FWS_EC_0118	O2:H25	stx2g	✓	✓
10-8268	FWS_EC_0119	O146:H21	stx1c, stx2a, stx2b	✓	✓
10-8270	FWS_EC_0120	O154:H31	stx1d	✓	✓
10-8272	FWS_EC_0122	O48:H21	stx1a, stx2a		✓
10-8273	FWS_EC_0123	O174:H21	stx2b	✓	✓
10-8275	FWS_EC_0124	O118:H12	stx2b	✓	✓
10-8279	FWS_EC_0127	O128ab:NM	stx2f	✓	✓
11-2646	FWS_EC_0132	O177:NM	stx2c	✓	✓
11-3088	FWS_EC_0009	O104:H4	stx2a		✓
11-4633	FWS_EC_0156	O121:H19	stx2a		✓
11-5594	FWS_EC_0140	O121:H1	stx2a	✓	✓
11-6686	FWS_EC_0159	O111:NM	stx1a, stx2a	✓	✓
11-7063	FWS_EC_0160	O121:H19	stx2a		✓
12-2966	FWS_EC_0021	O26:H11	stx1a		✓

12-2977	FWS_EC_0028	O103:H2	stx1a, stx2a		✓
12-2978	FWS_EC_0033	O111:H8	stx1a	✓	✓
12-2987	FWS_EC_0041	O145:NM	stx1a	✓	✓
12-2988	FWS_EC_0042	O145:H25	stx2a	✓	✓
12-2990	FWS_EC_0044	O145:NM	stx1a, stx2a	✓	✓
12-2995	FWS_EC_0045	O91:NM	stx1a, stx2b	✓	✓
12-2996	FWS_EC_0046	O91:NM	stx1a, stx2b	✓	✓
12-2997	FWS_EC_0047	O91:H21	stx2d	✓	✓
12-2998	FWS_EC_0048	O91:H21	stx1a, stx2a	✓	✓
12-2999	FWS_EC_0049	O113:H4	stx1a, stx2d	✓	✓
12-3000	FWS_EC_0050	O113:H4	stx1a, stx2d	✓	✓
12-3001	FWS_EC_0051	O113:H21	stx2d	✓	✓
12-3002	FWS_EC_0010	O113:H21	stx2a	✓	✓
12-3003	FWS_EC_0052	O128:NM	stx1c	✓	✓
12-3004	FWS_EC_0053	O128:H2	stx1c	✓	✓
12-3005	FWS_EC_0054	O128:H10	stx1a, stx1c	✓	✓
12-6191	FWS_EC_0011	O113:H21	stx2d	✓	✓
14-0585	FWS_EC_0302	O121:H19	stx2a		✓
14-0586	FWS_EC_0303	O121:H19	stx2a		
14-0587	FWS_EC_0304	O121:H19	stx2a		

---

**Supplementary Table S6.** Summary of the Stx-negative isolates used to evaluate the PRM Stx detection assay.

<b>NML lab number</b>	<b><i>E. coli</i> pathotype</b>	<b>Stx subtype</b>
17-2	EAEC	Negative
01-5871	EAEC	Negative
042	EAEC	Negative
01-8001	EAEC	Negative
01-7987	EAEC	Negative
01-8000	EAEC	Negative
10-7591	EAEC	Negative
11-7485	EAEC	Negative
55989	EAEC	Negative
88-501A	EPEC	Negative
88-557A	EPEC	Negative
88-263B	EPEC	Negative
03-5069	EPEC	Negative
01-7986	EPEC	Negative
01-7999	EPEC	Negative
02-6956	ETEC	Negative
03-5090	ETEC	Negative
01-7992	ETEC	Negative
03-6474	ETEC	Negative
78-10376	ETEC	Negative
78-10377	ETEC	Negative
78-10373	ETEC	Negative
82-10281	ETEC	Negative
83-7032	ETEC	Negative
86-5227	ETEC	Negative
86-5230	ETEC	Negative
86-5420	ETEC	Negative
2547T	Shigella spp.	Negative
SH-62	Shigella spp.	Negative